Title
The catalytic mechanism tRNA (m_5U54)-Methyltransferase

Author
Kealey, James T.

Publication Date
1994

Peer reviewed|Thesis/dissertation

The Catalytic Mechanism tRNA (m^5U54)-Methyltransferase

by

James T. Kealey

DISSERTATION

Submitted in partial satisfaction of the requirements for the degree of

DOCTOR OF PHILOSOPHY

in

Pharmaceutical Chemistry

in the

GRADUATE DIVISION

of the

UNIVERSITY OF CALIFORNIA

San Francisco

For Michael

Forward

I have been fascinated with biology ever since I was a kid-- and I decided to pursue it as a career when it became clear that I had little chance of playing professional baseball. I enrolled at UC Santa Cruz with the intent of becoming a marine biologist, but after spending much enjoyable time in the tide pools of the California coast, I realized that my interest in biology lay on a smaller scale, and I switched majors to biochemistry. As a senior at Santa Cruz, I worked for the academic year in Harry Noller's laboratory, where I gained a reverent appreciation of RNA, and became interested in protein-RNA interactions.

For my graduate studies, I chose a project that encompassed my interests in enzymology, RNA, and protein-RNA recognition. I chose to study an enzyme [tRNA (m^5U54)-methyltransferase, RUMT] that employs a complex chemical mechanism to introduce a methyl group at the 5-position of a specific uridine in transfer RNA. The RUMT-tRNA interaction represents an ideal system for the study of protein-RNA recognition-- in particular, how protein-RNA interactions contribute to catalysis. My work has mainly focused on the chemical mechanism of RUMT, and has, I believe, provided a strong foundation for further analysis of the enzyme and its catalytic mechanism by X-ray crystallography.

Acknowledgments

I thank Glenn Björk (Umeå, Sweden) for isolating *trmA* , making the work on RUMT possible, and Claes Gustaffson (Umeå, Sweden) for many stimulating discussions on *trmA*. I thank Andras Patthy (Budapest, Hungary) for friendship and teaching me the "Hungarian way" of science. I thank past and present members of the Santi Lab who have made this experience educational, as well as pleasurable, especially Chris Carreras, Jens Eckstein, and Jim Newell, who I hope will be lifelong scientific colleagues and friends. I am especially indebted to Chris Carreras, who read and edited the entire thesis. I thank Xiangrong Gu for sharing his enthusiasm for RNA, and Kathryn Ivanetich and Patricia Greene for useful advice and criticism. I thank Uli Schmitz for advice on NMR and for stimulating discussions. The completion of this work was greatly facilitated by my familys' tremendous support and steadfast encouragement through some difficult times, and I cannot thank them enough. My academic advisor, Martin Shetlar, went beyond the call of duty to remind me of administrative deadlines and policies, and generally kept me out of bureaucratic trouble. I thank my undergraduate research advisor, Harry Noller, for introducing me to science and to RNA and for giving me the opportunity to work in a stellar research laboratory as an undergraduate. I am indebted to my graduate advisor and good friend, Dan Santi, who has taught me to be a scientist and has generously provided the tools necessary to do first-rate work. Finally, I thank my son, Michael, for helping to put the vicissitudes of a career in research into perspective.

Abstract

The Catalytic Mechanism tRNA (m^5U54)-Methyltransferase

James T. Kealey

This dissertation focuses on mechanistic studies of the enzyme tRNA (m^5U54)methyltransferase (RUMT), which catalyzes the*S*-adenosyl-L-methionine (AdoMet) dependent methylation of uridine 54 in tRNA. The thesis is primarily comprised of work that I have previously published, and these accounts are cited where appropriate. The introductory chapter reviews what is currently known about the chemical and kinetic mechanism, and substrate recognition of RUMT, and provides an historical account of studies on the molecular biology of the RUMT gene, *trmA*. In addition, chapter 1 discusses the role of 5-methyluridine (m^5U) in tRNA, and how the inhibition of RUMT by tRNA containing 5-fluorouridine (FUtRNA) might be related to the anti-cancer properties of the drug 5-fluorouracil.

RUMT ultilizes covalent catalysis to activate the 5-carbon of the target uracil base for electrophilic substitution. In chapter 2 I describe a set of experiments that identified cysteine 324 of RUMT as the nucleophilic catalyst [Kealey, J. T. and D. V. Santi (1991) *Biochemistry* **30**: 9724-9728]. Nucleophilic addition of cysteine 324 to C6 of U54 produces a potent nucleophile (anion equivalent) at C5, which is subsequently methylated. It is shown in chapter 3 that the methyl group is transferred from AdoMet to C5 in a single S_N2 displacement reaction [Kealey, J. T., S. Lee, H. G. Floss and D. V. Santi (1991)*Nucleic. Acids. Res.* **19**: 6465-6468]. Following methylation the C5

proton is abstracted and β-elimination yields free enzyme and methylated product.

In the presence of AdoMet, FUtRNA is a potent mechanism based inhibitor of RUMT, which forms a methylated FUtRNA-RUMT covalent complex. ^{19}F nuclear magnetic resonance (NMR) studies of this complex indicated that the catalytic nucleophile and methyl group add *cis* across the 5-6 double bond of U54, and the subsequent elimination occurs *trans* (chapter 5). Based on the data presented in chapter 5 and in previous chapters, I propose a complete chemical mechanism of RUMT catalyzed transmethylation (chapter 5). The NMR studies required milligrams of enzyme, which were provided by the overexpression and streamlined purification of RUMT, described in chapter 4 [Kealey, J. T. and D. V. Santi (1994) *Prot. Exp. Purif.* **5**: 149-152]. In chapter 6, I relate the curious finding that greater than 80% of RUMT in homogeneous preparations contains tightly bound AdoMet, which is chemically competent for methylation of RNA.

Table of Contents

Tables

Figures

"It can be foreseen that the enzyme responsible for this interesting feature of the tRNA structure will be fully characterized before long."

Glenn Björk, 1975

CHAPTER 1

INTRODUCTION

tRNA (m^5U54)methyltransferase: A Review of the Catalytic Mechanism, Gene Structure, and the Biochemical Role of m^5U54 in tRNA.

Introduction

One of the unique features of transfer RNA (tRNA) is its extensive post-transcriptional modification (for reviews see Kersten, 1984; Björk et al., 1987; Björk, 1992). In yeast $tRNA^{Phe}$, for example, 20% of the nucleosides are modified versions of the four canonical nucleosides, adenosine, uridine, cytidine, and guanosine (see Figure 1.1). To date, over 50 different types of tRNA modifications have been identified, which vary from base or sugar methylations to hypermodifications resulting from multistep syntheses requiring several enzymes. Because of the pivotal role tRNA plays in protein synthesis, an understanding of how modifications affect tRNA function is of great interest. Since most mutants defective in tRNA modification are viable, it is believed that tRNA modifications are not essential for cell growth, but may serve to "fine tune" tRNA function. Nevertheless, tRNA modifications confer a selective advantage for the cell, which is underscored by the fact that wild type strains generally outgrow strains defective in tRNA modifying activities. Moreover, it has been estimated that four times more genetic information codes for tRNA modifying enzymes than for primary tRNA transcripts (Björk, 1992), which further emphasizes the *in vivo* significance of tRNA modification.

Although modification patterns in tRNA show sequence specific variations (modified nucleosides are located at 61 different positions in tRNA), 5-methyluridine (m^5U) [1] and pseudouridine (Ψrd) are found at

---

[1] The nucleosides in tRNA are numbered 1-76, and the positions of modified nucleosides are identified as follows: Base methylations are indicated by the letter "m" preceding the atom position (superscript) and residue type and number . For example, m^5U54 denotes a base methylation at the 5 position of uridine 54 (m^5U is also referred to by the trivial name ribothymidine, or rT). Sugar methylations are indicated by an "m" following the residue type. For example, Gm18, denotes a ribose methylation at guanosine 18. Some modifications are referred to by their trivial names, such as pseudouridine (5-β-D-ribofuranosyluracil), abbreviated Ψrd.

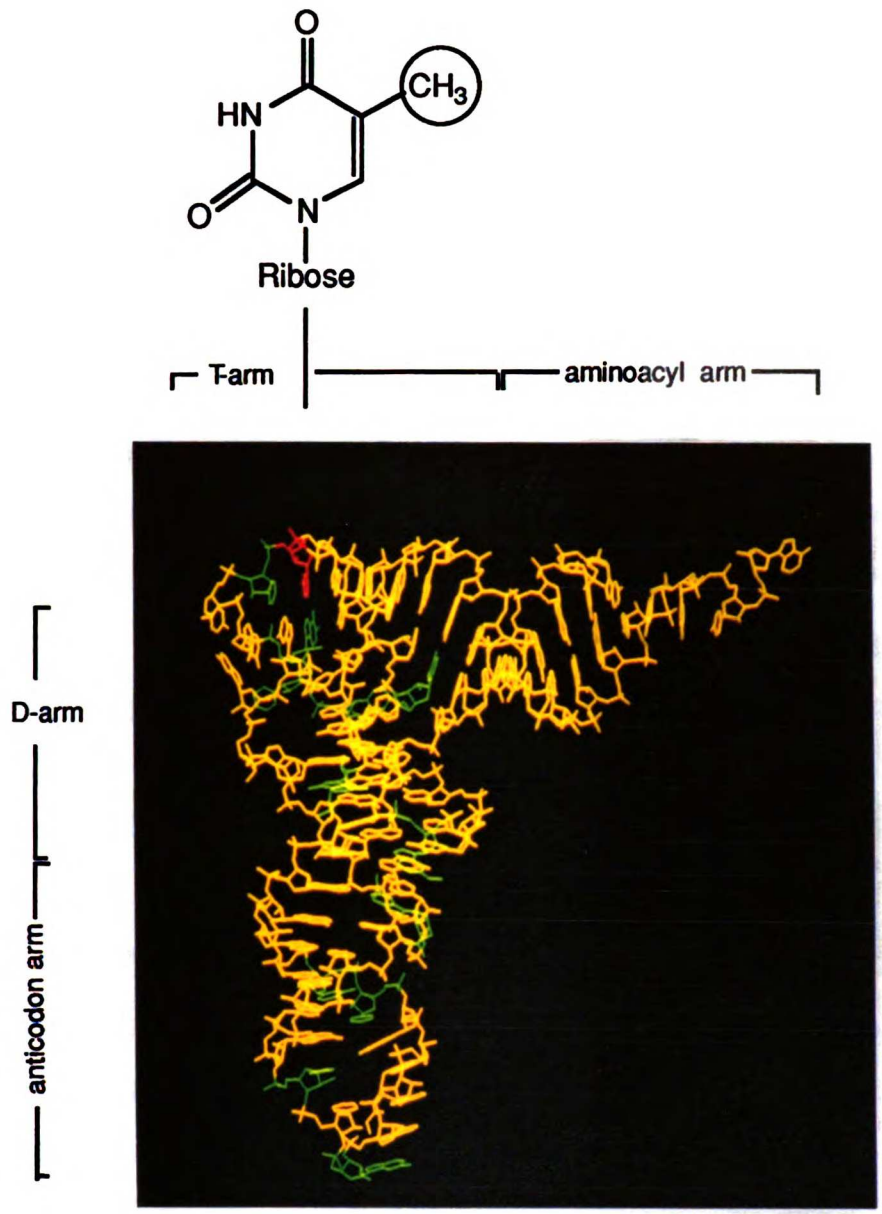

Figure 1.1. Modified Nucleosides in yeast $tRNA^{Phe}$. All minor or modified nucleosides are colored green, except m^5U, which is colored red. The structure and position of m^5U is shown .

Hypermodifications are denoted as described above. For example, mnm^5s^2U34, refers to 2-thio-5-carboxymethylaminomethyl uridine 34.

positions 54 and 55, respectively, in virtually all tRNAs. The invariance of these two modified bases is likely due to their key roles in maintaining the tertiary structure of tRNA (see below). Of all modification enzymes studied to date, *E. coli* tRNA (m^5U54)methyltransferase (RUMT, EC 2.1.1.35), the *trmA* gene product , is the most thoroughly characterized in terms of gene organization and regulation (Ny and Björk, 1977; Ny and Björk, 1980; Ny and Björk, 1980a; Gustafsson et al., 1991; Gustafsson and Warne, 1992; Persson et al., 1992; Gustafsson and Björk, 1993).

This dissertation focuses on the catalytic mechanism of RUMT, and the work described herein places our understanding of the enzymology of RUMT on par with that of the molecular biology of its gene, *trmA*. Table 1.1 provides a summary of RUMT's major properties, which are elaborated upon in the text that follows.

Catalytic Mechanism of RUMT

The catalytic mechanism of RUMT is comprised of both methyl transfer and substrate recognition: (1) RUMT employs covalent catalysis via Michael addition to facilitate the chemistry of transmethylation, (2) by binding the substrate tRNA in a manner that exposes the target atoms of U54 to the catalytic groups on the enzyme, RUMT utilizes binding energy to assist in catalysis.

Mechanism of Transmethylation of U54 in tRNA

RUMT exploits covalent catalysis via Michael addition to activate the 5-carbon of the target pyrimidine for the methyl transfer reaction [for a review see (Ivanetich and Santi, 1992)]. Thymidylate synthase (TS) serves as a mechanistic model for this class of enzymes (Santi and Danenberg, 1984; Matthews et al., 1990; Matthews et al., 1990a; Montfort et al., 1990) which also

Table 1.1

Properties of tRNA m^5U54 methyltransferase

PROPERTY	COMMENT
Reaction Catalyzed	Methyl transfer (U54 + AdoMet --> m^5U54 + AdoHcy)
Substrates	tRNA, T-arm [a], rRNA (in vitro) [b]
Cofactor	*S*-adenosylmethionine
k_{cat} ($tRNA^{Phe}$)	5.5 min^{-1} (15 °C)[a,c]
K_m ($tRNA^{Phe}$)	0.8 µM (15 °C)[a,c]
k_{cat}/K_m ($tRNA^{Phe}$)	10^5 M^{-1} s^{-1} [a,c]
K_d ($tRNA^{Phe}$)	80 nM [a,c]
K_m (AdoMet)	12 µM [d,e]
M_r	42 kD [d,e]
Isoelectric point (pI)	4.7 [d]
Gene, # a.a., MW	cloned /sequenced. 366 aa (42,112 g/m) [f]
Active form	monomer [g]
Sulfhydryl requirement	yes (contains active site cys) [h]
Association with RNA *in vivo*	50% of RUMT covalently bound to RNA *in vivo* (various tRNAs, and 16S rRNA[i])
Other Function	Methylating Activity *is not* essential for cell growth. Gene *is* essential for cell growth [j]. Possible second function.

[a] Gu and Santi, 1991
[b] Gu and Santi, 1994
[c] Gu and Santi, 1992
[d] Ny et al., 1988; [e] Greenberg and Dudock, 1980
[f] Gustafsson et al., 1991
[g] Kealey, J.T., unpublished observation
[h] Kealey and Santi, 1991
[i] Gustafsson and Björk, 1993
[j] Persson et al., 1992

includes dUMP and dCMP hydroxymethylases (Kunitani and Santi, 1980; Lee et al., 1988), and DNA (Cyt-5-)methyltransferases (Wu and Santi, 1987; Osterman et al., 1988). Michael addition to pyrimidines of RNA has been proposed to occur in complexes between the aminoacyl tRNA synthetases and tRNA (Starzyk et al., 1982), the R17 coat protein and bacteriophage R17 replicase gene (Romaniuk and Uhlenbeck, 1985), and a 55 kDa protein and RNA in the 5' noncoding region of poliovirus (Najita and Sarnow, 1990). Hence, in addition to catalyzing electrophilic substitution, the above examples suggest that Michael addition may play a more general role in protein-RNA interactions.

Based on the established mechanism of TS, and as shown in Scheme I, the reaction catalyzed by RUMT is believed to occur by Michael addition of a thiolate nucleophile of the enzyme to the 6-carbon of U54, followed by methyl transfer from AdoMet to the 5-carbon of U54, 5-proton abstraction, and finally, β-elimination of the enzyme to yield m^5U (**3a**). This mechanism is supported by the experimental observations that (1) RUMT catalyzes proton exchange between [5-^{3}H]-uridine-tRNA and solvent water in the absence of AdoMet (**2** to **2a** interconversion), and (2) RUMT is inactivated by the mechanism based inhibitor, 5-fluorouridine-tRNA (Scheme II)(Santi and Hardy, 1987).

Since 5-H exchange differs from methylation only in the nature of the electrophile-- a proton rather than an activated methyl-- it is an excellent model reaction. Santi and Brewer established chemical precedence for the enzyme catalyzed 5-hydrogen exchange reaction by showing that the rate of base catalyzed 5-H exchange from 1-substituted uracils was dependent on the nature of the 1-substituent (Santi and Brewer, 1973). Based on these data, they proposed a mechanism for exchange that involved intramolecular attack of the anion of the 1-substituent on C-6, producing a dihydrouridine intermediate (analogous to **2a**, Scheme I), followed by reversal of these steps.

When fluorine is substituted for hydrogen at the 5 position of uridine, RUMT forms an irreversible, covalent complex with FUtRNA in the presence of AdoMet. Because of the stability of the carbon-fluorine bond, the putative Michael adduct is trapped as the FUtRNA-CH_3-RUMT complex (**3**, Scheme II), and can be observed on SDS-PAGE (Figure 1.2). The observation of this inhibitory complex is further evidence for the mechanism proposed in schemes I and II. Moreover, as revealed in the chapters that follow, FUtRNA is a powerful tool for probing the RUMT mechanism.

SCHEME I

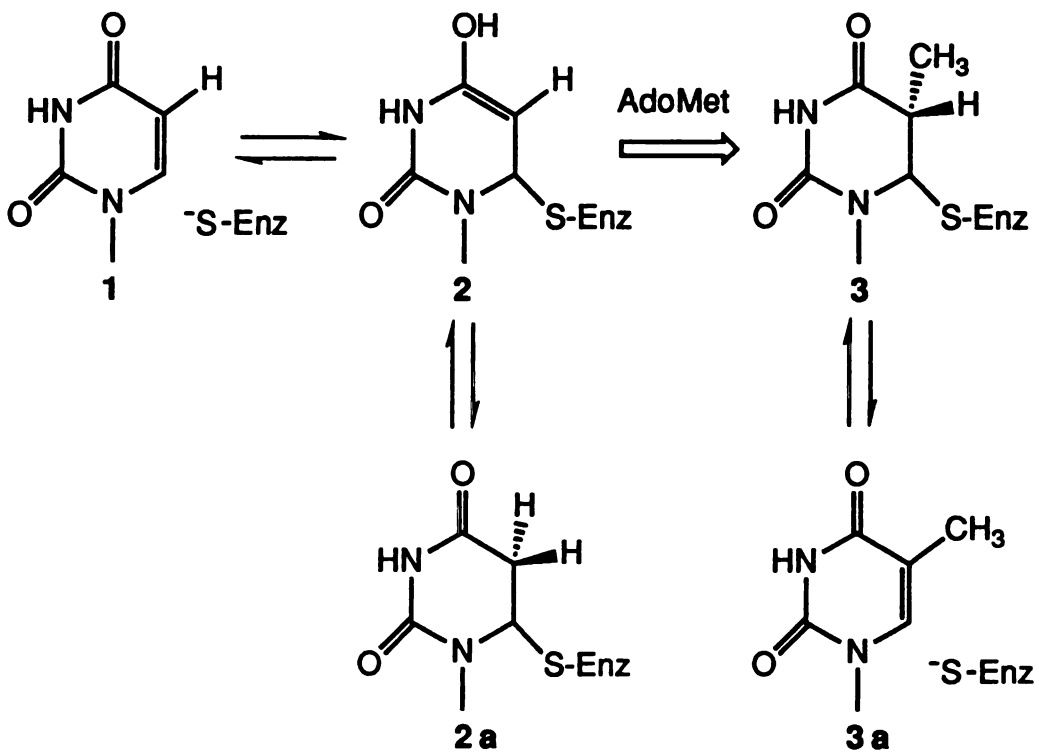

SHEME II

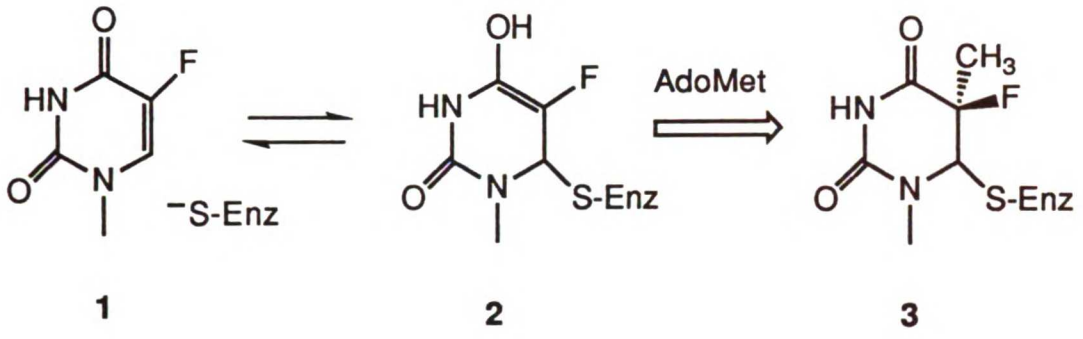

1 **2** **3**

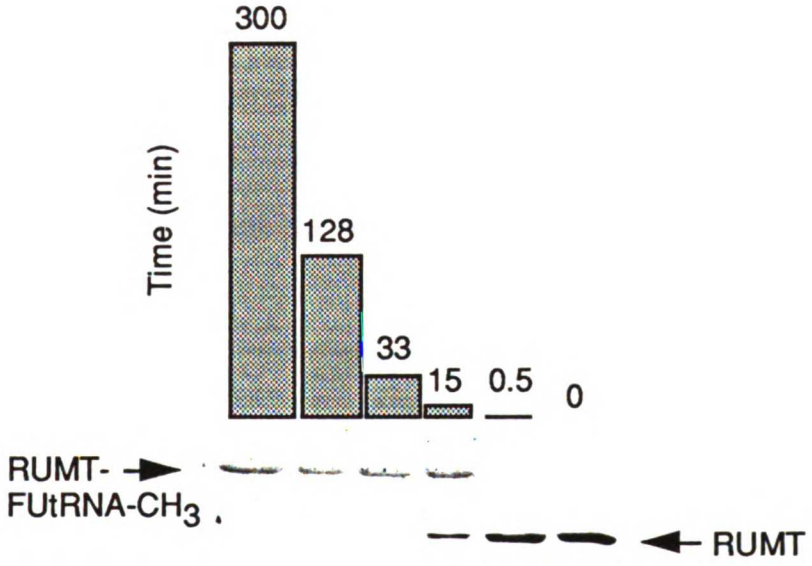

Figure 1.2. Band shift of RUMT on SDS-PAGE upon formation of the RUMT-FUtRNA-CH_3 complex. RUMT was incubated with excess FUtRNA and AdoMet for various lengths of time at room temperature, and aliquots were subjected to SDS-PAGE. RUMT was stained with coomassie R-250.

tRNA Recognition

Since RUMT methylates all tRNAs from *E. coli*, it must recognize common elements of tRNA primary, secondary or tertiary structure. The tRNA recognition problem faced by RUMT is thus similar to that of elongation factor TU (EF-Tu), which must also recognize common features of all tRNAs. The aminoacyl tRNA synthetases face the opposite dilemma, since they must distinguish cognate from structurally similar non-cognate tRNA molecules.

Yeast $tRNA^{Phe}$, whose 3-dimensional structure is shown in Figure 1.3 a,b (see also Figure 1.1), serves as a model substrate for RUMT. Like most tRNAs, its characteristic "L" shape is comprised of two perpendicular coaxial stacked A-type helices (Kim et al., 1973; Kim et al., 1974). Each helix consists of stem and loop structures: the aminoacyl stem: T-stem/loop, and the D-stem/loop: anticodon stem/loop. The vertex of the "L" is held together by tertiary interactions between T- and D-loop residues (Figure 1.3c). C56 forms a Watson-Crick base pair with G19 of the D-loop, and O_4 of Ψ55 forms H-bonds with N_1 and N_2 of G18. In addition, bases of the D-loop intercalate between those of the T-loop: the semi-conserved G57 stacks between G18 and G19 of the D-loop, and the invariant A58 stacks between G18 and C61. In the T-loop itself, m^5U54 stacks between the last 5' base of the T-stem, G53, and the second base of the loop, Ψ55. In addition m^5U54 participates in a reverse Hoogstein base pair with A58 across the loop. Base stacking of m^5U54 and the tertiary interaction across the loop effectively stabilize and extend the RNA helix into the loop, whence it is disrupted by a sharp turn (π-turn) of the phosphate backbone at residue 55. The π-turn is stabilized by (i) a hydrogen bond between the N_3 of Ψ55 (H-bond donor) and a phosphate oxygen from A58

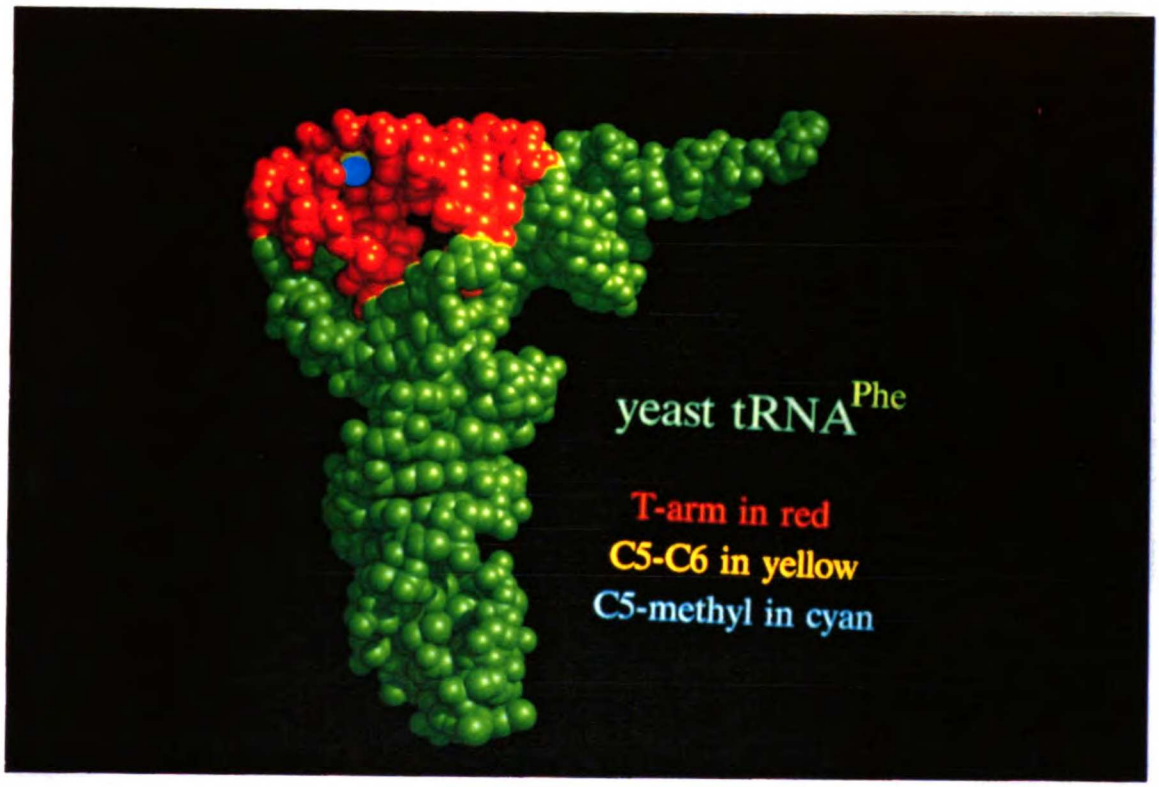

Figure 1.3a. Space filling model of yeast tRNA^{Phe}, showing the T-arm (red), C6, C5 (yellow) and the C5 methyl group (cyan).

(ii) the m^5U54- A58 reverse Hoogstein base pair, and (iii) a stacking interaction between Ψ55 and the G57 phosphate. The π-turn is an example of a conserved element of tertiary structure which might be exploited by RUMT for T-loop recognition. The T-loop is further stabilized by a hydrogen bond between N_4 of the invariant C61 and the phosphate oxygen of residue 60. In summary base stacking, base-base and base-backbone tertiary interactions collectively stabilize the highly structured T-loop.

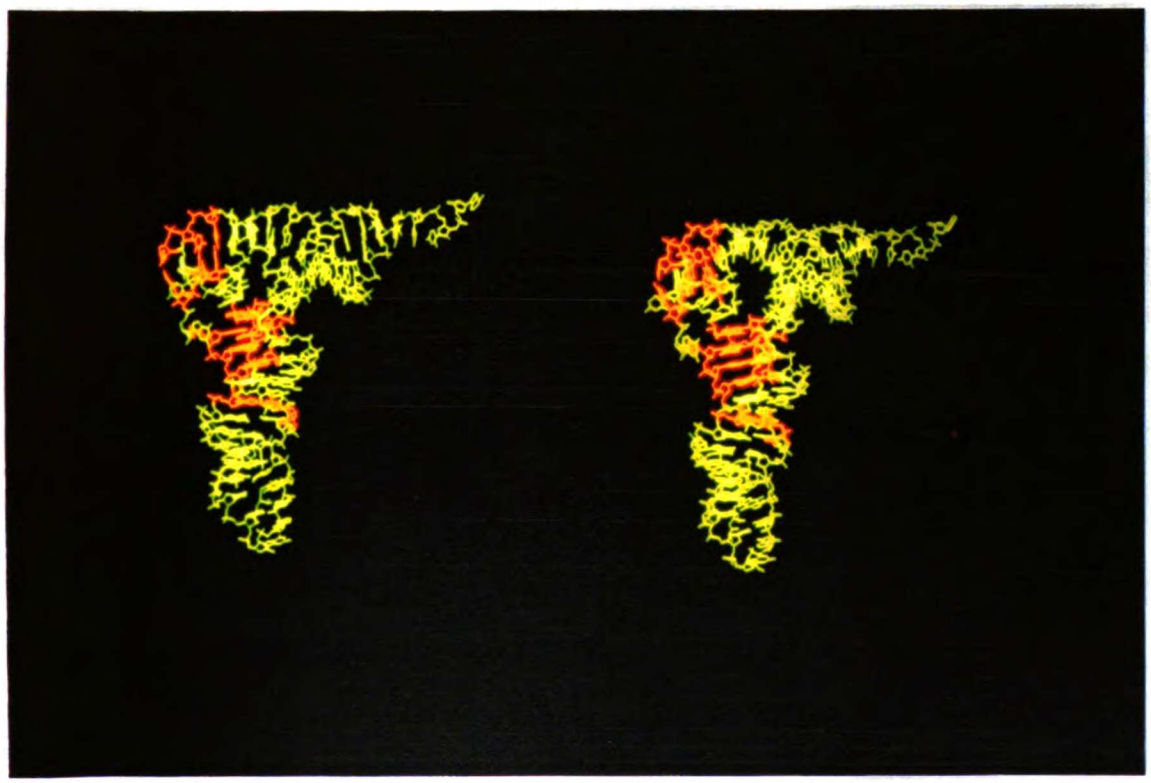

Figure 1.3b. "Cross-eye" stereo view of the tertiary Structure of yeast $tRNA^{Phe}$. Residues that participate in major tertiary interactions are shown in red.

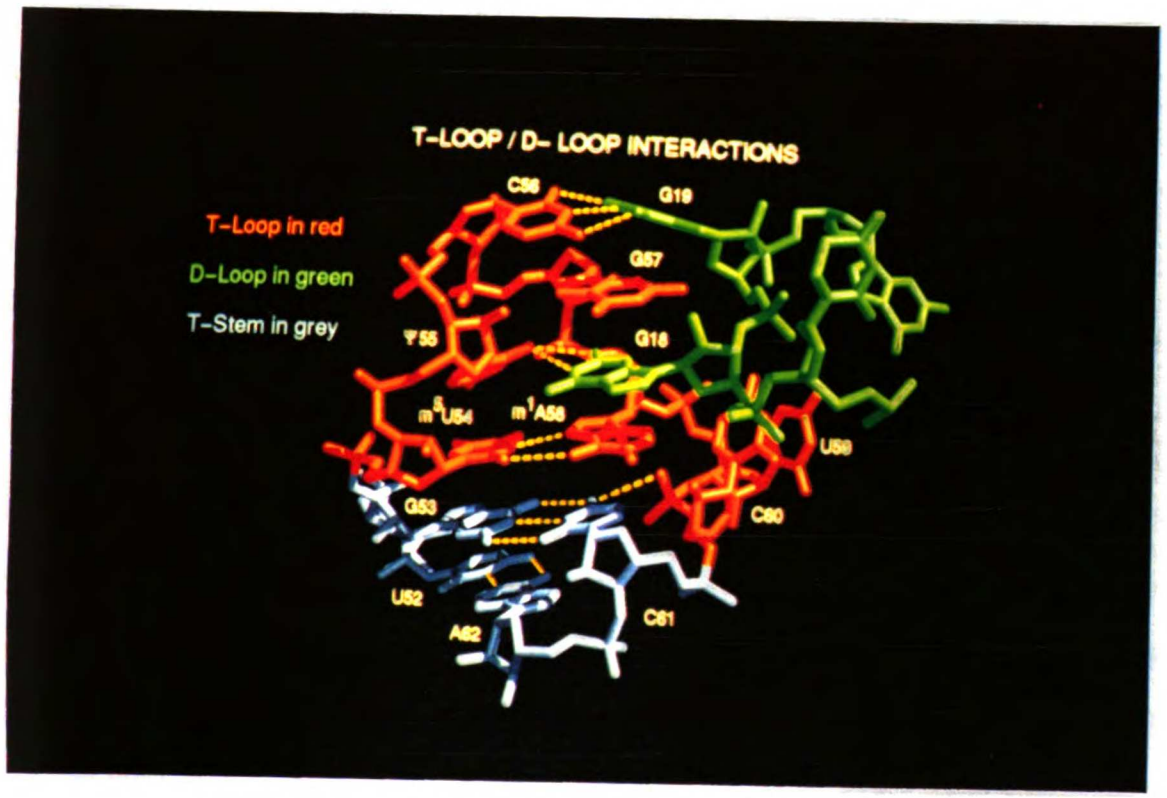

Figure 1.3c. T-loop/D-loop interactions. T-loop residues are red, T-stem residues are grey (shown is a 2 base-pair stem), and D-loop residues are green.

The T-arm of tRNA is a Substrate for RUMT

Recently, Gu and Santi showed that the 17 nucleotide T-arm of tRNA is an excellent substrate for RUMT, displaying only a 3-fold reduction in k_{cat} and a 6-fold increase in K_m compared to unmodified tRNA (Gu and Santi, 1991). This suggests that most of the discrimination elements for the RUMT-tRNA interaction are contained within the T-loop. By comparing over 40 tRNA sequences from *E.coli*, Gu and Santi (1991) deduced a consensus sequence for T-arm methylation (Figure 1.4a), which not surprisingly, consists of predominantly invariant bases. The consensus sequence was tested by mutagenizing individual loop residues, which resulted in a more "broad" consensus (Figure 1.4b). As shown in Figure 1.4b, most of the active T-loop mutants bind RUMT well, as evidenced by their similar relative K_ds (second number in parenthesis), but they differ significantly in their initial rates of methylation (first number in parenthesis). Positions that are hypersensitive to mutation include U55 (A is the only allowable substitution), C56 (only A is allowed), and A58 (G is the only permittable substitution, with substantial loss in activity). Interestingly, A appears to be a rather neutral mutation, since it is allowed at every loop position (except, of course, 54). This might reflect the ability of A to display H-bond donor/acceptor patterns similar to those of both U and C. In general, the mutagenesis data confirm that the the evolutionarily-derived consensus sequence, but also suggest that the consensus is fairly broad.

Although the T-arm mutations represent non-conservative changes that may disrupt RNA structure as well as hydrogen bond donor/acceptor patterns, they have, nevertheless, implicated residues that are crucial for RNA recognition and catalysis. The next step is to make more specific changes at A58, U55, and C56 in an attempt to delineate the role of individual atoms in the

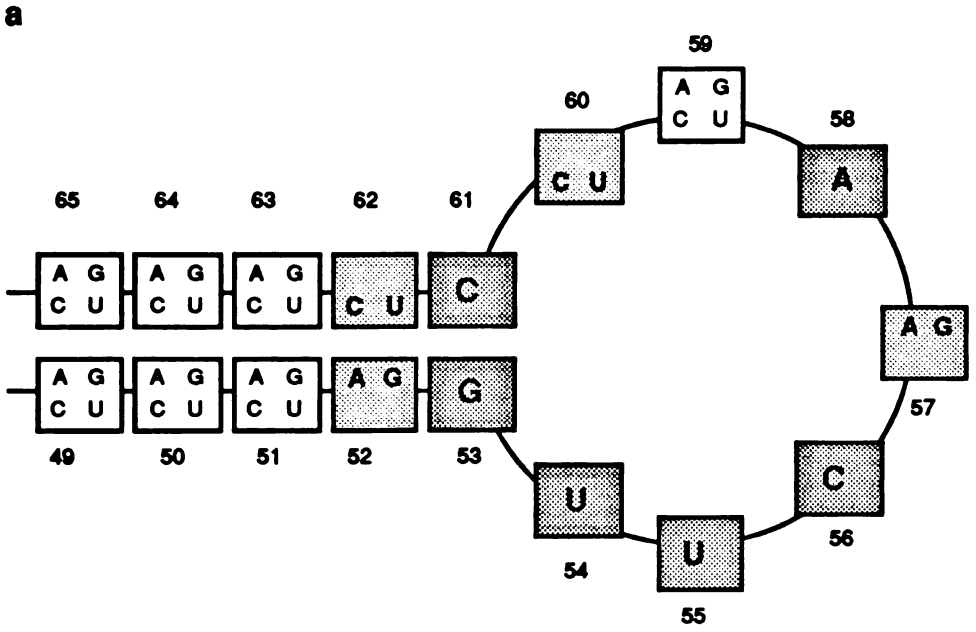

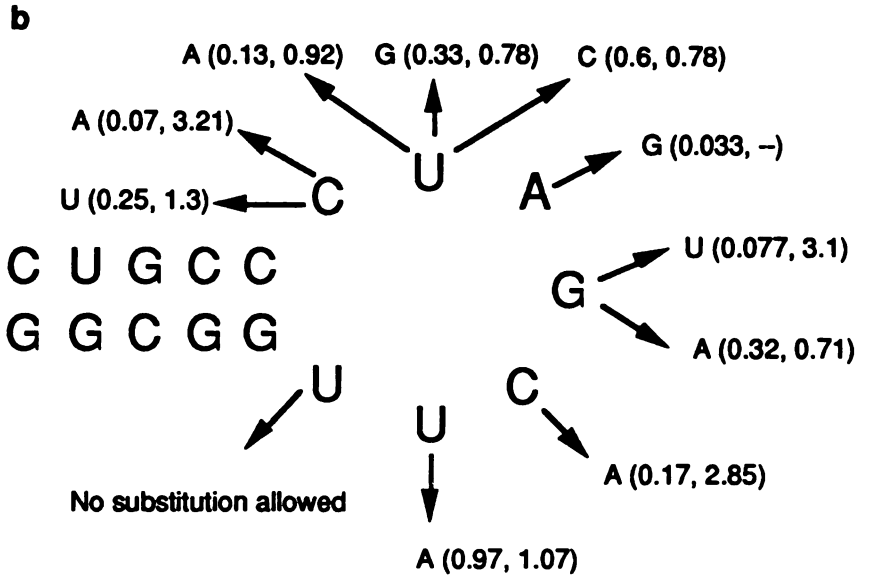

Figure 1.4 (a) Consensus sequence of the T-arm derived from the sequences of *E. coli* tRNAs. Dark shade indicates complete conservation of base, light shade indicates conservation of Py or Pu, and unshaded indicates non-conserved positions. Within each box is shown acceptable bases or base parirs (b) Mutangenesis of the T-loop. Each nucleotide was changed to each of the other 3 nucleotides, such that 4 different RNAs (including wt) were obtained for each varied position. Shown are acceptable nucleotide substitutions at each position. A mutant T-arm is considered inactive (and its nucleotide substitution unacceptable) if its activity is less than about 1 % of wt. The first number in parenthesis following the nucleotide change is the initial rate of methylation, normalized to the wt rate, and the second number is the K_d for RUMT-RNA binary complex formation, normalized to wt (unpublished data from Gu, X. and D.V. Santi).

RUMT-RNA interaction. For example, one could assess the role of N_7 of A58 by preparing a T-arm containing 7-deazaguanosine at that position. This represents an extremely conservative change aimed at assessing the role of one hydrogen bond acceptor.

A study on the effect of free T-arm loop size on binding and methylation indicated that a loop of seven nucleotides is essential for substrate recognition and catalysis (X. R. Gu, unpublished). The strict loop size requirement is surprising considering that the structure of the free T-loop probably differs significantly from that in tRNA. For example, in tRNA, the T-loop actually consists of 8 residues, due to intercalation of G18 from the D-loop between residues A58 and G57 (see Figure 1.3c). Indeed, the fact that the free T-arm is such a good substrate suggests that the ground state tRNA structure (i.e. crystal structure) differs significantly from the RNA structure recognized by RUMT.

The Catalytic Mechanism Involves Conformational Changes of the RNA Substrate

The chemical mechanism outlined in Scheme I and detailed in Chapter 7 imposes stereochemical and stereoelectronic constraints on intermediates and high energy species along the reaction pathway: the reaction requires precise positioning of the catalytic nucleophile and the methyl electrophile with respect to C6 and C5 of U54. In the T-loop, however, C6 of U54 is completetly solvent inaccessible, and C5 is 95% buried. This is dramatically illustrated in Figure 1.5, where it is clear that C6 and C5 are not accessible to RUMT. This poses an intriguing mechanistic problem: how does RUMT negotiate RNA structure to gain access to C6 and C5? As we have already suggested (Kealey et al., 1991; see also chapters 2, 3, and 5), it appears certain that RUMT must dramatically

disrupt the RNA structure in the vicinity of U54 to access target atoms and to catalyze methylation. Insight into this aspect of the RUMT mechanism will be greatly facilitated by an X-ray structure of the RUMT-FUtRNA-CH_3 complex, and

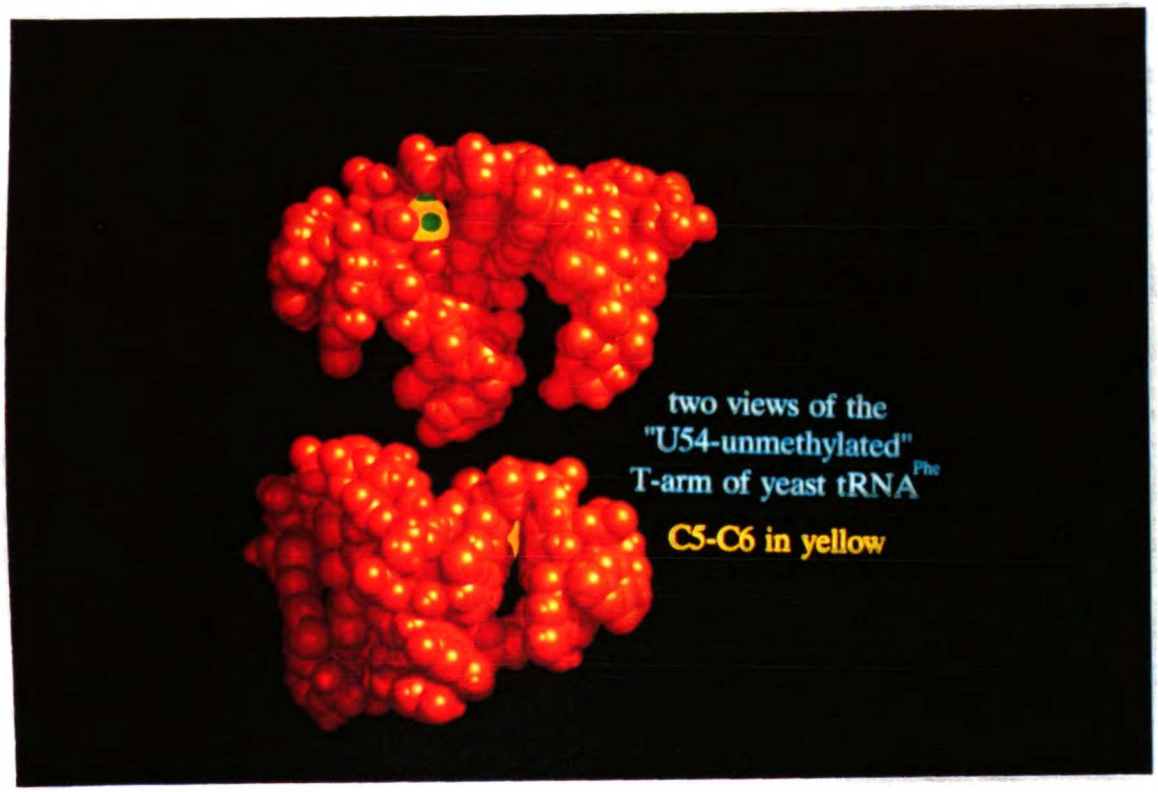

Figure 1.5. Space filling model of two views of the T-arm of yeast tRNA^{Phe}. The methyl group has been deleted so that C5 (yellow) and C6 (yellow) are more visible. The two views are related by a 180° rotation about the z-axis. As is apparent from the rendering, C5 and C6 are quite inaccessible from both the "front" and "back" of the loop.

crystallization trials are in progress. In the meantime, we consulted mechanistically similar enzymes (whose X-ray structures are known) for insight into RUMT-tRNA interactions during catalysis. In terms of substrate recognition, the wealth of structural information available on TS-substrate complexes

provides few clues into the RUMT mechanism, since TS interacts with a mononucleotide, where target atoms are completely accessible. A co-crystal structure of a *Hha* I methylase-5FdCyd)DNA complex has recently been reported (Klimasauskas et al., 1994) and may, by analogy, shed light on the RUMT-tRNA interaction. Remarkably, in the *Hha* I -(5FdCyd)DNA structure, the target cytidine has been "flipped out" of the DNA double helix, allowing the enzyme access to the C6-C5 double bond from above and below the plane of the pyrimidine ring. It thus appears likely that for RUMT to gain access to the C6-C5 double bond, RUMT must "pull" U54 out of the G53/U55 stack and break the U54-A58 reverse Hoogstein hydrogen bond (see Figure 1.3c). A detailed understanding of how the enzyme accomplishes this will not only illuminate the RUMT mechanism, but will also yield valuable information concerning the more general problem of protein-RNA recognition.

Kinetics of Binary Complex Formation

The current kinetic scheme for RUMT catalyzed transmethylation is shown in Figure 1.6. The first step, characterized by k_1, is a rapid association of tRNA and RUMT, and occurs at a rate approaching the diffusion controlled encounter frequency of RUMT and tRNA (J. Newell and D. Santi, unpublished). Following the initial encounter complex, a slow step occurs (k_2), which yields non-covalent and transiently covalent complexes that can be trapped on nitrocellulose filters. This step (or composite of steps) probably involves conformational changes of both RNA and RUMT that occur prior to the chemical

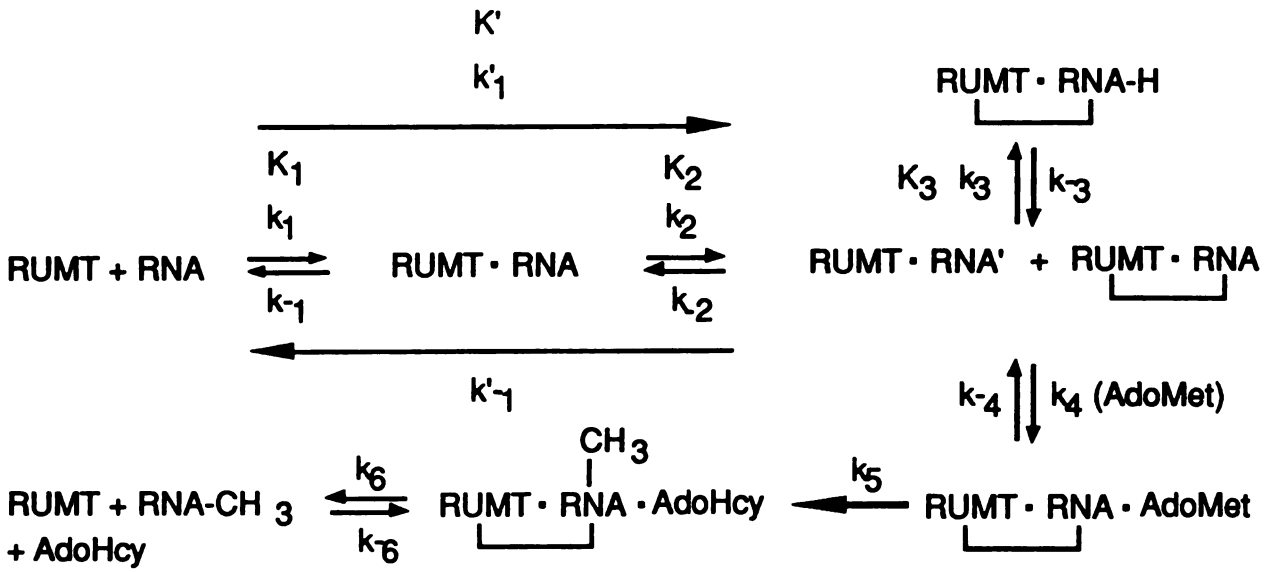

Figure 1.6. Kinetic model for RUMT-catalyzed methylation of tRNA showing conformational changes and formation of covalent adducts. See Scheme I for structures of covalent complexes.

step, k5. Most of the rate constants indicated in Figure 1.6 have been measured, calculated or esitmated, and their values are listed in Table 1.2.

The dihydrouridine species, which is the obligatory intermediate in the 5-H exchange reaction, is obtained by tautomerization of the enol intermediate, via k_3 (see also Scheme 1). Interestingly, this intermediate is not catalytically competent for methylation, since k_3 is less than k_{cat}, and k_{cat} places a *lower* limit on any first-order rate constant on the forward reaction pathway (Fersht, 1985). The dihydrouridine intermediate is, however, chemically competent for methylation, since it was shown by a pulse-chase experiment that tRNA does not dissociate from the enzyme (via k_{-2} and k_{-1}) prior to methylation (via k_4 and k_5)(Gu and Santi, 1992). In *E. coli* up to 50% of RUMT is covalently bound to various species of RNA, including several tRNAs and the 3' end of 16S rRNA (Ny et al., 1988; Gu and Santi, 1990; Gustafsson and Björk, 1993). It is likely that

Table 1.2

Kinetic and Equilibrium Constants for RUMT-tRNA Binary Complex Formation

Constant	Value	Reference or method of calculation
k_1	1E8 $M^{-1}s^{-1}$	J. Newell and D.V Santi (unpublished)
k_{-1}	45.9 s^{-1}	from $k_{-1} = k_1 \times k_2 \times K'/ k_{-2}$
k_2	0.03 s^{-1}	assuming $k_2 = k_{cat}$
k_{-2}	3.2 E^{-3} s^{-1}	$k_{-2} \approx k_{-1}'$
k'_1	6.6E4 $M^{-1}s^{-1}$	k_1 from Gu and Santi, 1992
k'_{-1}	3.2E^{-3} s^{-1}	k_{-1} from Gu and Santi, 1992
k_3	2.5 E^{-4} s^{-1}	k_2 from Gu and Santi, 1992
k_{-3}	4.3E^{-4} s^{-1}	k_{-2} from Gu and Santi, 1992
K_1	4.59E^{-7} M	$K_1 = k_{-1}/k_1$
K_2	0.106	$K_2 = K'/K_1$
K'	4.90E^{-8} M	K_1 from Gu and Santi, 1992
K_3	1.2	K_2 from Gu and Santi, 1992
k_{cat}	3.0E^{-2} s^{-1}	from Gu and Santi, 1992
K_m	3.10 E^{-7} M	from Gu and Santi, 1992
k_{cat}/K_m	9.7 E4 $M^{-1}s^{-1}$	from Gu and Santi, 1992

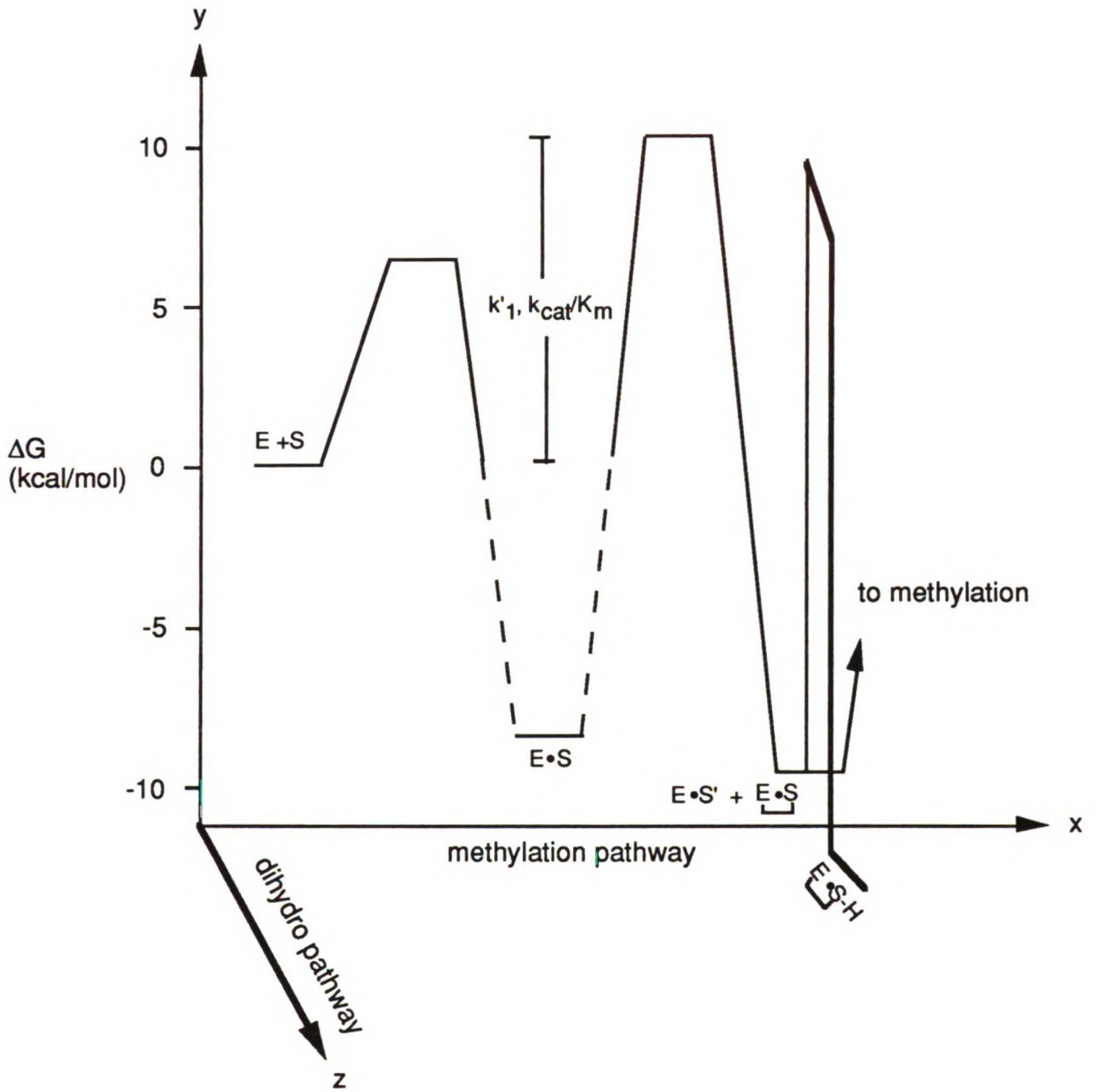

Figure 1.7. Free energy diagram for the RUMT-tRNA interaction.

these complexes exist as dihydrouridine intermediates, similar or identical to **2a** in Scheme I. It has been suggested that these covalent binary adducts may serve as reservoirs of RUMT-tRNA complexes primed for methylation, or in

unknown roles with RNAs other than tRNA (Gu and Santi, 1992).The rate and equilibrium constants listed in Table 2 have been used to generate a free energy profile for RUMT-yeast $tRNA^{Phe}$ binary complex formation (see Figure 1.7). This profile was constructed using two experimentally determined rate constants, k_1 and k'_1, and the equilibrium constant, K'. Unfortunately, K_1 has not yet been determined experimentally, so it was not possible to calculate k_2. However, if k_2 is arbitrarily set equal to k_{cat}, which is the lowest value that it could possibly have, then the diagram can be completed (the dashed lines indicate that K_1 is uncertain). The free energy profile is represented in three dimensions to illustrate that the dihydrouridine intermediate is not on the reaction pathway leading to methylation. The free energy diagram will be refined and updated, as missing microscopic rate constants are determined.

The specificity constant, k_{cat}/K_m, measures the slowest bimolecular rate constant in an enzymatic reaction (Fersht, 1985). It is noteworthy that k_{cat}/K_m is almost identical to k'_1, the bimolecular rate constant for the conversion of RUMT and RNA to nitrocellulose isolable non-covalent and transient covalent complexes (Gu and Santi, 1992; see also Table 1.2). This suggests that the lowest bimolecular rate constant in the reaction reflects a binding interaction between tRNA and RUMT. As mentioned above, RUMT must significantly disrupt RNA structure to gain access to the target atoms of U54. The relatively low value of k'_1 (and k_{cat}/K_m) probably reflects conformational changes in both RNA and RUMT, prior to methylation.

The idea that RNA structure is perturbed by RUMT prior to methylation is further substantiated by recent kinetic work on D-arm mutants of tRNA. As noted above, the T- and D-loops of tRNA are held together by tertiary interactions between G18 and Ψ55, and G19 and C56 (see Figure 1.3c). By preparing tRNA mutants that cannot form T-loop/D-loop tertiary interactions, it was possible to

ascertain whether these tertiary interactions affect the tRNA-RUMT interaction. In the G19C mutant, the G19-C56 Watson-Crick tertiary base pair cannot form and in the G18A mutant, the G18-Ψ55 H-bond interaction is abolished. As shown in Figure 1.8, for both mutants, k'_1 is significantly increased relative to wild type tRNA. This suggests that the steps described by k'_1 reflect disruption of tertiary contacts between the T- and D-loops. Apparently, these interactions preclude access to U54 by RUMT, and therefore must be disrupted prior to methylation.

The inverse dependence of k'_1 on the degree of hydrogen bonding between T- and D-loops suggests that the T-loop itself should have a higher k'_1 than both wt tRNA and D-loop mutants. As shown in Figure 1.8, this is clearly not the case. The discrepancy could be explained by a change in the rate limiting step when the substrate is changed from tRNA to the T-arm. It is possible that the interaction between RUMT and the T-arm, described by k_1, does not occur at the diffusion controlled limit, and that k_1 for the T-arm is actually less than k'_1 for tRNA. Although the T-loop is the main discrimination element in tRNA, there is a high probability that RUMT makes additional contacts with other parts of tRNA. Multiple RUMT-tRNA contact sites may help to insure that each encounter is productive (i.e. leads to complex formation). In the T-arm, which is presumably lacking important RUMT contact sites, there is a greater probability that each encounter will <u>not</u> be productive, which is reflected in a lower k_1, relative to tRNA. This idea could be tested by measuring k_1 for the T-arm-RUMT interaction. Unfortunately, k_1 cannot be determined by fluorescent quenching techniques (as was done with tRNA), because, unlike tRNA, the T-arm does not quench intrinsic RUMT fluorescence (J. Newell, personal communication). Indeed, this fact alone suggests differences in binding interactions between tRNA and free T-arm. Of course, it is also conceivable that

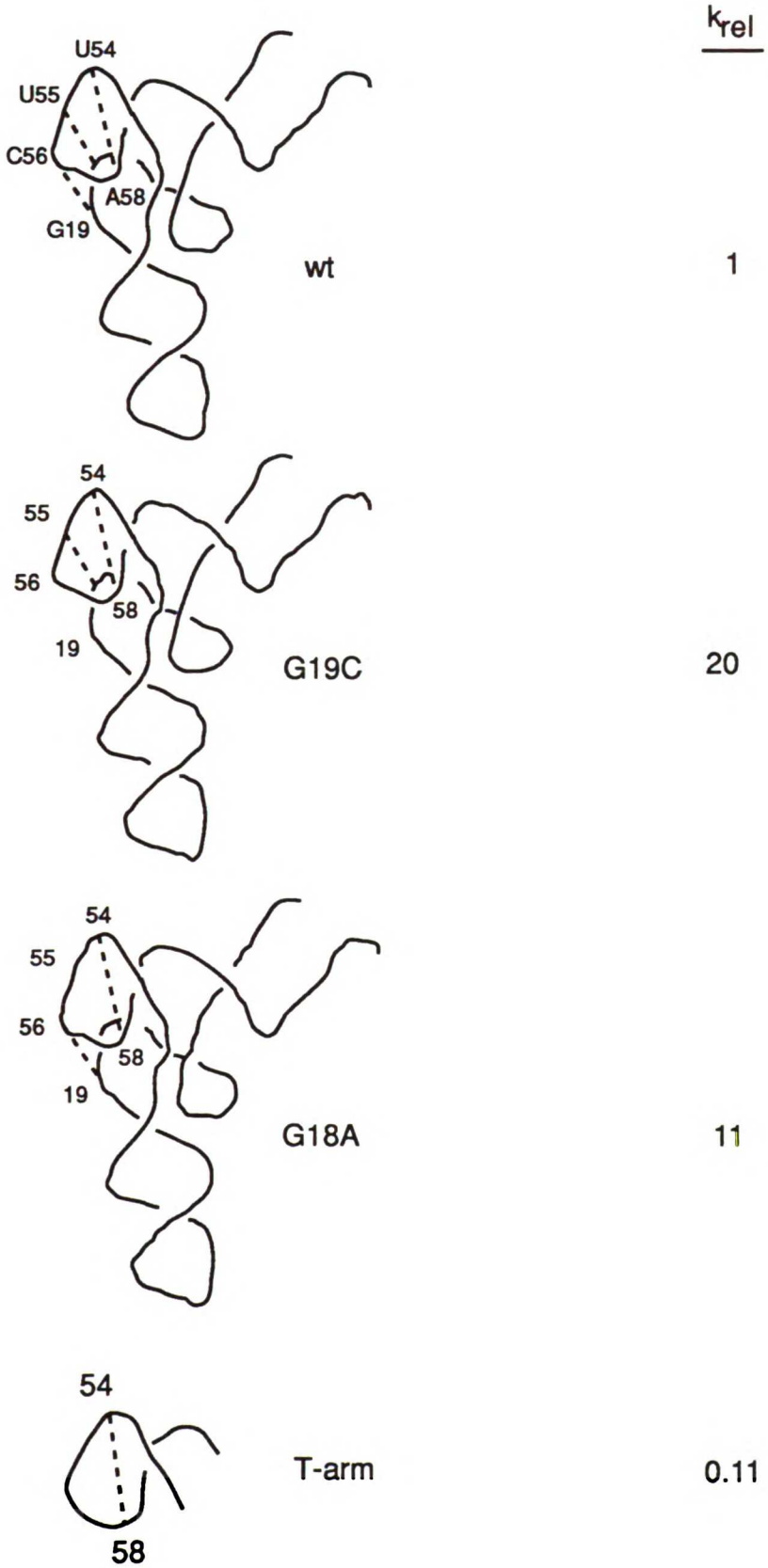

Figure 1.8 Activity of T-arm mutants. k_{rel} is the ratio of the second order rate constant (k'_1) of the mutant relative to wild type.

when removed from the context of tRNA, only a small fraction of the free T-arm exists in a state that is competent for binding RUMT. This is an equally valid explanation for the low k_{rel} (ratio of mutant k'_1 to wt k'_1, see Figure 1.8) for T-arm.

The History of *trmA* (RUMT gene) and Biological Significance of m^5U54

History and Structure of trmA

The *trmA* gene was identified in the early 1970s by chemical mutagenesis of *E. coli*, and screening for mutants that contained undermethylated tRNA, which could be subsequently methylated by a crude *E. coli* enzyme preparation (Björk and Isaksson, 1970). A second level of screening led to the isolation of a strain of *E. coli* that lacked m^5U54 in its tRNA, and was thus deficient in the tRNA m^5U54 methylating activity. Genetic mapping localized the *trmA* gene to minute 89 on the *E. coli* (K12) chromosome. (Björk, 1975; See Figure 1.9). The *trmA* gene was cloned (Ny and Björk, 1980), and more recently, the *trmA* gene and 5' and 3' untranslated regions were sequenced (Gustafsson et al., 1991), which revealed that *trmA* is monocistronic, which is unique among genes coding for tRNA modifying enzymes (they are typically located within multigene operons), and *trmA* contains a promoter sequence homologous to the rRNA P1 promoters, which appears to be unique among protein encoded genes and could be related to stringent control and growth dependent regulation of RUMT mRNA (Ny and Björk, 1977; Ny and Björk, 1980a).

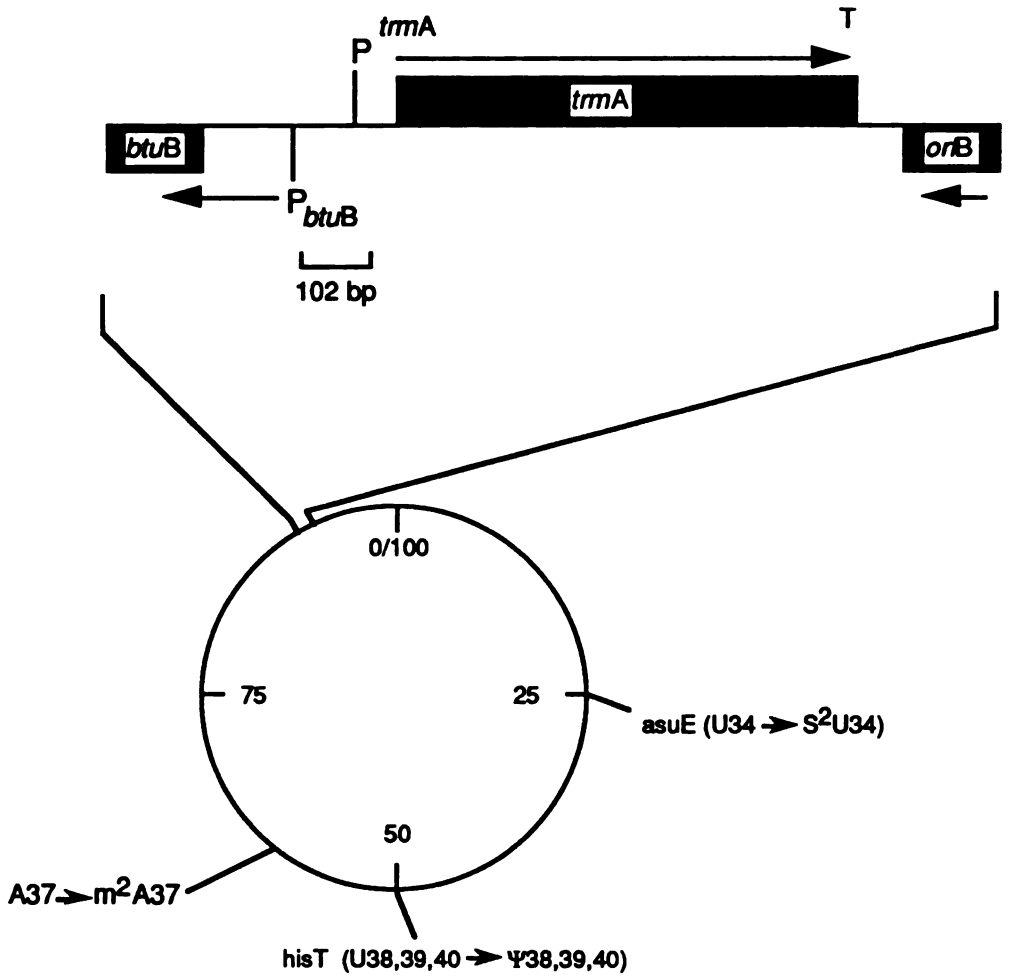

Figure 1.9. Circular map of the *E. coli* chromosome showing the monocistronic *trm*A operon. For reference, several other tRNA modification genes are also shown. P denotes promoters, and T denotes a transcriptional terminator. Note that the *Btu*B (receptor for vitamin B_{12}) gene is divergently transcribed from an initiating position 102 bp 5' of +1 of the *trmA* transcript. There is probably insufficient room for two polymerase molecules to simultaneously bind the *trm*A and *btu*B promoters. There is an open reading frame immediately down stream of *trmA*, which is transcribed in the opposite direction. [Adapted from (Gustafsson, 1992)].

Biological Significance of m^5U54 in tRNA

m^5U54 is one of the most common base modifications in prokaryotic and eukaryotic tRNAs. It is present in all *E. coli* tRNAs and most eubacterial and eukaryotic tRNAs, with a few exceptions (Steinberg et al., 1993). In archeabacteria, $m^1\Psi$ replaces m^5U at position 54 (Pang et al., 1982); however, the U54 and $\Psi54$ methyl groups occupy the same spacial location (i.e. they are isosteric), which suggests an evolutionary convergence and underscores the significance of the U54 methyl group in tRNA structure and function. Considering the ubiquity of m^5U54 in tRNA, it is surprising that a non-conditional *E. coli* mutant (*trmA*5), which completely lacks m^5U in its tRNA, is fully viable, displaying only a marginal (4%) reduction in growth rate (Björk et al., 1987, p281). Moreover, a yeast mutant which lacks the m^5U54-methyltransferase activity is also viable (Hopper et al., 1982), and *Mycobacterium smegmatis* tRNA completely lack m^5U54 (Vani et al., 1979). The m^5U54 activity is thus non-essential, suggesting that the biological role of m^5U54 in tRNA is subtle. In mixed cultures wild type *E. coli* outgrows the *trmA*$^-$ strain, which demonstrates that, although non-essential, tRNA containing m^5U54 is selectively advantageous (Björk and Neidhardt, 1975). A recent study by Persson et al. showed that, although the tRNA-methylating activity is not essential for *E. coli* growth, the *trmA* gene is (Persson et al., 1992). This implies that RUMT performs a second function *in vivo* which is essential for cell growth. There are now several documented cases of multifunctional enzymes in tRNA modification and RNA metabolism: the *nuvC* gene product is involved in the synthesis of s^4U8 in tRNA and in the synthesis of thiamine (Ryals et al., 1982); the *trmC* gene product catalyzes the reactions $cmnm^5s^2U$ --> nm^5s^2U and nm^5s^2U => mnm^5s^2U at position 37 of some tRNAs (Hagervall et al., 1987); the iron-response element binding protein regulates expression of the transferrin

receptor and ferritin in response to iron, and has aconitase activity (Kaptain et al., 1991); the nuclear encoded mitochondrial tyrosyl-tRNA synthetases from *Neurospora crassa* and *Podospora anserina* and leucyl-tRNA synthetase from yeast function in RNA splicing (Kamper et al., 1992; Akins and Lambowitz, 1987) [for a review see (Lambowitz and Perlman, 1990)]; glyceraldehyde -3-phosphate dehydrogenase facilitates tRNA export from the nucleus (Singh and Green, 1993). If multifunctionality in tRNA modification enzymes proves to be a general phenomenon, this may explain why so much genetic information is dedicated to the synthesis of enzymes that perform selectively advantageous, but presumably non-essential functions.

Although tRNA lacking m^5U has been available for *in vitro* studies for over twenty years, the functional role of m^5U in tRNA remains elusive. In the mid 1970's evidence was presented that the conserved TΨCG sequence within TΨC-loop of tRNA (see Figure 1.3) interacts directly with the ribosome (Sprinzl et al., 1976), stimulating studies on the role of m^5U in translation. Kersten et al. investigated the role of m^5U in aminoacylation, EF-Tu binding, A and P site binding, and translocation (Kersten et al., 1981). According to their study, lack of m^5U in *E. coli* $tRNA^{Phe}$ and $tRNA^{Lys}$ had no effect on aminoacylation or EFTu-GTP binding, but increased the missence error frequency (as determined by misincorporation of Leu for Phe) of polyU directed poly Phe synthesis by a factor of 10, and increased the rate of polyA directed poly Lys synthesis. The rate of polyU directed poly Phe synthesis was identical for $tRNA^{Phe}$ containing or lacking m^5U. The authors suggested that the increased rate of poly Lys synthesis with $tRNA^{Lys}$ lacking m^5U was due to reduced A site binding and an increased rate of translocation. The authors further speculated that reduced A site binding may decrease the time needed for proof reading, thereby leading to an increase in translational errors. In a recent study, Harrington et al. assessed

the difference between fully modified and unmodified $tRNA^{Phe}$ (Harrington et al., 1993), using an *in vitro* translation system that enabled the measurement of equilibrium and rate constants for EF-Tu•GTP•phe-tRNA binding to the ribosome, GTP hydrolysis, peptide bond formation, or release of the tRNA from the ribosome without peptide bond formation (proofreading). These workers found that tRNA modifications increased the accuracy of translation 8.6-fold by decreasing the rate of dipeptide synthesis (thus allowing a longer time to reject the non-cognate codon) and by increasing the rate of rejection of non-cognate codons. An 8.6-fold increase in misincorporation would yield one error per 116 amino acids, compared to the wild type misincorporation rate of 1 error per 1000 amino acids. Hence, tRNA modifications appear to be crucial for translational accuracy. It is noteworthy that the results of the studies on completely unmodified tRNA are consistent with the earlier work of Kersten et al. on m^5U54 deficient tRNA.

The role of m^5U54 in eukaryotic tRNAs has also been studied (Marcu and Dudock, 1976; Roe and Tsen, 1977). In wheat germ, all glycine and several threonine tRNAs, and one tyrosine tRNA contain an unmodified U54, which can be methylated by a crude preparation of *E. coli* RUMT (Marcu and Dudock, 1976). Marcu and Dudock found that incorporation of [^{3}H]Gly into a polypeptide in an *in vitro* translation system was markedly slowed when the $tRNA^{Gly}$ was methylated by RUMT *in vitro*; however, the inhibitory effect could be overcome by addition of spermine. The authors speculated that the levels of m^5U54-tRNA and spermine might vary in cells and serve to regulate the kinetics of protein synthesis. In some tRNAs from mammalian tissues U54 has been only partially converted to m^5U54. Again, these tRNAs can be quantitatively methylated *in vitro* with a crude preparation of *E. coli* RUMT. Roe and Tsen found that increasing the m^5U54 content of $tRNA^{Phe}$ in this class of partially methylated

tRNAs caused an *increase* in the apparent rate (V_{max}) of protein synthesis (Roe and Tsen, 1977). Although these data appear in conflict with those of Marcu and Dudock (1976), the data do corroborate the idea that m^5U54 might be involved in the regulation of eukaryotic protein synthesis at the level of translation.

To fully understand the role of m^5U54 in tRNA, it is necessary to determine how the C5 methyl moiety affects RNA structure, and how this, in turn, is manifested in biological function. Davanloo et al. found that tRNA containing m^5U54 exhibited a 6 °C higher melting temperature than tRNA lacking m^5U54, suggesting that the C5 methylation stabilizes tRNA structure (Davanloo et al., 1979). I have observed that the methylated T-arm migrates faster on semi-denaturing polyacylamide gels than the unmethylated T-arm, and that the melting temperature (stem to coil transition) for the methylated T-arm is about 2 degrees below that of the unmethylated counterpart. Thus, the methyl group clearly influences RNA structure, and the affect appears to depend on whether the T-arm is free, or in the context of tRNA. Just how the methyl group contributes to RNA stability (or apparent lack thereof) is not known, however. Is the structural effect confined to the T-loop or propagated to distal parts of the tRNA, such as the anticodon? In support of the latter idea is the observation that an anticodon-anticodon interaction in the yeast $tRNA^{Asp}$ crystal lattice results in disruption of the G19-C56 base pair (Moras et al., 1986). It is tempting to speculate that the C5 methyl group at U54 might serve to modulate RNA-RNA or RNA-protein interactions on the ribosome during translation, thereby affecting the accuracy of protein synthesis.

RUMT and Cancer Chemotherapy

It is commonly believed that the cytotoxic action of the anticancer drug, 5-fluorouracil (5FU), is due to its metabolic conversion to 5-fluoro-2'-deoxyuridine

5'- monophosphate (FdUMP), and subsequent inhibition of thymidylate synthase (Cohen, 1958; Heidelberger et al., 1983). Since the TS reaction represents the sole *de novo* pathway for the production of thymidylate, inhibition of TS reduces thymidylate pools and halts DNA synthesis, thus leading to cytotoxicity. Since 5FU is incorporated into RNA (Heidelberger et al., 1983), enzymes that catalyze reactions similar to that of TS, but with RNA substrates, might also be inhibited by 5FU metabolites (see scheme II). Indeed, it has been shown that tRNA uracil-5-methyltransferase from mouse liver and mouse mammary tumor is significantly inhibited following 5FU treatment (Tseng et al., 1978). This indicates that the cytotoxic effects (or possible side effects) of 5FU may involve inhibition of enzymes that modify RNA, and/or disruption of important protein-RNA contacts in large RNA-protein complexes, such as ribosomes and small nuclear spiceosomes. This is supported by the observation that thymidine cannot reverse the effects of 5FU in some prokaryotic and eukaryotic cells (Mandel, 1969; Tseng et al., 1978), and that the cytotoxicity caused by exposure of Novicoff hepatoma cells to 5FUrd in culture can be reversed by uridine but not by thymidine (Wilkinson and Crumly, 1976).

It has already been noted that the tRNA U54 methylating function of RUMT is not essential for cell growth (Björk and Neidhardt, 1975), so it might be argued that the cytotoxic effects of 5FU cannot involve inhibition of RUMT. However, it is noteworthy to add that RUMT performs a second "essential" function (Persson et al., 1992), which could be inhibited by a FUra metabolite, and that the effects of RUMT-FUtRNA complexes (Scheme II) on cell physiology are unknown. Moreover, although the catalytic mechanism of methyl transfer deduced for *E. coli* RUMT will be directly analogous to that in eukaryotic systems, "other" RUMT functions may differ significantly between prokaryotes and eukaryotes.

REFERENCES

Akins, R. A. and A. M. Lambowitz (1987). A protein required for splicing group I introns in Neurospora mitochondria is mitochondrial tyrosyl-tRNA synthetase or a derivative thereof.*Cell* **50**: 331-45.

Björk, G. R. (1975). Transductional mapping of gene *trmA* responsible for the production of 5-methyluridine in the transfer ribonucleic acid of *Escherichia coli. J. Bacteriol.* **124**: 92-98.

Björk, G. R. (1992). The Role of Modified Nucleosides in tRNA Interactions. in Transfer RNA In Protein Synthesis. CRC Press, Boca Raton, FL. 23-85.

Björk, G. R., J. U. Ericson, C. E. D. Gustafsson, T. G. Hagervall, Y. H. Jonsson and P. M. Wikstrom (1987). Transfer RNA Modification. *Ann. Rev. Biochem* **56**: 263-287.

Björk, G. R. and L. A. Isaksson (1970). Isolation of Mutants of *Escherichia coli* lacking 5-methyluracil in transfer ribonucleic acid of 1- methyl-guanine in ribosomal RNA. *J. Mol. Biol.* **51**: 83-100.

Björk, G. R. and F. C. Neidhardt (1975). Physiological and Biochemical Studies on the function of 5-Methyluridine in the Transfer Ribonucleic Acid of *Escherichia coli. J. Bacteriol.* **124**: 99-111.

Cohen, S. S., Flaks, J.G., Barner, H.D., Loeb, M.R., and Lichtenstein, J. (1958). The Mode of Action of 5-fluoruracil and Its Derivatives. *Proc. Natl. Acad. Sci. U.S.A.* **44**: 1004-1012.

Davanloo, P., M. Sprinzl, K. Watanabe, M. Albani and H. Kersten (1979). Role of ribothymidine in the thermal stability of transfer RNA as monitored by proton magnetic resonance. *Nucleic Acids Res.* **6**: 1571-1581.

Fersht, A. (1985). Enzyme Structure and Mechanism. Second Edition. W. H. Freeman and Company. New York. p 104.

Greenberg, R. and B. Dudock (1980). Isolation and Characterization of m5U-methyltransferase from *Escherichia coli. J. Biol. Chem.* **255**: 8296-8302.

Gu, X. and D. V. Santi (1990). High-Level Expression of *Escherichia coli* tRNA(m5U54)-Methyltransferase. *DNA and Cell Bliology* **9**: 273-278.

Gu, X. and D. V. Santi (1991). The T-arm of tRNA is a Substrate for tRNA (m5U54)-Methyltransferase. *Biochemistry* **30**: 2999-3002.

Gu, X. and D. V. Santi (1992). Covalent Adducts between tRNA (m^5U54)-Methyltransferase and RNA Substrates. *Biochemistry* **31**: 10295-10302.

Gu, X. and D. V. Santi (1994). *In Vitro* Methylation of *Escherichia coli* 16S rRNA by tRNA (m^5U54)-methyltransferase. *Biochemistry* **33**: 2255-2261.

Gustafsson, C. (1992). The tRNA modifying enzyme tRNA(m^5U54)methyltransferase and its structural gene *trm*A. Doctoral Dissertation. University of Umeå, Umeå Sweden.

Gustafsson, C. and G. R. Björk (1993). The tRNA-(m5U54)-methyltransferase of *Escherichia coli* is present in two forms in vivo, one of which is present as bound to tRNA and to a 3'-end fragment of 16 S rRNA. *J. Biol. Chem.* **268**: 1326-31.

Gustafsson, C., P. H. R. Lindstrom, T. G. Hagervall, K. B. Esberg and G. R. Björk (1991). The *trmA* Promotor Has Regulatory Features and Sequence Elements in Common with the rRNA P1 Promotor Family of *Escherichia coli. J. Bacteriol.* **173**: 1757-1764.

Gustafsson, C. and S. R. Warne (1992). Physical Map of the *oxyR-trmA* Region (Minute 89.3) of the *Escherichia coli* Chromosome. *J. Bacteriol.* **174**: 7878-7879.

Hagervall, T. G., C. G. Edmonds, J. A. McCloskey and G. R. Björk (1987). Transfer RNA(5-methylaminomethyl-2-thiouridine)-methyltransferase from *Escherichia coli* K-12 has two enzymatic activities. *J. Biol. Chem.* **262**: 8488-8495.

Harrington, K. M., I. A. Nazarenko, D. B. Dix, R. C. Thompson and O. C. Uhlenbeck (1993). In Vitro Analysis of Translational Rate and Accuracy wih an Unmodified tRNA. *Biochemistry* **32**: 7617-7622.

Heidelberger, C., P. V. Danenberg and R. G. Moran (1983). Fluorinated pyrimidines and their nucleosides. . *Adv. Enzymol*. **54**: 58-119.

Hopper, A. K., A. H. Funakawa, H. D. Phau and N. C. Martin (1982). Defects in modification of cytoplasmic and mitochondrial transfer RNAs are caused by single nuclear mutations. *Cell* **28**: 543-550.

Ivanetich, K. M. and D. V. Santi (1992). 5,6-Dihydropyrimidine Adducts in the Reactions and Interactions of Pyrimidines with Proteins. *Prog. Nuc. Acid. Res. Mol. Biol.* **42**: 127-156.

Kamper, U., U. Kuck, A. D. Cherniack and A. M. Lambowitz (1992). The Mitochondrial Tyrosyl-tRNA Synthetase of Podospora anserina Is a Bifunctional Enzyme Active in Protein Synthesis and RNA Splicing. *Mol. Cell. Biol.* **12**: 499-511.

Kaptain, S., W. E. Downey, C. Tang, C. Philpott, D. Haile, D. G. Orloff, J. B. Harford, T. Rouault and R. D. Klausner (1991). A regulated RNA binding protein also possesses acontase activity. *Proc. Natl. Acad. Sci. U.S.A* **88**: 10109-10113.

Kealey, J. T., S. Lee, H. G. Floss and D. V. Santi (1991). Stereochemistry of methyl transfer catalyzed by tRNA (m5U54)-methyltransferase-- evidence for a single displacement mechanism. *Nucleic. Acids. Res.* **19**: 6465-6468.

Kealey, J. T. and D. V. Santi (1991). Identification of the Catalytic Nucleophile of tRNA (m^5U54)Methyltransferase. *Biochemistry* **30**: 9724-9728.

Kealey, J. T. and D. V. Santi (1994). High Level Expression and Rapid Purification of tRNA m5U54 methyltransferase. *Prot. Exp. Purif.* **5**: 149-152

Kersten, H. (1984). On the Biological Significance of Modified Nucleosides in tRNA. *Prog. Nuc. Acid Res.* **31**: 62-114.

Kersten, H., M. Albani, E. Mannlein, R. Praisler, P. Wurmbach and K. Nierhaus (1981). On the Role of Ribosylthymine in Prokaryotic tRNA Function. *Eur. J. Biochem.* **114**: 451-456.

Kim, S., G. J. Quigly, A. Suddath, A. McPherson, D. Sneden, J. J. Kim, J. Weinzierl and A. Rich (1973). Three-dimensional structure of yeast phenylalanine transfer RNA: Folding of the polynucleotide chain. *Science* **179**: 285-288.

Kim, S., J. L. Sussman, A. Suddath, G. J. Quigly, A. McPherson, A. H. J. Wang, N. C. Seeman and A. Rich (1974). The general structure of transfer RNA molecules. *Proc. Natl. Acad. Sci. U.S.A* **71**: 4970-4974.

Klimasauskas, S., S. Kumar, R. R.J. and X. D. Cheng (1994). *Hha*1 Methyltransferase Flips its Target Base out of the DNA Helix. *Cell* **76**: 357-369.

Kunitani, M. G., and D. V. Santi (1980). On the mechanism of 2'-deoxyuridylate hydroxymethylase. *Biochemistry* **19**: 1271-1275

Lambowitz, A. M. and P. S. Perlman (1990). Involvement of aminoacyl-tRNA synthetases and other proteins in group I and group II intron splicing. *T.I.B.S* **15**: 440-4.

Lee, M.H., M. Gautam-Basak, C. Woolley, and E. G.Sander (1988). Deoxycytidylate hydroxymethylase: purification, properties, and the role of a thiol group in catalysis. *Biochemistry* **27**:1367-1373.

Mandel, H. G. (1969). The Incorporation of 5-Fluorouracil into RNA and its Molecular Consequences. *Progr. Mol. Subcellular Biol.* **1**: 82-135.

Marcu, K. B. and B. S. Dudock (1976). Effect of ribothymidine in specific eukaryotic tRNAs on their efficiency in in vitro protein synthesis. *Nature* **261**: 159-162.

Matthews, D. A., K. Appelt, S. J. Oatley and N. H. Xuong (1990). Crystal structure of *Escherichia coli* thymidylate synthase containing bound 5-fluoro-2'-deoxyuridylate and 10-propargyl-5,8-dideazafolate. *J. Mol.Biol*. **214**: 923-936.

Matthews, D. A., J. E. Villafranca, C. A. Janson, W. W. Smith, K. Welsh and S. Freer (1990a). Stereochemical mechanism of action for thymidylate synthase based on the X-ray structure of the covalent inhibitory ternary complex with 5-fluoro-2'-deoxyuridylate and 5,10-methylenetetrahydrofolate. . *J Mol Biol* **214**(4): 937-48.

Montfort, W. R., K. M. Perry, E. B. Fauman, M. J. S. Finer, G. F. Maley, L. Hardy, F. Maley and R. M. Stroud (1990). Structure, multiple site binding, and segmental accommodation in thymidylate synthase on binding dUMP and an anti-folate.*Biochemistry* **29**: 6964-6977.

Moras, D., A.-C. Dock, P. Dumas, E. Westhof, P. Romby, J.-P. Ebel and R. Giege (1986). Anticodon-anticodon interaction induces conformational changes in tRNA: Yeast $tRNA^{Asp}$, a model for tRNA-mRNA recognition. *Proc. Acad. Natl. Sci. U.S.A* **83**: 932-936.

Najita, L. and P. Sarnow (1990). Oxidation-Reduction sensitive interaction of a cellular 50-kDa protein with an RNA hairpin in the 5' noncoding region the polio virus genome. *Proc. Natl. Acad. Sci. U.S.A* **87**: 5846-5850.

Ny, T. and G. R. Björk (1977). Stringent Regulation of the Synthesis of a Transfer Ribonucleic Acid Biosynthetic Enzyme: Transfer Ribonucleic Acid (m^5U)methyltransferase from *Escherichia coli*.. *Journal of Bacteriology*, **130**:635-641.

Ny, T. and G. R. Björk (1980). Cloning and Restriction Mapping of the *trmA* Gene Coding for Transfer Ribonucleic Acid (5-methyluridine)-Methyltransferase in *Escherichia coli* K-12. *J. Bacteriol.* **142**: 371-379.

Ny, T. and G. R. Björk (1980). Growth Rate-Dependent Regulation of Transfer Ribonucleic Acid (5-Methyluridine)Methyltransferase in *Escherichia coli. J. Bacteriol.* **141**: 67-73.

Ny, T., P. Lindstrom, T. Hagervall and G. Björk (1988). Purification of transfer RNA (m^5U54)-methyltransferase from *Escherichia coli* Association with RNA. *Eur. J. Biochem.* **117**: 467-475.

Osterman, D. G., G. D. DePillis, J. C. Wu, A. Matsuda and D. Santi V. (1988). 5-Fluorcytosine in DNA Is a Mechanism-Based Inhibitor of *Hhal* Methylase. *Biochemistry* **27**: 5204-5210.

Pang, H., M. Ihara, Y. Kuchino, S. Nishimura, R. Gupta, C. R. Woese and J. A. McCloskey (1982). Structure of a modified nucleoside in archeabacterial tRNA which replaces ribosylthymine. 1-methylpsuedouridine. *J. Biol. Chem.* **257**: 3589-3592.

Persson, B., C. Gustafsson, D. Berg and G. R. Björk (1992). The gene for a tRNA modifying enzyme, m5U54-methyltransferase, is essential for viability in *E. coli. Proc. Natl. Acad. Sci. U.S.A* **80**: 3995-3998.

Roe, B. A. and H.-Y. Tsen (1977). Role of ribothymidine in mammalian tRNAPhe. *Proc. Natl. Acad. Sci. U.S.A* **74**: 3696-3700.

Romaniuk, P. J. and O. C. Uhlenbeck (1985). Nucleoside and Nucleotide Inactivation of R17 Coat Protein: Evidence for a Transient Covalent RNA-Protein Bond. *Biochemistry* **24**: 4239-4244.

Ryals, J., R. Y. Hsu, M. N. Lipsett and H. Bremer (1982). Isolation of single-site *Escherichia coli* mutants deficient in thiamine and 4-thiouridine syntheses: Identification of a nuvC mutant. *J. Bacteriol.* **151**: 899-904.

Santi, D. V. and C. F. Brewer (1973). Model studies of thymidylate synthetase. Intramolecular catalysis of 5-hydrogen exchange and 5-hydroxymethylation of 1-substituted uracils. *Biochemistry* **12**: 2416-2424.

Santi, D. V. and P. V. Danenberg (1984). Folates in pyrimidine nucleotide biosynthesis. in Folates and Pterins. John Wiley & Sons, Inc. New York. pps. 345-398.

Santi, D. V. and L. W. Hardy (1987). Catalytic Mechanism and Inhibition of tRNA (Uracil-5-) methyltransferase: Evidence for Covalent Catalysis. *Biochemistry* **26**: 8599-8606.

Singh, R. and M. R. Green (1993). Sequence-Specific Binding of Transfer RNA by Glyceraldehyde-3-Phosphate Dehydrogenase. *Science* **259**: 365-368.

Sprinzl, M., T. Wagner, S. Lorenz and V. A. Erdmann (1976). Regions of tRNA Important for Binding to the Ribosomal A and P Sites. *Biochemistry* **15**: 3031-3039.

Starzyk, R. M., S. W. Koontz and P. Schimmel (1982). A covalent adduct between the uracil ring and the active site of an aminoacyl tRNA sythetase. *Nature* **298**: 136-140.

Steinberg, S., A. Misch and M. Sprinzl (1993). Compilation of tRNA sequences and sequences of tRNA genes. *Nucleic Acids Res.* **21**: 3011-3015.

Tseng, W.-C., D. Medina and K. Randerath (1978). Specific Inhibition of Transfer RNA Methylation and Modification in Tissue of Mice Treated with 5-fluorouracil. *Cancer Res.* **38**: 1250-1257.

Vani, B. R., T. Ramakrishnan, Y. Taya, S. Noguchi, Z. Yamaizumi and S. Nishimura (1979). Occurrence of 1-Methyladenosine and Absence of Ribothymidine in Transfer Ribonucleic Acid of *Mycobacterium smegmatis*. *J. Bacteriol.* **137**: 1084-1087.

Wilkinson, D. S. and J. Crumly (1976). The Mechanism of 5-fluorouridine Toxicity in Novikoff Hepatoma Cells. *Cancer Res.* **36**: 4032-4038.

Wu, J. C. and D. V. Santi (1987). Kinetic and catalytic mechanism of Hhal methyltransferase. *J. Biol. Chem.* **262**: 4778-4786.

CHAPTER 2

Identification of the Catalytic Nucleophile of tRNA (m^5U54)-methyltransferase

(A published account of this work appears as: *Identification of the Catalytic Nucleophile of tRNA (m^5U54)-methyltransferase*, James T. Kealey and Daniel V. Santi. *Biochemistry* **30**: 9724-9728)

ABSTRACT

A covalent complex between tRNA (m^5U54)-methyltransferase, 5-fluorouridine $tRNA^{Phe}$ and *S*-Adenosyl-L-[methyl-^{3}H]-methionine was formed *in vitro* and purified. Previously, it was shown that in this complex the 6-position of fluorouridine-54 is covalently linked to a catalytic nucleophile, and the 5-position is bound to the transferred methyl group of AdoMet (Santi, D. V.& Hardy, L W. , (1987) *Biochemistry 26*, 8599-8606). Proteolysis of the complex generated a [^{3}H]-methyl-FUtRNA-bound peptide, which was purified by 7M urea-15% polyacrylamide gel electrophoresis. The peptide component of the complex was sequenced by gas phase Edman degradation and found to contain two cysteines. The tritium was shown to be associated with Cys 324 of the methyltransferase, which unequivocally identifies this residue as the catalytic nucleophile.

INTRODUCTION

The quintessential proof of covalent catalysis is the identifcation of the catalytic nucleophile. In 1987 Santi and Hardy showed that RUMT catalyzed transmethylation of U54 in tRNA proceeded by covalent catalysis and that the catalytic nucleophile was probably a cysteine (Santi and Hardy, 1987). Since RUMT forms an isolable covalent complex with FUtRNA and a methyl group derived from AdoMet (Scheme II, Chapter 1), it provides a model system for detailed study of protein-mediated Michael addition to a pyrimidine of RNA. The obligatory first step of the reaction can be established by elucidation of the amino acid residue that is covalently bound to FUtRNA. In this paper we report the isolation and primary sequence of a fragment of RUMT which remains covalently bound to FUtRNA, following proteolysis of the covalent complex. We have also identified Cys 324 of RUMT as the nucleophile which is covalently bound to the ribopyrimidine. The work described below represents the first direct proof that a Michael adduct between a protein and RNA is mediated through a specific cysteine nucleophile.

MATERIALS AND METHODS

Acrylamide, Bis acrylamide and CAPS were from Biorad. AdoMet was from Boehringer Mannheim. Ribonucleotide triphosphates were from Pharmacia. 5-Fluorouridine-triphosphate was from Sierra Bioresearch. *S*-Adenosyl-L-[methyl-^{3}H]- Methionine (79 Ci/millimole), and [^{14}C]-iodoacetamide (59 Ci/mole) were from Amersham. Aquasol II was from Dupont. ProBlott PVDF membrane was from Applied Biosystems. LEP was from Wako. T-7 RNA polymerase was prepared as described (Davanloo et al., 1984). Unless otherwise specified,

DEAE-cellulose was DE-52 from Whatman. DITC Sequalon membranes and associated reagents were from Millipore. Peptide sequencing was performed on an Applied Biosystems 470A gas phase protein sequencer with an on-line 120A PTH analyzer at the Biomolecular Resource Center, University of California, San Francisco. EtOH precipitations were performed by addition of 2.5 vols of cold 95% EtOH, followed by cooling at -20 °C overnight or at -80 °C for 1 hr.

Purification of RUMT: RUMT was purified to 800 units/mg (ca. 50% pure) as described (Gu & Santi, 1990), except the final DEAE purification step was omitted. One unit is the amount of enzyme that transfers one picomole of methyl groups to U54 methyl- deficient tRNA per minute at 30 °C under standard assay conditions (Santi and Hardy, 1987).

Preparation and Purification of FUtRNA^{Phe}. FUtRNA^{Phe} was prepared by *in vitro* transcription as described (Sampson and Uhlenbeck, 1988), using 4 mM NTPs and replacing UTP with FUTP. After phenol/chloroform extraction and EtOH precipitation, the RNA pellet was dissolved in water and applied to a Nucleogen 4000-10 DEAE column (1x12 cm), equilibrated with 20 mM Tris-HCl, pH 7.6, containing 0.1 M NaCl (Buffer A). The column was washed with Buffer A for 5 min at 0.5 ml/min, followed by a linear ramp to 40% Buffer B (20 mM Tris-HCl, pH 7.6, 1 M NaCl) over 5 min; from 40% to 65% B over 40 min; from 65 to 100% B over five min; and 100% B for 5 min (the flow rate of all gradient steps was 0.5 ml/min) . The major peak eluted at ca. 0.5 M NaCl (50% B), was precipitated with EtOH and dissolved in 10 mM Tris-HCl, pH 7.6, 1 mM EDTA. Prior to formation of the RUMT-[^{3}H]-methyl-FUtRNA complex, FUtRNA was heated at 80 °C for five min, and then renatured by slowly cooling to room temperature.

Preparation and Purification of Enzyme-[^{3}H]-methyl-FUtRNA Complex. A reaction mixture (3.78 mL) containing RUMT (0.64 mg, 800 units/mg), FUtRNA^{Phe} (14.4 nmol), [^{3}H]-methyl-AdoMet (200 nmol, 0.54 Ci/mmole), 50 mM Tris-HCl, pH 7.6, 1 mM EDTA, 2 mM $MgCl_2$, 5 mM DTT, and 50 mM NaCl was incubated at 18 °C. After 30 min, an additional 0.26 mg of RUMT in 0.8 mL of 20 mM Tris-HCl, pH 7.6, 0.5 mM DTT, 0.5 mM EDTA, and 20% w/v glycerol was added and incubation was continued for 1.5 hour at 18 °C.

The complex was purified by adsorption to a 1.5 mL DE-52 column (0.9x6 cm), equilibrated with 20 mM Tris-HCl, pH 7.6, 1 mM EDTA and 50 mM KCl. The column was washed with 10.2 mL of this buffer until tritium in the wash reached background (ca. 50 dpm/mL), and then washed with 11.9 mL of 20 mM Tris-HCl, pH 7.6, 1 mM EDTA and 250 mM KCl to remove excess protein. The complex was eluted in 1.7 mL of 20 mM Tris-HCl, pH 7.6, 1 mM EDTA and 1 M KCl, and concentrated/desalted by precipitation with EtOH .

Lysylendopeptidase digestion of RUMT-[^{3}H]-methyl -FUtRNA Complex RUMT-FUtRNA-[^{3}H]-methyl complex (1.8 nmol) in 100 µL of 100 mM Tris-HCl, pH 8.9, and 2 M Gdn-HCl was digested with 0.045 unit of LEP at 30 °C. After 70 min of incubation, EDTA and DTT were added to final concentrations of 2.5 and 20 mM, respectively, and an additional aliquot of LEP (0.045 unit) was added; the sample was flushed with argon and incubated for 60 min at 30 °C. The extent of digestion was assayed by monitoring the shift in electrophoretic mobility, using 7M urea- 15% PAGE and EtBr to stain RNA. After complete proteolytic digestion, the peptide-[^{3}H]-methyl -FUtRNA complex was precipitated with EtOH .

Separation of tRNA-peptides by 7M Urea-15% PAGE and Electroblotting to PVDF Membrane. The EtOH precipitated peptide-[^{3}H]-methyl -FUtRNA complex was dissolved in water, and then diluted with an equal volume of formamide

containing 0.03% bromophenol blue and 0.03% xylene cyanole. The sample (ca. 400 pmol) was loaded to a 7M urea-15%-polyacrylamide "mini gel" (8 cm x 10 cm x 0.75mm) as follows: Five percent was loaded to one lane of the gel to serve as a marker, and the remainder was loaded to an adjacent lane. Electrophoresis was carried out at 200 V until the xylene cyanole band reached the bottom of the gel. Following electrophoresis, the lane containing the marker was excised and stained with EtBr. The remainder of the gel was electroblotted to Problott PVDF membrane in a Biorad Mini-Transblot Electrophoretic Transfer Cell. Electroblotting was carried out for 35 min at 50 V in CAPS/ MeOH, pH 11, as described in the Applied Biosystem's ProBlott Brochure. To localize the peptide-[^{3}H]-methyl -FUtRNA complex on the membrane, the PVDF strip was sliced horizontally into twelve 0.5 cm x 1.5 cm segments. One-tenth of each segment (0.5 cm x 0.15 cm) was suspended in 5 mL Aquasol II, and the radioactivity measured by liquid scintillation counting. The PVDF segment exhibiting the greatest amount of radioactivity and containing the putative peptide-tRNA was loaded to a gas phase protein sequencer, and N-terminal sequencing was performed.

[^{14}C]- Carboxyamidomethylation of Peptide-FUtRNA-[^{3}H]-methyl Complex. Following LEP digestion, the peptide-[^{3}H]-methyl-FUtRNA complex was precipitated with EtOH to remove excess DTT. The pellet was washed with cold 70% EtOH, dried briefly under vacuum, and dissolved in 60 µL of 0.1 M Tris-HCl, pH 8.9, and 5.33 M Gdn-HCl containing 1µCi of [^{14}C]-iodoacetamide (59 mCi/mm). The sample was flushed with argon and incubated for 60 min at 23 °C. The complex was precipitated EtOH, and the pellet was washed with cold 70% EtOH until the [^{14}C] in the supernatant reached a constant value (ca. 200 dpm/mL).

V-8 Protease Digestion of the [^{14}C]-peptide-[^{3}H]-methyl-FUtRNA Complex. To 125 pmoles of [^{14}C]-peptide-[^{3}H]-methyl-FUtRNA in 100µL of 0.1M Tris-HCl, pH 7.5 was added 2 µg of V-8 protease. Following incubation at 37 °C for 2 hr the complex was precipitated with EtOH, washed with cold 70% EtOH and dissolved in water. Aliquots from both supernatant and dissolved pellet were counted in Aquasol II to quantitate [^{14}C] and monitor the extent of proteolytic digestion. Since these results indicated incomplete digestion, the dissolved pellet was adjusted to 0.1 M Tris-HCl, pH 7.5, an additional 2 µg of V-8 protease was added, and the sample was incubated at 37 °C for 1 hour. The peptide-[^{3}H]-methyl-FUtRNA was recovered by EtOH precipitation and dissolved in 60µl of water. One half of this solution was subjected to gas phase Edman degradation.

Covalent Protein Sequencing of the [^{14}C]-peptide-[^{3}H]-methyl-FUtRNA Complex. The [^{14}C]-peptide-[^{3}H]-methyl-FUtRNA (250 pmoles) was attached to a DITC Sequalon membrane via the ε-amino group of the carboxyterminal lysine, as described in the bulletin provided by the manufacturer of the membrane. Edman degradation (O3CPTH cycle) and PTH analyses were performed for 9 cycles as described above, except that the O3CBGN cycle was omitted. After 9 PTH cycles, Solvent 1 (S1, n-heptane), Solvent 2 (S2, ethylacetate) and Solvent 3 (S3, butylchloride) were changed to ethylacetate/ n-hepane (50:50,v/v) (S1'), 100% MeOH (S2') and 20mM sodium phosphate, pH 7.0/ MeOH (10:90, v/v)(S3') (Wettenhall et al., 1990). ATZ cycles were then commenced, as described (Wettenhall et al., 1990) with minor modifications: to prevent blockage by salt precipitation, the ATZ transfer line was changed from 0.3 i.d. to 0.5 i.d., and after each cycle the line was extensively washed with S2' . Each ATZ fraction was counted in 4 mL Aquasol II until the standard error was less than 1%.

RESULTS

Upon formation of the RUMT-[^{3}H]-methyl -FUtRNA complex, the apparent molecular weight of RUMT shifted from 42 to 67 kDa on SDS PAGE (Santi & Hardy, 1987). The 67 kDa band was approximately 50% pure as indicated by SDS PAGE. Due to its RNA component, the complex eluted from DEAE-cellulose in high salt, whereas contaminating proteins eluted in medium salt. Using a RUMT preparation that was about 50% pure, DEAE-cellulose purification gave a complex which was greater than 95% homogeneous. (Figure 2.1).

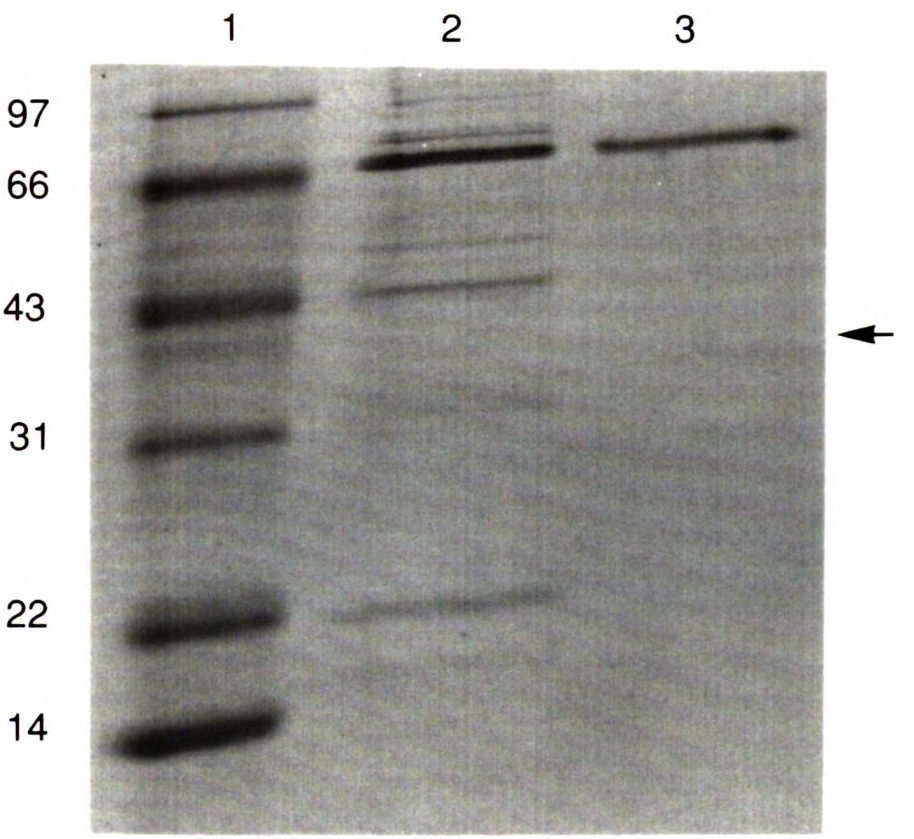

Figure 2.1: Purification of the Covalent Complex. Shown is a Coomassie stained SDS gel of crude complex (lane 2) and the DEAE purified complex (lane 3). Lanes 1 shows the migration of standard molecular weight markers (97.4, 66.2, 42.7.,31.0, 21.5, and 14.4 kDa). The arrow marks the position of free RUMT.

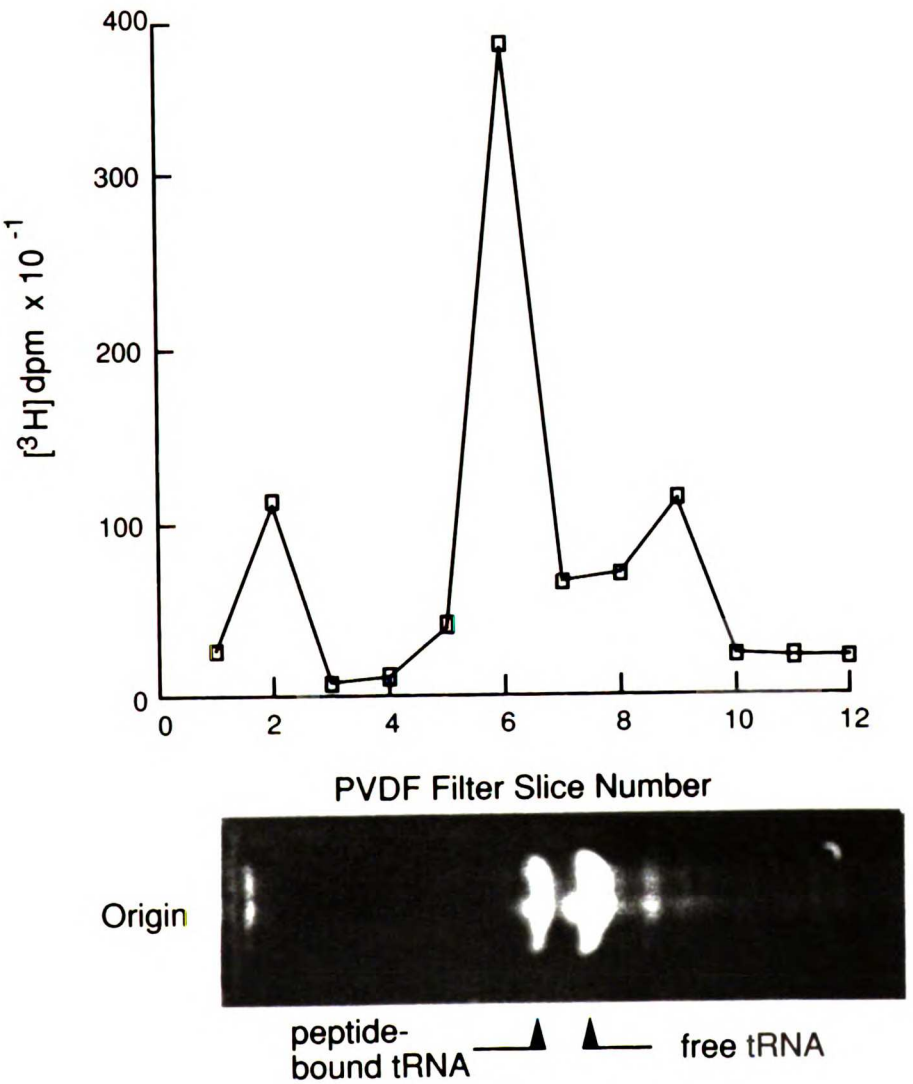

Figure 2.2: Electroblotting of peptide-[^{3}H]-methyl-FUtRNA complex to PVDF membrane. Shown is an ethidium bromide stained portion of a7M urea-15% polyacrylamide gel (depicted horizontally from the origin) contiguous to the gel section which was electroblotted to PVDF paper. Dpm per PVDF slice is plotted, such that it corresponds to gel position.

The purity of the complex was also assessed by N-terminal protein sequencing, which yielded homogeneous PTH amino acids for 5 cycles and confirmed the N-terminus of RUMT (data not shown).

The LEP digestion of the purified RUMT-[^{3}H]-methyl-FUtRNA complex was monitored by 7M urea-15% PAGE. After 70 min at 30 °C several FUtRNA-peptides were observed, which upon continued incubation, converged to a single band, migrating slightly slower than free FUtRNA (data not shown). In a parallel experiment the gel was blotted to a PVDF membrane and the peptide-[^{3}H]-methyl-FUtRNA complex was localized on the electroblot by measuring the radioactivity in segments of the membrane (Figure 2.1). The PVDF segment exhibiting the highest number of recovered counts corresponded to the putative peptide-[^{3}H]-methyl-FUtRNA complex, as determined by EtBr staining.

The PVDF segment containing the complex was subjected to 22 cycles of Edman degradation. With the exception of cycle 13, unambiguous amino acid assignments could be made for 18 consecutive cycles (Figure 2.3). When compared to the DNA sequence of RUMT (Gustafsson et al., 1991), the LEP fragment that remained attached to FUtRNA corresponded to residues 312-331: MVQAYPRILYISCNPETLCK (Figure 2.4). The C-terminus of the peptide was presumed to be Lys 331, since LEP cleaves at the C-terminal side of lysine. Thus, the catalytic nucleophile was concluded to be either Cys 324 (circled, figure 2.4) or Cys 330 (boxed, Figure 2.4) of the protein. However, a definitive assignment could not be made since neither Cys residue could be directly identified under normal operation of the gas phase sequencer.

In order to distinguish free cysteine from nucleotide bound cysteine, the peptide-[^{3}H]-methyl-FUtRNA complex was treated with [^{14}C]-iodoacetamide to alkylate and label the free thiol (Figure 2.4). This yielded a doubly labelled complex in which one of the cysteines was labelled with ^{3}H and the other with

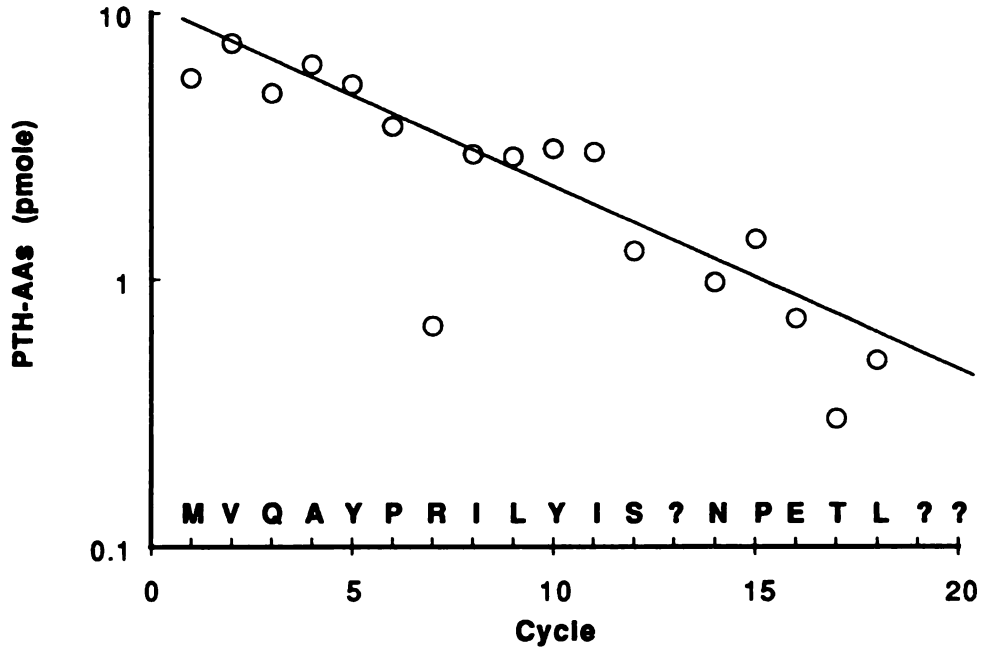

Figure 2.3: N-terminal Protein sequence of peptide-[^{3}H]-methyl-FUtRNA complex. The theoretical initial PTH yield was 10.7 pmole and average repetitive yield was 85%.

^{14}C. The [^{14}C]-peptide-[^{3}H]-methyl-FUtRNA complex was digested with V-8 protease, which cleaves at the C-terminal side of glutamic acid. Proteolysis should occur at Glu 327 and yield two peptides, one containing Cys-[^{3}H]-methyl-FUtRNA, and the other containing [^{14}C]-carboxyamidomethyl-cysteine. The peptide that contained [^{3}H]-FUtRNA was purified by EtOH precipitation and washed free of the [^{14}C]- peptide (over 99% removal). The peptide that remained attached to [^{3}H]-FUtRNA was sequenced and found to contain the same N-terminus as did the peptide prior to protease removal of the ^{14}C modified cysteine. Further, the sequence abruptly terminated at Glu 327. This

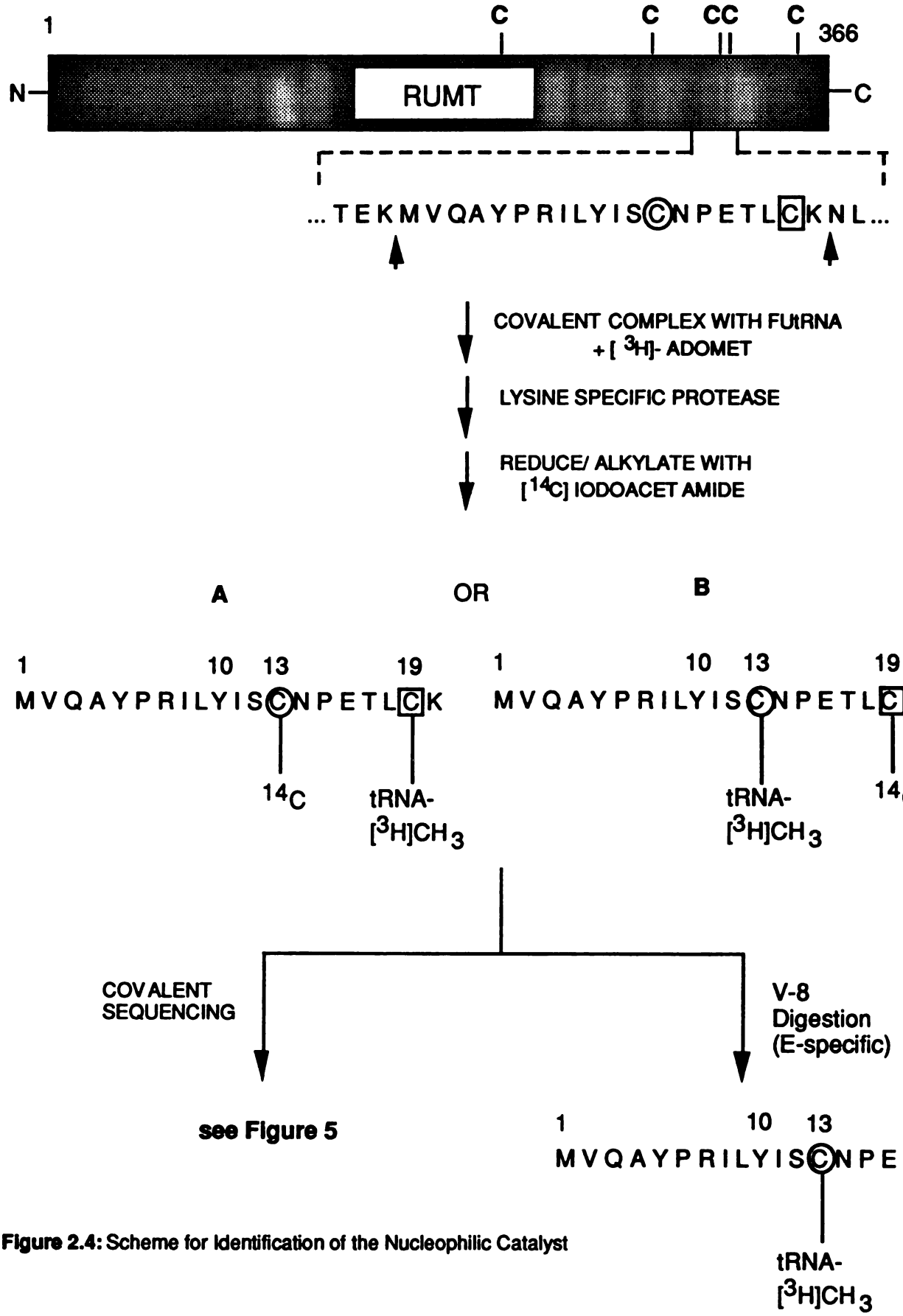

Figure 2.4: Scheme for Identification of the Nucleophilic Catalyst

provides indirect evidence that cysteine 324 of the original LEP fragment is attached to FUtRNA, and that cysteine 330 is carboxyamidomethylated.

To definitively demonstrate that cysteine 324 is bound to FUtRNA, we sought to identify the sequencer cycles in which ^{3}H and ^{14}C were released and to correlate those cycles with the known peptide sequence (figure 2.4). This approach is not feasible by "non-covalent" gas phase sequencing due to the inability to extract [^{3}H]-FUtRNA-Cys from a glass fiber or PVDF membrane, during conventional operation of the gas phase protein sequencer. To recover ATZ-[^{3}H]-FUtRNA-Cys, more rigorous extraction conditions were required, which necessitated covalent attachment of the [^{14}C]-peptide-[^{3}H]-methyl-FUtRNA to a solid support. The [^{14}C]-peptide-[^{3}H]-methyl-FUtRNA was covalently attached to a Sequalon® DITC membrane through the ε- amino group of the putative C-terminal lysine, and conventional protein sequencing was performed for 9 cycles (PTH derivatives analyzed), and then ATZ -amino acids were collected using the vigorous extraction conditions. As shown in Figure 2.5, tritium is released in cycle 13 and ^{14}C in cycle 19. These results clearly establish that Cys 324 (circle, figure 2.4) is bound to FUtRNA and Cys 330 is carboxyamidomethylated.

DISCUSSION

The objective of this work was to identify the nucleophilic catalyst of RUMT which is believed to form a transient covalent adduct with U54 of tRNA. The strategy was to form a RUMT-[^{3}H]-methyl -FUtRNA covalent complex, which mimicked a steady state intermediate of the normal enzymic reaction; to convert the complex to a small peptide-[^{3}H]-methyl-FUtRNA complex, and then to sequence the peptide to determine which amino acid was attached to the RNA.

The covalent complex was formed with RUMT, [^{3}H]-methyl-AdoMet and FUtRNA, purified from extraneous proteins by exploiting properties of RNA on anion exchange chromatography, and treated with LEP to convert it to a peptide-[^{3}H]-methyl-FUtRNA complex. The presence of tRNA in the complex allowed the peptide-RNA complex to be purified and desalted by simple EtOH precipitation, and to be visualized on PAGE by EtBr staining.

The active site peptide had the twenty amino acid sequence MVQAYPRILYISCNPETLCK which contained two cysteine residues that were candidates for the nucleophilic catalyst. The cysteine covalently attached to [^{3}H]-methyl-FUtRNA could not be identified by conventional protein sequencing because it was not possible to extract the modified amino acid from a glass fiber or PVDF membrane. To unequivocally identify the catalytic nucleophile, two complementary strategies were employed (see figure 2.4).

First, the peptide-[^{3}H]-methyl-FUtRNA complex was reacted with [^{14}C]-iodoacetamide to produced a peptide doubly labelled at the two cysteine residues. The [^{14}C]-peptide-[^{3}H]-methyl-FUtRNA was then cleaved with V-8 protease at the Glu between the two cysteines, and the peptide that remained attached to FUtRNA was isolated and sequenced. It was determined that the peptide containing Cys 324 remained attached to FUtRNA, and the peptide containing Cys 331 was released from the complex.

In a second approach, the [^{14}C]-peptide-[^{3}H]-methyl-FUtRNA was covalently attached to a PVDF membrane, and the peptide component was sequenced using a modified Edman degradation protocol. After nine conventional sequencer cycles, ATZ-amino acids were collected using rigorous extraction conditions; tritium was released at Cys 324 and ^{14}C at Cys 331 (see Figure 2.5). These results unequivocally show that Cys 324 of RUMT is the residue attached to [^{3}H]-methyl-FUtRNA in the covalent complex. We believe that the

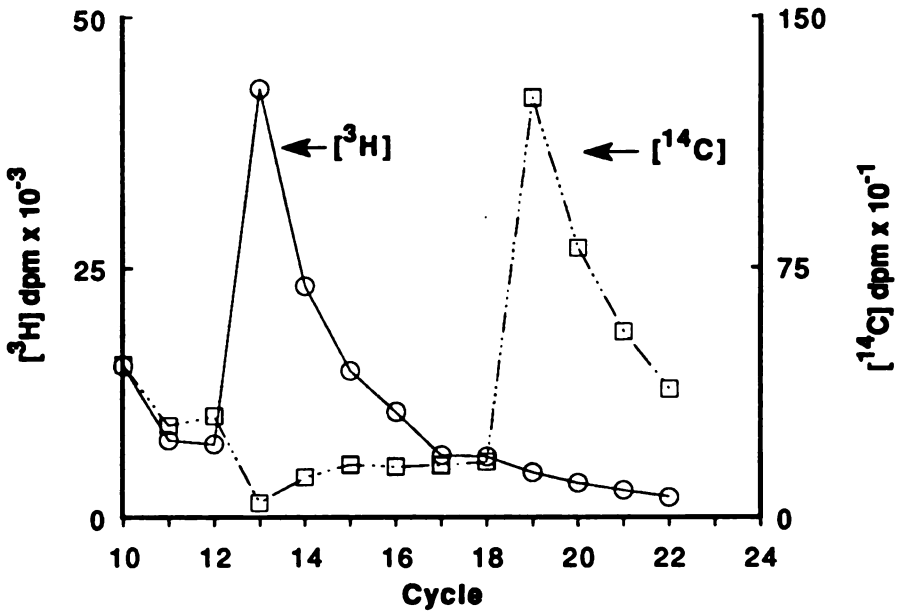

Figure 2.5: Covalent protein sequencing of the [^{14}C]-peptide-[^{3}H]-methyl-FUtRNA complex. For Edman degradation cycles 10-22, ATZ amino acids were collected and quantitated by scintillation counting. The ATZ yields in cycles 13 and 19, as determined by radiochemical quantitation, were 36 and 10 pmoles respectively. The relative picomole yields of [^{3}H] and [^{14}C] are consistent with the theoretical initial yield of the peptide.

interaction of the mechanism based inhibitor, FUtRNA, with RUMT mimics that of the natural tRNA substrate, so we conclude that Cys 324 is the nucleophilic catalyst in the normal enzymic reaction.

We can deduce that nucleophilic catalysis by RUMT requires substantial conformational change of the tRNA substrate. In the crystal structure of yeast tRNA^{Phe}, C6 of U54 is completely solvent inaccessible. Access to C6 is precluded from above and below the plane of the pyrimidine ring by base stacking of U54 between adjacent residues, Ψ55 and G53. Therefore, at an early stage of the reaction, the structure of the T-loop must be opened so that

the sulfhydryl of Cys 324 can access C6 of U54 to form the covalent adduct. RUMT might accomplish this either by facilitating a conformational change in the RNA upon binding, or by stabilizing a high energy conformation of the RNA, where C6 of U54 is solvent accessible. It has recently been shown that the methyl transfer step occurs by direct displacement of the C5 anion equivalent on the sulfonium ion of AdoMet (see Chapter 3). This places further constraint on the structure of the T-loop during methylation, since C5 and the methyl electrophile must be colinear for S_N2 displacement.

Several other proteins are believed to form Michael adducts with RNA and DNA as a means of enhancing binding specificity and catalysis. These include other RNA-pyrimidine methyltransferases, DNA-Cytosine methyltransferases, pseudouridine synthases and other unrecognized proteins (Santi et al., 1978)(Santi and Hardy, 1987). The approach used here for *E. coli* RUMT should be applicable to the purification of other proteins which form stable Michael adducts, as well as identification of nucleophilic residues involved in covalent bond formation.

ACKNOWLEDGEMENTS

We thank Ralph Reid for his assistance in protein sequencing.

REFERENCES

Davanloo, P., A. H. Rosenberg, J. J. Dunn and F. W. Studier (1984). Cloning and expression of the gene for bacteriophage T-7 RNA polymerase. *Proc. Natl. Acad. Sci. USA* **81**: 2035-2039.

Gustafsson, C., P. H. R. Lindsrom, T. G. Hagervall, B. K. Esberg and G. R. Bjork (1991). The trmA Promoter Has Regulatory Features and Sequence Elements in Common with the rRNA P1 Promoter Family of Escherichia coli. *J. Bacteriol.*. **173**(5): 1757-1764.

Kealey, J. T., S. Lee, H. G. Floss and D. V. Danti :

Sampson, J. R. and O. C. Uhlenbeck (1988). Biochemical and physical characterization of an unmodified yeast phenylalanine transfer RNA transcribed *in vitro*. *Proc. Natl. Acad. Sci. USA* **85**: 1033-1037.

Santi, D. V. and L. W. Hardy (1987). Catalytic Mechanism and Inhibition of tRNA (Uracil-5-) methyltransferase: Evidence for Covalent Catalysis. *Biochemistry* **26**: 8599-8606.

Santi, D. V., Y. Wataya and A. Matsuda (1978). Approaches to the design of mechanism-based inhibitors of pyrimidine metabolism. Enzyme-activated irreversible inhibitors. Proceedings of the international symposium on substrate-induced irreversible inhibition of enzymes., Strasbourg, France, Elsevier/North Holland Biomedical Press.

Wettenhall, R. E. H., R. H. Aebersold and L. E. Hood (1991). Solid-phase sequencing of 32P-labeled phosphopeptides at picomole and subpicomole levels. *Methods in Enzymology* **201**:186-199.

CHAPTER 3

Stereochemistry of Methyl Transfer Catalyzed by tRNA (m^5U54)-methyltransferase--Evidence for a Single Displacement Mechanism

James T. Kealey[1], Sungsook Lee[2], Heinz G. Floss[2], and Daniel V. Santi [1,*]

[1]Departments of Pharmaceutical Chemistry and Biochemistry and Biophysics, University of California, San Francisco, CA., 94143; and [2] Department of Chemistry, University of Washington, Seattle, WA., 98195

(A published account of this work appears as: *Stereochemistry of methyl transfer catalyzed by tRNA (m5U54)-methyltransferase-- evidence for a single displacement mechanism*, James T. Kealey, S. Lee, H. G. Floss and D. V. Santi (1991). *Nucleic. Acids. Res.* **19**: 6465-6468.

ABSTRACT

tRNA (m^5U54)-methyltransferase (RUMT) catalyzes the transfer of a methyl group from *S*-adenosyl-L-methionine (AdoMet) to the 5-carbon of uridine 54 of tRNA. We have determined the steric course of methyl transfer, using (*methyl*-R)- and (*methyl*-S)-[*methyl*-$^2H_1$,^3H]-AdoMet as the chiral methyl donors, and tRNA lacking the 5-methyl group at position 54 as the acceptor. Following methyl transfer, ribothymidine was isolated and degraded to chiral acetic acid for configurational analysis. Transfer of the chiral methyl group to U54 proceeded with inversion of configuration of the chiral methyl group, suggesting that RUMT catalyzed methyl transfer occurs by a single SN2 displacement mechanism.

INTRODUCTION

tRNA (m^5U54)-methyltransferase (RUMT, EC 2.1.1.35) catalyzes the methylation of uridine 54 (U54) of tRNA by S-adenosyl-L-methionine (AdoMet). The product of the reaction is the modified nucleoside, ribothymidine, which is invariant in the TΨC-loop of most eubacterial and eukaryotic tRNAs (1). As currently understood, the mechanism of RUMT-catalyzed transmethylation is shown in Scheme I (Chapter 1). In the first step the thiol group of cysteine 324 reacts with C6 of U54 to produce a nucleophilic center (enol or enolate) at C5 (2)(3). Next, the methyl group from AdoMet is transferred to C5 of U54, and then β- elimination produces the methylated tRNA product and free enzyme. As shown in Scheme II (this chapter), the methyl transfer proceeds by either (a) direct displacement of the methyl group of AdoMet by C5 of the U54 covalent adduct, or (b) by a double displacement reaction, whereby the methyl group is first transferred to a nucleophile on the enzyme, and subsequently to C5 (Scheme II, Chapter 3). These two mechanisms can be distinguished by performing the methylation reaction with chiral methyl AdoMet ([*methyl*-$^2H_1$,^3H]-AdoMet) as the cofactor and monitoring the stereochemical fate of the methyl group. The single displacement mechanism predicts inversion of configuration of the chiral methyl group, whereas the double displacement mechanism would proceed by double inversion and predict overall retention of configuration of the chiral methyl group.

In this paper we show that the RUMT catalyzed methyl transfer proceeds with inversion of configuration of the chiral methyl group derived from AdoMet; therefore, the reaction must occur by a single displacement mechanism.

Scheme II

(a) Single displacement

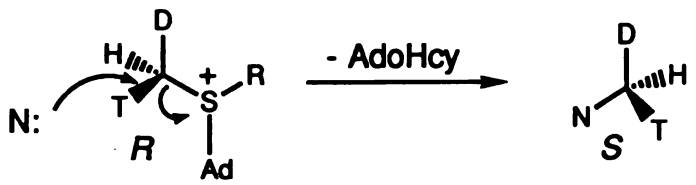

Inversion

(b) Double displacement

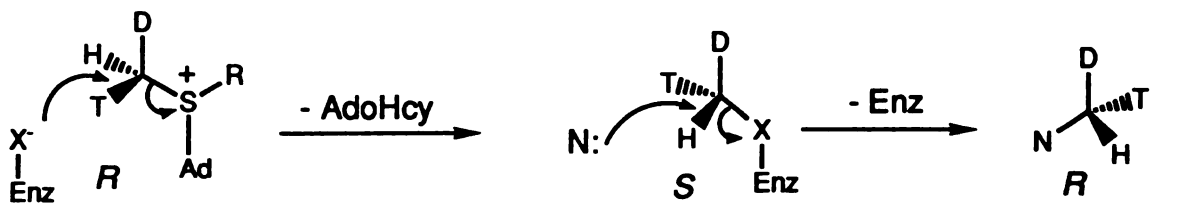

Retention

X = a nucleophile on the enzyme; N: = U54 C5 nucleophile

EXPERIMENTAL

General Materials and Methods

Escherichia coli GB1-5-39, a strain deficient in tRNA (m^5U54)-methyltransferase, was a gift from Glenn Björk of the University of Umeå, Umeå, Sweden. Calf intestinal alkaline phosphatase was purchased from Pharmacia, P-1 Nuclease from Boehringer Mannheim, [^{3}H]-methyl-AdoMet (70 Ci/mmol) from Amersham, and DEAE-cellulose was DE-52 obtained from Whatman. Tri-N-octyl-amine and Freon-TF (1,1,2-trichlorotrifluoroethane) were purchased from Aldrich. One unit of RUMT is the amount of enzyme that methylates one pmol of U54 methyl-deficient tRNA per min at 30 °C under standard assay conditions (2). (*Methyl*-R)- and (*Methyl*-S)-[*methyl*-$^2H_1$,^{3}H]AdoMet (80 mCi/mmol, 91% and 86% ee, respectively) were prepared as described (4, 5).

Preparation of m^5U54-deficient tRNA

A single colony of tRNA (m^5U54) methyltransferase-deficient *E. coli* GB1-5-39 was grown in 30 mL of Luria broth (6) at 37 °C overnight. Three liters of Luria broth were inoculated with the overnight culture and the cells were grown until the A_{590} reached 3.4. The cells were harvested by centrifugation and frozen at -20 °C. Frozen cells were resuspended in 50 mL of 0.1M Tris-HCl, pH 7.5, 10 mM $MgCl_2$, and bulk methyl- deficient tRNA was purified as described (7).

Preparation of RUMT

RUMT was prepared from *E. coli* HB101 /pMTXR1 as described (8) with the following modifications. To concentrate the enzyme, a pooled protein fraction from phosphocellulose chromatography containing RUMT (100 ml at 0.33 mg/ml; 610 units/ml; ca. 50% pure), was adsorbed to a 25 ml DEAE-cellulose column (2.5 x 12.5 cm) previously equilibrated with Buffer A (20 mM Tris-HCl, pH 7.5, 0.5 mM EDTA, 0.5 mM DTT, and 20% glycerol). After washing the column with 50 ml of Buffer A containing 50 mM KCl, RUMT was eluted at 1.5 ml/min in Buffer A containing 0.33 M KCl, and 3 ml fractions were collected. Based on protein assay (9), fractions 7-11 were pooled, yielding a final concentration of 1.8 mg protein/ ml.

Methyl Transfer from [*methyl*-$^2H_1$,^3H]AdoMet to Methyl-deficient tRNA and Purification of the Methylated tRNA

A 3.1 ml reaction mixture containing chiral *methyl-R* AdoMet (100 nmoles, 10 μCi), 50 mM Tris-HCl, pH 7.6, 1 mM EDTA, 2 mM $MgCl_2$, 5 mM DTT, 22 μM RUMT (1750 units) and 82 μM methyl- deficient tRNA was kept at room temperature for 45 minutes. A second aliquot of RUMT (21 nmoles, 550 units)

was added and the reaction was allowed to continue for 45 minutes, then terminated by freezing at -20 °C.

The methylated tRNA was adsorbed to a 17 mL DEAE-cellulose column (2.5 x 12.5 cm), equilibrated with 20 mM Tris-HCl, pH 7.6, 0.2 mM EDTA (Buffer B), containing 50 mM KCl. The column was washed with 65 mL equilibration buffer to remove unreacted AdoMet, and then washed with 60 mL Buffer B containing 250 mM KCl to remove protein. The tRNA was eluted in Buffer B in 1 M KCl, and 2.3 ml fractions were collected. Fractions containing radioactivity (7-9) were pooled, and the RNA was precipitated with 2.5 volumes of cold 95% ethanol. The tRNA precipitate was collected by centrifugation, washed with 70% cold ethanol, and dried under vacuum. The yield of methylated tRNA derived from *methyl-R* AdoMet following DEAE-cellulose chromatography was 29 nmoles. Methyl transfer from *methyl-S* AdoMet (98 nmoles, 7.85 μCi) to methyl-deficient tRNA and purification of the methylated tRNA were performed as described for the *methyl-R* AdoMet. The yield of methylated tRNA following DEAE-cellulose chromatography was 28 nmoles.

Nuclease Digestion of tRNA and Isolation of [*methyl*-$^2H_1$,^3H] Ribothymidine

The pellets of chiral methyl tRNA, derived from either (*methyl-R*)- or (*methyl-S*)-AdoMet, were each dissolved in 400 μl of water, heated at 90 °C for 2 min, and cooled on ice. To these solutions were added 40 μl of 100 mM $ZnCl_2$, 50 μl of 100 mM NH_4OAc, pH 6.2, and 100 μg of P-1 nuclease (at 1 mg/ml). After 2 hours incubation at 37 °C, a second 50 μg aliquot of P-1 nuclease was added, and digestion was continued for 1 hour. The resulting solutions were adjusted to 0.2 M Tris (pH 8.9) with 1 M Tris-HCl, and 20 units of alkaline phosphatase (1 u/μl) were added to each sample. After 2 hours of incubation at 37 °C, 10 more

units of alkaline phosphatase were added and incubation was continued for 45 min. Conversion of tRNA to nucleosides was verified by analytical DEAE-cellulose chromatography. Nucleosides eluted in Buffer B containing 50 mM KCl, mononucleotides eluted in Buffer B containing 250 mM KCl, and tRNA eluted in Buffer B containing 1 M KCl.

To each solution of nucleosides, one-tenth volume of 50% w/v TCA was added and the samples were kept at 4 °C for 30 min. The precipitated protein was removed by centrifugation, and the supernatants were extracted with an equal volume of 0.5 M tri-N-octyl-amine/ 78% v/v Freon-TF (1,1,2-trichlorotrifluoroethane) to remove TCA (10)(11). The aqueous phase was clarified by centrifugation and applied to HPLC.

Reverse Phase HPLC was performed on a Rainin Rabbit *HP* system, equipped with a Vydak C18 column (4.6 mm x 25 cm), using the following conditions: Solvent A, 0.25 M ammonium acetate, pH 6; Solvent B, 40/60 (v/v) acetonitrile/water; gradient: 0-3 min 0% B, 3-10 min 0-5% B, 10-25 min 5-25% B, 25-30 min 25-50% B, 30-34 min 50-75% B, 34-37 min 75% B, 37-45 min 75-100% B; flow rate, 1.0 ml/min (7). Prior to chromatography of the [*methyl*-$^{2}H_{1}$,^{3}H]ribothymidine samples, the system was calibrated with a mixture of standard ribonucleosides, which exhibited the following retention times: Cyd, 5.1 min; Urd, 6.0 min; ribothymidine, 13.2 min; Guo, 14.5 min; and Ado,19.2 min. This system afforded base-line separation of ribothymidine from Guo, its closest neighbor. For preparative isolation of [*methyl*-$^{2}H_{1}$,^{3}H]ribothymidine, each nucleoside solution was loaded separately to the HPLC, and the [^{3}H]-labeled ribothymidine peak from each run was collected, and dried under vacuum. The yields of [*methyl*-$^{2}H_{1}$,^{3}H]ribothymidine from (*methyl-R*)- and (*methyl-S*)-[*methyl*-$^{2}H_{1}$, ^{3}H]AdoMet were 17.6 and 13.2 nmoles, respectively.

Degradation of [*methyl*-$^2H_1$,^3H]Ribothymidine

Individual reaction mixtures (2.1 mL) containing 2 mg (15.8 μmol) thymine, 300 mg (1.28 mmol) potassium periodate, 0.8 mg (5.7 μmol) potassium permanganate and 0.58 μCi (*methyl-R*)- or 0.68 μCi (*methyl-S*)-[*methyl*-$^2H_1$, ^3H]ribothymidine were stirred at room temperature for 2.5 hour, then filtered. The filtrate was diluted with 30 ml water and transferred to a 100 ml round bottom flask. After addition of 6 ml of 6 N NaOH the solution was concentrated to 3 mL by distillation (oil bath at 140 °C). The residue was acidified with 10 ml of 5 N H_2SO_4 and distilled to obtain chiral acetic acid. The distillate was brought to pH 10 with 0.1 N NaOH, evaporated to dryness in vacuo, and the [*methyl*-$^2H_1$, ^3H]acetate was subjected to configurational analysis as described (12).

In separate experiments, transfer by lyophilization was used to recover the chiral acetates. After filtering insoluble salts from the reaction mixture, the filtrate was acidified with 50 μl of 5N sulfuric acid. The solution was placed in a round bottom flask, which was connected to a receiving flask immersed in a dry ice/isopropanol bath. The sample flask was frozen in a dry ice/isopropanol bath, the bath was removed, and the system was evacuated to about 500 Torr to cause transfer of volatiles to the cooled receiving flask. The transferred material was thawed, adjusted to pH 10 with 0.1 N NaOH to convert acetic acid to sodium acetate, and then lyophilized to dryness. The chiral acetate residue was dissolved in 1 ml of water, lyophilized, and subjected to configurational analysis as described (12).

RESULTS AND DISCUSSION

The U54 methyl-deficient tRNA used in this study was derived from a strain of *E. coli* that did not contain active methylase. This non-conditional mutant displays

a 4 % reduction in growth rate compared to wild type *E coli*, but is fully viable (13). In a control experiment, it was shown that over 95% of the methyl-deficient tRNA was methylated by [^{3}H]-methyl-AdoMet and RUMT. The chiral methyl group from (*methyl-R*)- or (*methyl-S*)-[*methyl*-$^2H_1$, ^{3}H]AdoMet was transferred to U54 of the methyl-deficient tRNA using reagent amounts of RUMT, and the labeled tRNAs were isolated in 23 to 28 % overall yield. The tRNAs were extensively digested with P-1 nuclease and alkaline phosphatase to give a 99% conversion to nucleosides as determined by DEAE-cellulose chromatography. The labeled ribothymidine was then purified by reverse-phase HPLC using a system which separates all nucleosides of tRNA (7) (Fig 1.). The labeled ribothymidine product was isolated in 13 to 14 % overall yield.

The samples of [*methyl*-$^2H_1$,^{3}H] ribothymidine were diluted with carrier thymine and degraded by a Lemieux-von Rudloff oxidation with potassium periodate and a catalytic amount of potassium permanganate (14). The resulting [*methyl*-$^2H_1$,^{3}H]acetic acid products were recovered by distillation or lyophilization, and subjected to configurational analysis (15, 16), using a method routinely employed in one of our laboratories (12). In this procedure (Figure 2), the chiral acetate (excess R or S enantiomer) is phosphorylated, converted to acetyl-coenzyme A with phosphotransacetylase, and subsequently condensed with glyoxylate to form malate in the presence of malate synthase. The latter reaction involves abstraction of a proton from the methyl group of acetyl-Coenzyme A, and due to a large primary kinetic isotope effect (k_H/k_D = 3.8)(17), results in an uneven distribution of tritium between the two methylene hydrogens of the resulting L-malate. Since the methyl group of acetyl-coenzyme A is converted into the methylene of malate with inversion of configuration, (3-R)-L- malate is produced from S-acetate. The L-malate is then converted to fumarate with fumarase, which stereoselectively equilibrates the *pro-3R*

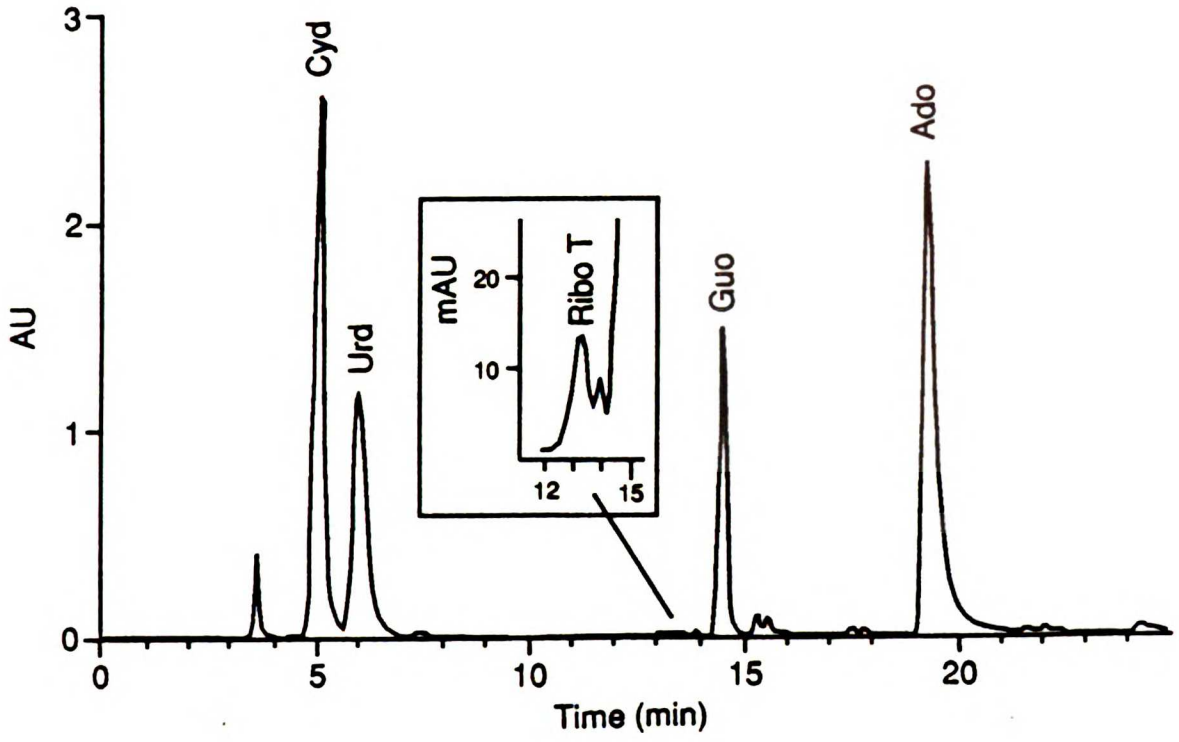

Figure 3.1: Analytical HPLC of nucleosides derived from tRNA methylated at U54 with (*methyl-R*)-[*methyl*-$^{2}H_{1}$,^{3}H] AdoMet. The inset shows an expanded region of the chromatogram corresponding to the elution position of [^{3}H]-labeled Ribo T. The Ribo T elution position was verified by co-injection of an authentic Ribo T standard (data not shown).

hydrogen of L-malate with solvent protons. If tritium is present in the *pro-3R* position of L-malate, it is released into the solvent by fumarase; if it is present in the *pro-3S* position, it is retained in fumarate. The enantiomeric excess (ee) is the percent excess of one enantiomer of the chiral methyl group in the product, as described by equation 1.

$$ee = \text{enantiomeric excess} = \frac{|[methyl\text{-}R] - [methyl\text{-}S]|}{[methyl\text{-}R] + [methyl\text{-}S]} \times 100\ (\%) \qquad (1)$$

The percentage of tritium retention in fumarate is called the F value and, by calibration of the assay procedure, has been shown to be related to the ee by

equation 2. For this assay, stereochemical purity (i.e. 100 % ee) is defined as a deviation of 29 from the 50 % (racemic) value(16).

$$ee(\%) = [|50 - F| \times 100] / 29 \qquad (2)$$

Hence, chirally pure R acetate will give an F value of 79 and chirally pure S-acetate will give an F value of 21. The results of the chirality analyses are shown in Table 1. Isolation of acetate by lyophilization rather than distillation gave slightly higher ee values, probably because heating in strong base causes some exchange of the chiral acetate samples (18).

The data in Table 1 clearly show that the methyl group transfer catalyzed by tRNA (m^5U54)-methyltransferase proceeds with inversion of configuration of the methyl group. This is consistent with a mechanism of methyl transfer that involves S_N2 attack of the C5 of U54 on the methyl group of AdoMet. The results rule out a mechanism which might occur by two sequential displacements at the methyl group, first by a nucleophile of the enzyme, and then by the U54, since this should give overall retention of configuration of the methyl group (Scheme II, chater 3). The data also argue against formation of a stable carbonium ion since an exposed carbonium ion would have resulted in racemization; however, a carbonium ion stabilized by the enzyme as an ion pair, *albeit* unlikely, cannot be ruled out.

Although the tRNA substrate used in this study lacked ribothymidine, there is good evidence that its structural features are homologous to those of yeast $tRNA^{Phe}$. First, unmodified and fully processed yeast $tRNA^{Phe}$ have similar tertiary interactions (19). Notably, both the U54-A58 and U55-G18 tertiary contacts are preserved in the unmodified tRNA. Second, since Ψ55 is present in the methyl deficient tRNA (20), the local base stacking arrangement

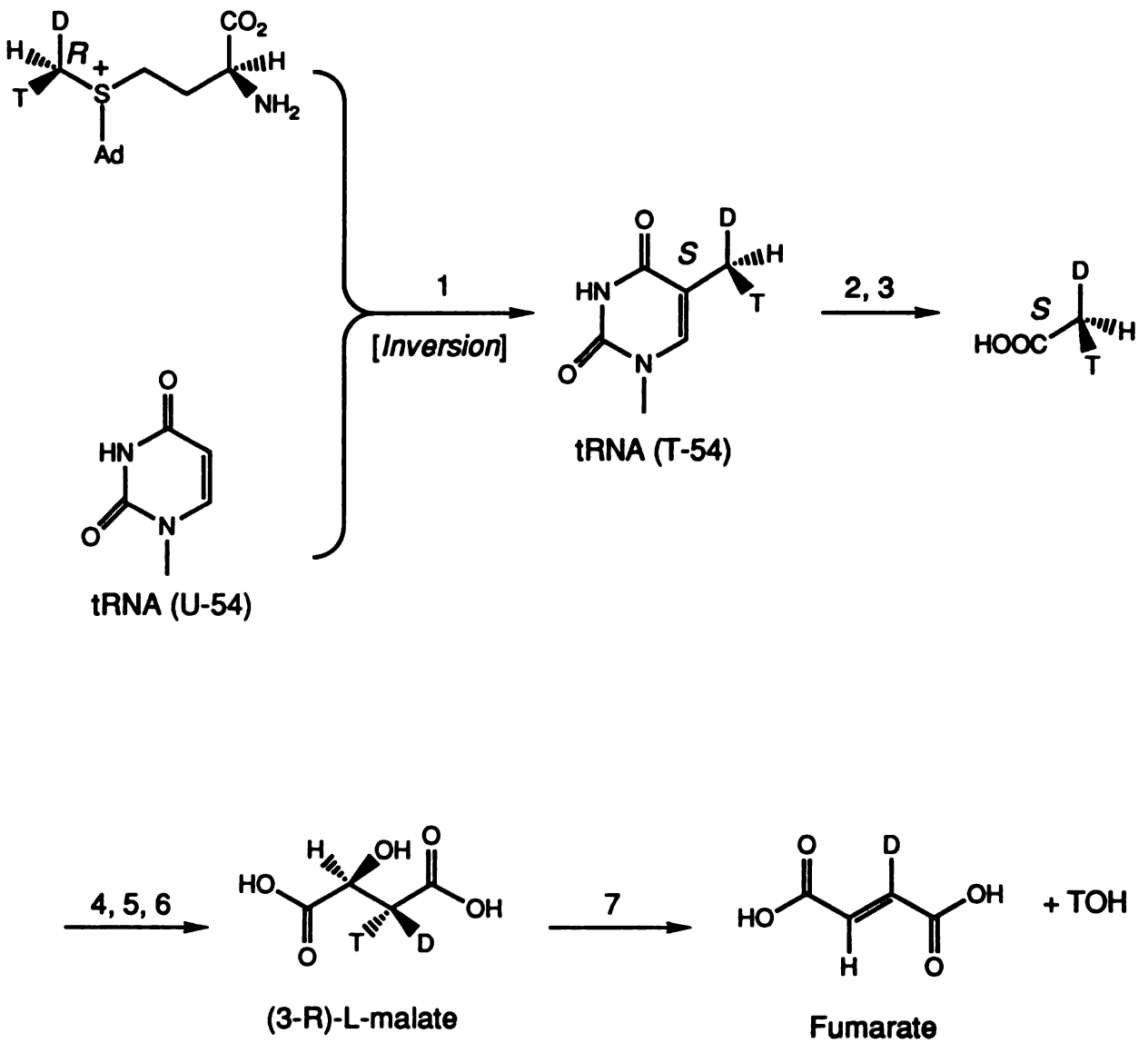

Figure 3.2. Methylation of tRNA with (*methyl-R*)-[*methyl*-$^{2}H_1$,^{3}H] AdoMet, degradation to chiral acetate, and synthesis of malate. 1, tRNA (m^5U54)-Methyltransferase; 2, nuclease, phosphatase, HPLC; 3, KIO_4, $KMnO_4$; 4, Acetate kinase, ATP; 5, Phosphotransacetylase, CoASH; 6, Malate synthase, glyoxylate; 7, Fumarase.

in this RNA is probably the same as that observed in yeast $tRNA^{Phe}$. In the crystal structure of yeast $tRNA^{Phe}$ U54 stacks between adjacent bases G53 and Ψ55, and as a result C5 and C6 of U54 are buried. Solvent accessibility calculations have shown that C5 is 95% buried and C6 is completely solvent

Table 3.1. Stereochemical Analysis of the tRNA (m^5U54)-methyltransferase Reaction.

Substrate	F Value[e] (acetate)	% ee
(*methyl-R*)-[*methyl*-$^2H_1$,^3H] AdoMet[c]	25.9[a]	83
	23.8[b]	90
(*methyl-S*)-[*methyl*-$^2H_1$,^3H] AdoMet[d]	73.8[a]	82
	80.1[b]	100

[a] Acetate as recovered by distillation.

[b] Acetate as recovered by lyophilization.

[c] 91% ee.

[d] 86% ee.

[e] F values are accurate to about ± 2 under the assay conditions used

inaccessible. We have previously concluded that in order to form the covalent adduct between C6 of U54 and Cys 324, RUMT must facilitate opening of the T-loop of tRNA (3). The results of this study suggest additional structural constraints on reactive intermediates. That is, the C5 anion of the U54 adduct of tRNA must be positioned to accommodate an S_N2 transition state in which the *p*-orbital of C5 of the U54 adduct, the methyl group, and the sulfur of AdoMet are co-linear for S_N2 displacement. (21).

A number of methyltransferases have been examined for the steric course of the methyl group transfer. In a compilation of thirteen such reactions, eleven proceeded by inversion of configuration and two with retention (18). The

two enzymes studied which catalyze N- or C-methylation of DNA bases both proceed with inversion. RUMT is the first RNA modification enzyme for which the steric course of methyl transfer has been determined. Our results clearly show that the steric course conforms to the majority of the methyltransferases thus far studied in that methyl transfer occurs with inversion of configuration.

REFERENCES

1. M. Sprinzl, J. Moll, F. Meissner and T. Hartmann, *Nucleic Acids Res.* **13**, r1-r49 (1985).

2. D. V. Santi and L. W. Hardy, *Biochemistry* **26**, 8599-8606 (1987).

3. J. T. Kealey and D. V. Santi, *Biochemistry* **30**, 9724-9728 (1991).

4. R. W. Woodard, L. Mascaro, R. Horhammer, S. Eisenstein and H. G. Floss, *J. Amer. Chem Soc.* **102**, 6314-6318 (1980).

5. R. W. Woodard, M.-D. Tsai, H. G. Floss, P. A. Crooks and J. K. Coward, *J. Biol. Chem* **255**, 9124-9127 (1980).

6. J. Sambrook, E. F. Fritsch and T. Maniatis, *Molecular Cloning, A laboratory Manual* (Cold Spring Harbor Laboratory Press, 1989).

7. M. Buck, M. Connick and B. N. Ames, *Anal. Biochem.* **129**, 1-13 (1983).

8. X. Gu and D. V. Santi, *DNA and Cell Biology* **9**, 273-278 (1990).

9. M. M. Bradford, *Anal. Biochem.* **72**, 248-254 (1976).

10. J. Y. Khym, *Clin. Chem.* **21**, 1245-1252 (1975).

11. A. L. Pogolotti and D. V. Santi, *Anal. Biochem.* **126**, 335-345 (1982).

12. H. G. Floss and M.-D. Tsai, *Adv. Enzymol.* **50**, 243-302 (1979).

13. G. R. Bjork and F.C. Neidhardt, *J. Bacteriol.* **124**, 99-111 (1975).

14. R. U. Lemieux and E. von Rudloff, *Canad. J. Chem.* **33**, 1701-1709 (1955).

15. J. W. Cornforth, J. W. Redmond, H. Eggerer, W. Buckel and C. Gutschow, *Nature (London)* **221**, 1212-1213 (1969).

16. J. Lüthy, J. Retey and D. Arigoni, *Nature (London)* **221**, 1213-1215 (1969).

17. H. Lenz and H. Eggerer, *Eur. J. Biochem.* **65**, 237-246 (1976).

18. D. K. Ho, J. C. Wu, D. V. Santi and H. G. Floss, *Arch. Biochem. and Biophys.* **284**, 264-269 (1991).

19. K.B. Hall, J.R. Sampson, O.C. Uhlenbeck, and A.G. Redfield, *Biochemistry* **28**, 5794-5801 (1989)

20. S. Yang, E.R. Reinitz, and M.L. Gefter, *Arch. Biochem. and Biophys* **157**, 55-62 (1973).

21. J. March, *Advanced Organic Chemistry* (John Wiley & Sons, Inc., 1985), p. 258.

CHAPTER 4

High Level Expression and Rapid Purification of tRNA (m^5U54)-methyltransferase [1]

(A published account of this work appears as: *High Level Expression and Rapid Purification of tRNA (m^5U54)-methyltransferase* , James T. Kealey and Daniel V. Santi. *Protein Expression and Purification* **5**: 149-152)

ABSTRACT

We report an extremely high-level expression system for tRNA (m^5U54)-methyltransferase (RUMT), and a purification strategy which routinely yields 20 to 50 mg of homogeneous RUMT per liter of *E. coli* cells. The RUMT gene (trmA) was cloned into a pET vector and transformed into *E. coli* BL21 (DE3) cells. Following induction, this system produces active enzyme at a level approaching 50% of the total soluble protein. A purification scheme consisting of DEAE-cellulose chromatography to remove nucleic acids, followed by phosphocellulose chromatography, provides homogeneous enzyme. The entire procedure, from cell growth to purified enzyme, takes less than two days. This represents a significant improvement over the previously published expression/purification protocol for RUMT (Gu, X and Santi, D. V. (1991) *Protein Expression and Purification* **2** 66-68), which typically nets 5 to 10 -fold less enzyme per liter of cells and is substantially more labor intensive.

INTRODUCTION

We are studying the structure and mechanism of *E. coli* RUMT[1], both in terms of the chemistry of transmethylation and protein/RNA recognition (Santi and Hardy, 1987; Kealey et al., 1991; Kealey and Santi, 1991; Gu and Santi, 1992; Gu and Santi, 1991). We have begun crystallization trials of the enzyme and are investigating the RUMT-RNA interaction by ^{19}F and ^{1}H nmr spectroscopy. For structural studies large quantities of highly purified RUMT are required. In this paper, we report high level expression and rapid purification of RUMT, which should greatly facilitate mechanistic and biophysical studies of this enzyme.

MATERIAL AND METHODS

E. coli GB1-5-39/pTN102 was a gift from Glenn Bjork, University of Umea, Umea, Sweden. The T7 expression system, *E. coli* BL21(DE3)/pET-15b, was obtained from Novagen. Restriction enzymes and corresponding buffers were obtained from New England Biolabs (NEB), and all restriction digests were performed in buffers recommended by NEB. T-4 DNA polymerase and T-4 DNA ligase were obtained from Boehringer Mannheim. Phosphocellulose P11 and DEAE-cellulose (DE-52) were obtained from Whatman, and the resins were prepared as recommended by the manufacturer. Cell lysis buffer consisted of 2 mM DTT, 0.1 mM EDTA, 10 % glycerol (v/v) (Buffer 1), containing 150 mM potassium phosphate, pH 6.8 (13.5 mS, room temperature); phosphocellulose

[1] Abbreviations used: RUMT, *E. coli* tRNA (m^5U54)-methyltransferase; SDS-PAGE, sodium dodecyl sulfate polyacrylamide gel electrophoresis; IPTG, Isopropylthio-β-Galactoside; LB, Luria Broth; LB/amp, Luria Broth containing 100 μg/ ml ampicillin; dNTP, deoxynucleotide triphosphates; AdoMet, *S*-adenosyl-L-methionine.

buffer A consisted of Buffer 1 containing 100 mM potassium phosphate, pH 6.8 (9 mS, room temperature); phosphocellulose buffer B consisted of Buffer 1 containing 500 mM potassium phosphate, pH 7.2 (42 mS, room temperature). All molecular biology procedures not specifically outlined were according to Sambrook *et al.* (Sambrook et al., 1989). RUMT activity assays were performed essentially as described (Santi and Hardy, 1987), except all assays were performed at room temperature. SDS-PAGE (10 - 15% acrylamide gradient) was performed on a Pharmacia Phast System and gels were stained with Coomassie R-250.

Construction of the High-Level RUMT Expression Vector. One μg of pTN102 DNA was digested to completion with 12 units of *Eco*R V in a 10 μl reaction mixture. The *Eco* R V restricted DNA was further digested with 5 units of *Bsp*H I, the reaction was terminated by phenol extraction, and the DNA was recovered by ethanol precipitation. Two μg of pET-15b was digested to completion with 15 units of *Xho* I and the overhangs were filled in by incubating the DNA in a 17 μl reaction mixture, containing 2 mM dNTPs and 2 units of T-4 DNA polymerase. The reaction was terminated by phenol extraction and the DNA was recovered by ethanol precipitation. To generate a cloning site compatible with the *Bsp*H I restricted pTN102 DNA, the pET DNA was further digested with 20 units of *Nco* I in a 20 μl reaction mixture.

Approximately 150 ng of *Eco*R V/*Bsp*H I digested pTN102 and about 100 ng of linearized pET vector were ligated in a 20 μl reaction mixture, containing 20 units of DNA ligase. After 16 hours of incubation at 15°, 2 units of *Sac* II and 5 units of *Nco* I were added to the ligation mixtures, and the samples were incubated for 1 hour at 37°, followed by 20 minutes at 65°. One microliter from each reaction mixture was used to transform DH5α cells by the standard heat

shock procedure. Following transformation, 1 ml of LB was added to the cells and they were incubated for 30 minutes at 37°. The cells (50 µl and 200 µl of the 1 ml total) were spread on LB/ amp plates. The plate spread with 50 µl of cells yielded 15 colonies for vector plus insert and 6 colonies for vector alone (i.e. ligation without RUMT gene insert).

Twelve culture tubes, each containing 2 ml of LB/amp, were inoculated with random chosen colonies from the plate spread with 200 µl of transformed DH5α, and the cultures were incubated overnight at 37°. The plasmid DNA was liberated by phenol/$CHCl_3$ extraction, purified by ethanol precipitation, and the DNA pellets were dissolved in 20 µl of water. The plasmids were linearized with *Sac* I and analyzed on a 1% agarose gel. The electrophoretic mobility of two of the 12 linear plasmids was consistent with a combined size of the pET vector plus RUMT gene insert (6877 bp). The two plasmids of correct size were digested with *Xba* I and *Bam* H I, and one of the plasmids [pJKtrmA (pET-15b)] yielded the RUMT gene insert (1343 bp).

Expression and Purification of RUMT. pJKtrmA (pET-15b) was used to transform BL21(DE3) cells, and the transformation mixture was spread on LB/ amp plates. A single colony was picked and grown overnight in 2 ml of LB/ amp at 37°. LB/ amp (1 L) was inoculated with the overnight culture and the 1L culture was grown until the A_{600} reached 0.685, and then the synthesis of T-7 RNA polymerase was induced by addition of IPTG (1 mM final concentration) (Studier et al., 1990). The induced culture was grown for 3 hours at 37°, and the cells were harvested by centrifugation at 5000 xg for 20 minutes.

Cells from 660 ml of induced pJKtrmA (pET-15b) were suspended in 15 ml of cold lysis buffer, lysed by two passages through a French pressure cell at 18,000 psi, and the cellular debris was removed by centrifugation at 18,000xg

for 20 minutes (all steps were performed at 4°). The supernatant was loaded onto a 10 mL DEAE-cellulose column (2.5 x 10 cm) (ca. 2 ml/ minute), equilibrated with cell lysis buffer. The column was washed with 30 ml of cell lysis buffer and the load/ wash fraction (45 ml) which contained RUMT was collected. To the load/ wash fraction was added an equal volume of cold water, such that the final conductivity of the diluted sample was less than 9 mS (4°). This fraction was loaded onto a 37 ml phosphocellulose column (2.5 x 20 cm), equilibrated with phosphocellulose buffer A. The column was washed with 100 ml of buffer A (until A_{280} reached the baseline; 2-3 column volumes). The protein was eluted with a five column volume linear gradient to 100 % phosphocellulose buffer B, and 4 ml fractions were collected. Fractions were screened for protein by the Bradford assay (Bradford, 1976), for activity by the standard assay, and for purity by SDS-PAGE. Based on the SDS-PAGE data, the purest fractions from the phosphocellulose column were pooled and dialyzed against 20 mM potassium phosphate, pH 7.2, 10 % glycerol, 0.1 mM EDTA, and 1 mM DTT. In one experiment, the dialyzed phosphocellulose fraction was further purified by tRNA affinity chromatography as described (Gu and Santi, 1991), except Mg^{2+} was eliminated from all buffers.

RESULTS and DISCUSSION

Construction of the High-Level RUMT Expression Vector. The strategy for introducing the RUMT gene (trmA) into pET-15b is shown in Figure 4.1. pET15b contains an *Nco* I site at the ATG initiation codon. Since we required a blunt end site to accomodate the 3' end of the RUMT gene, pET-15b was first cut with *Xho* I, and the overhang was filled in with T-4 DNA polymerase and dNTPs. The

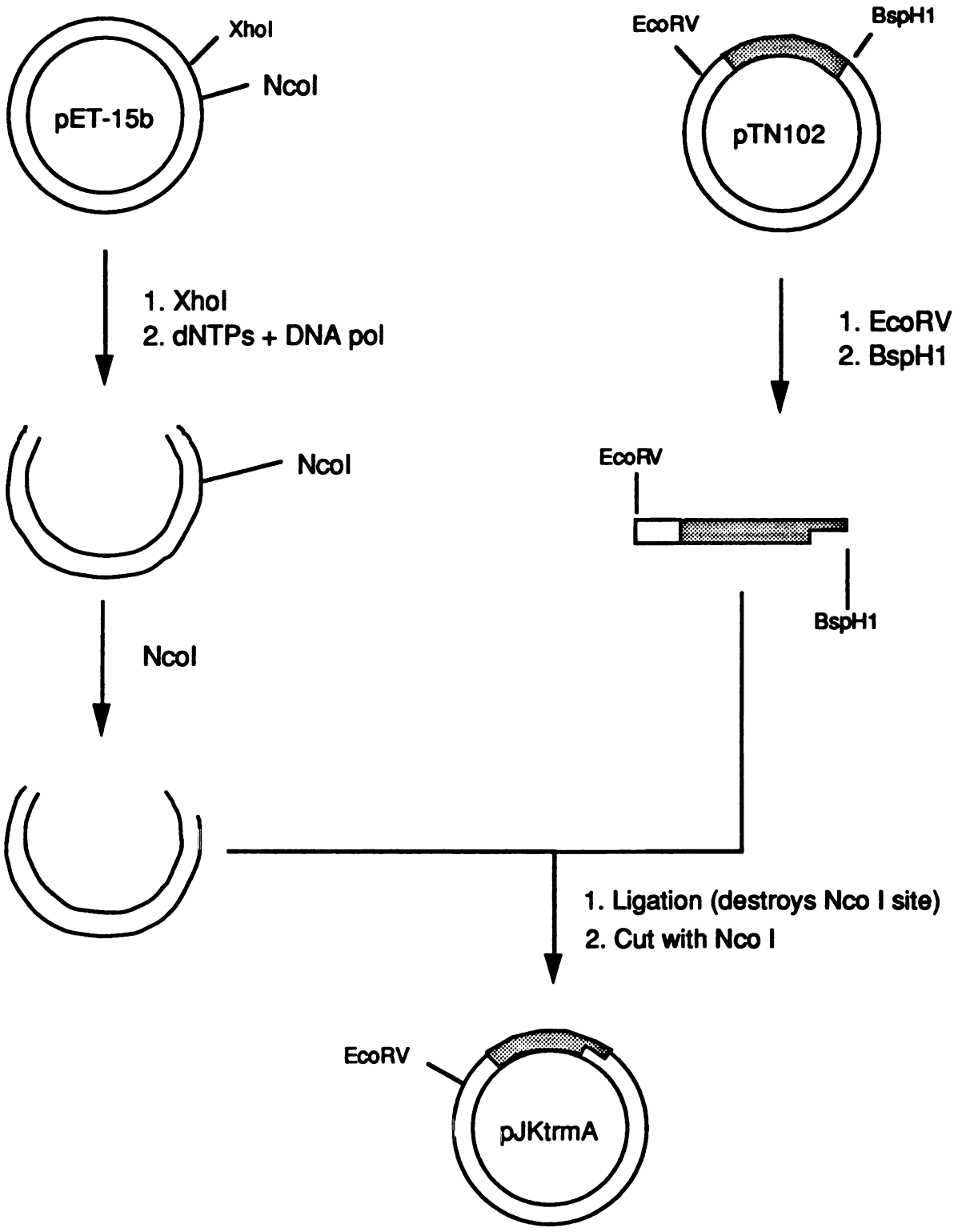

Figure 4.1. Strategy for the construction of the pJKtrmA (pET-15b) expression vector. The shaded bars indicate the TrmA (RUMT) coding sequence.

filled-in vector was next cut with *Nco* I, producing a vector with an overhang at the ATG site and a blunt end. The plasmid pTN102, carrying trmA, contained a *Bsp*H I site at the ATG inititation codon. Since *Nco* I and *Bsp*H I share compatible cohesive ends, the *Bsp*H I/*Eco*R V restricted trmA gene could be directly inserted into the *Nco* I/blunt-end vector. Following ligation the resulting plasmid pool was cut again with *Nco* I to destroy vector not containing the trmA insert (introduction of trmA destroys the *Nco* I site), and with *Sac* II to destroy uncut pTN102 (a *Sac* II site is present in the non-coding region of pTN102, but not in pET). The resulting plasmid pool was transformed into DH5α cells, and the clones were screened for the trmA insert by restriction analysis. One of 12 colonies selected for restriction analysis contained a plasmid carrying the trmA gene. This plasmid, pJKtrmA (pET-15b), was transformed into BL21 (DE3) cells for expression of RUMT. Upon induction with IPTG, these cells expressed RUMT at a level approaching 50% of the soluble cellular protein (Figure 4.2).

Purification of RUMT. The previously reported purification procedure for RUMT consisted of cell lysis, polyethyleneimine precipitation, ammonium sulfate precipitation, phosphocellulose chromatography, tRNA affinity chromatography, and finally DEAE-cellulose chromatography (Gu and Santi, 1990). Given the substantial expression of RUMT in BL21(DE3)/pJKtrmA (pET-15b), we sought to streamline purification by eliminating time consuming chromatographic steps and dialyses. First, we attempted to load the crude cell lysate directly onto phosphocellulose and thereby eliminate four steps of the original purification strategy. However, the crude lysate did not adsorb to the phosphocellulose column, probably because the extract's high nucleic acid content interfered with adsorption of RUMT to the column matrix. Nucleic acids could be removed by passing the extract (in 150 mM phosphate buffer) through a DEAE-cellulose

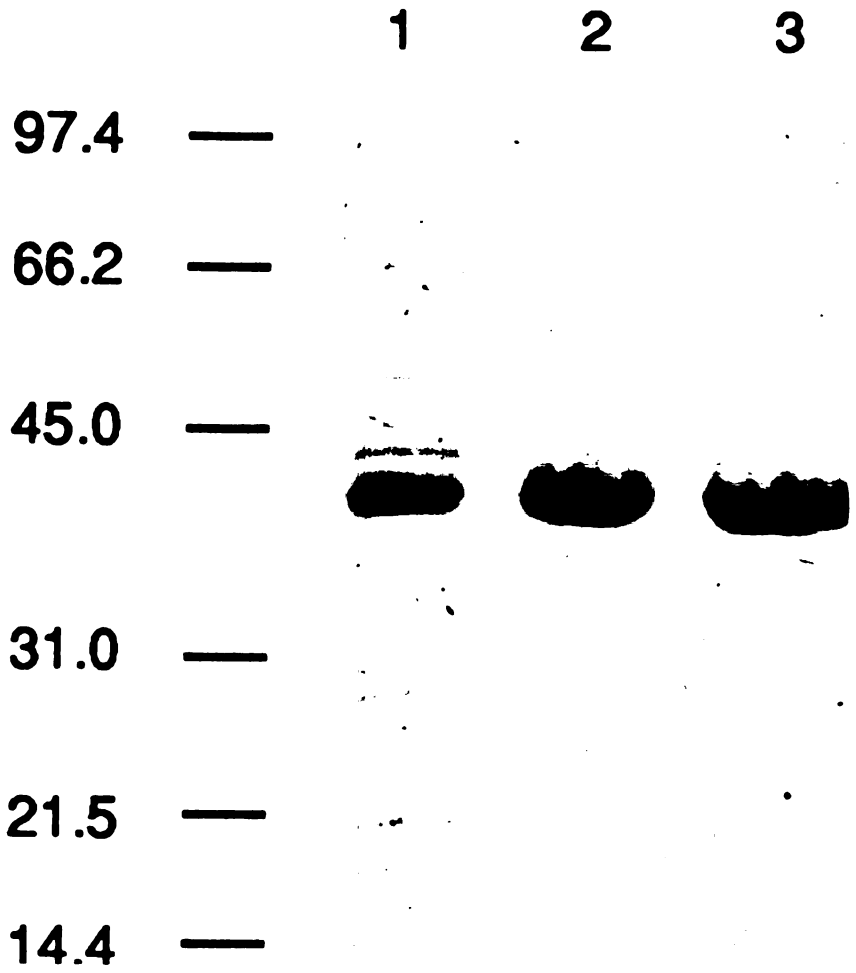

Figure 4.2. SDS-PAGE of samples from a typical RUMT purification: Lane 1, crude extract; Lane 2, phosphocellulose chromatography pool; Lane 3, pool after combined phosphocellulose chromatography and tRNA affinity chromatography. The positions of protein standards are indicated in kDs.

TABLE 4.1

Purification of RUMT from a 660 ml culture of BL21 (DE3)/pJKtrmA (pET15-b)

Fraction	Volume (ml)	Protein (mg)	Units (nmoles/ min)	Specific Activity (Units/mg)	Yield (%)
Crude extract	15.0	64.5	83.9	1.30	100
DEAE-cellulose	90.0	60.0	78.0	1.30	92
Phosphocellulose pool	48.0	30.0	49.6	1.65	59

column. Under these conditions RUMT flowed through and nucleic acids adsorbed to the column. After diluting the flow-through fraction with an equal volume of water, most of the RUMT adsorbed to the phosphocellulose column (see Table 4.1). After washing the phosphocellulose column with equilibration buffer, a five -column volume linear gradient from 100 mM potassium phosphate, pH 6.8 to 500 mM potassium phosphate, pH 7.2 was implemented and RUMT eluted at ca. 270 to 400 mM potassium phosphate. The RUMT in the pooled fractions was homogeneous, as judged by Coomassie-stained SDS-PAGE (Figure 4.2), and the specific activity was similar to that reported previously for homogeneous RUMT (Gu and Santi, 1990). Since the phosphocellulose column alone yielded enzyme of similar quality to that obtained by combined phosphocellulose- tRNA affinity chromatography (Figure 4.2), the affinity chromatography step was eliminated.

5-fluorouracil substituted tRNA (FUtRNA) is a potent mechanism based inhibitor of RUMT, and in the presence of AdoMet, forms a covalent complex with RUMT, which shifts its mobility on SDS-PAGE from a 42 kD free enzyme to a ca. 60 kD complex (Kealey and Santi, 1991). Active site titration of RUMT with FUtRNA indicated that greater than 95 % of the purified RUMT preparation was able to form the the 60 kD complex (see Figure 1.2).

Using the above purification scheme, the recovery of RUMT has ranged from 20 mg to over 50 mg of pure protein per liter of *E. coli*. The lower yields of enzyme were due to failure of RUMT to stick to the phosphocellulose column, and better yields are obtained if the flow through fraction is recirculated over the column.

This expression system and purification protocol represent a significant improvement over previously published expression/purification schemes for RUMT (Gu and Santi, 1990; Gu and Santi, 1991). Notably, this strategy avoids

the polyethyleneimine precipitation, where nearly 50% of RUMT is lost in the inextractable precipitate (Gu and Santi, 1990). In the past it took approximately two weeks to obtain 4 to 5 mg of RUMT per liter of cells. We now routinely obtain 20 to 50 mg of homogeneous RUMT per liter of *E. coli* in less than two days. The expression system and purification strategy reported here for *E. coli* RUMT will greatly facilitate ongoing mechanistic and biophysical studies of this enzyme.

ACKNOWLEDGMENT

We thank Patricia Greene for many helpful suggestions on cloning strategies.

RERERENCES

Bradford, M. M. (1976). *Anal. Biochem.* **72**: 248-254.

Gu, X. and D. V. Santi (1990). High-Level Expression of *Escherichia coli* tRNA (m^5U54)-Methyltransferase. *DNA and Cell Biology* **9**: 273-278.

Gu, X. and D. V. Santi (1991). Affinity Chromatography of Escherichia coli tRNA (m^5U54)-methyltransferase on tRNA-Agarose. *Protein Expression and Purification* **2**: 66-68.

Gu, X. and D. V. Santi (1991). The T-arm Is a Substrate for tRNA (m^5U54)-Methyltransferase. *Biochemistry* **30**: 2999-3002.

Gu, X. and D. V. Santi (1992). Covalent Adducts Between tRNA (m5U54)methyltransferase and RNA substrates. *Biochemistry* **31**: 9788.

Kealey, J. T., S. Lee, H. G. Floss and D. V. Santi (1991). Stereochemistry of methyl transfer catalyzed by tRNA (m^5U54)-methyltransferase-- evidence for a single displacement mechanism. *Nuc. Acid. Res.* **19**: 6465-6468.

Kealey, J. T. and D. V. Santi (1991). Identification of the Catalytic Nucleophile of tRNA (m5U54)-methyltransferase. *Biochem* **30**: 9724-9728.

Sambrook, J., E. F. Fritsch and T. Maniatis (1989). Molecular Cloning. A laboratory Manual. Cold Spring Harbor Laboratory Press.

Santi, D. V. and L. W. Hardy (1987). Catalytic Mechanism and Inhibition of tRNA (Uracil-5-) methyltransferase: Evidence for Covalent Catalysis. *Biochemistry* **26**: 8599-8606.

Studier, F. W., A. H. Rosenberg, J. J. Dunn and J. W. Dubendorff (1990). Use of T7 RNA Polymerase to Direct Expression of Cloned Genes. *Meth. Enzym.* **185**: 60-89.

CHAPTER 5

The Stereochemistry of Nucleophilic Addition of tRNA (m^5U54)-methyltransferase as Assessed by ^{19}F NMR Spectroscopy

James T. Kealey and Daniel V. Santi*

Departments of Pharmaceutical Chemistry and of Biochemistry and Biophysics

University of California, San Francisco, CA. 94143-0448

ABSTRACT

tRNA (m^5U54)-methyltransferase (RUMT) catalyzes the methylation of uridine 54 (U54) of tRNA by *S*-adenosyl-L-methionine (AdoMet). The catalytic mechanism involves the formation of a transient covalent adduct between RUMT and tRNA, in which Cys 324 of RUMT is bound to C_6 of U54 and C_5 of U54 is methylated. We used a substrate analog, containing a fluorine at the 5-position of U54, to trap the covalent adduct, which was analyzed by ^{19}F NMR spectroscopy. The ^{19}F spectrum of the adduct consisted of an overlapping doublet of quartets, which confirmed the previously proposed structure of the adduct and provided information on the stereochemistry of the nucleophilic addition reaction. Based on the magnitude of three-bond H_6-F coupling constant (J_{H6-F}, 4 Hz), we deduced that Cys 324 of RUMT and the methyl from AdoMet added to U54 in *cis* fashion, and the subsequent elimination was *trans*. Together with previous studies, the data presented here enable a complete chemical mechanism of RUMT-catalyzed methylation of U54 in tRNA to be proposed.

INTRODUCTION

tRNA (m^5U54)-methyltransferase (RUMT[2], EC 2.1.1.35) catalyzes the AdoMet dependent methylation of U54 in the TΨC-loop of all *Escherichia coli* tRNAs, and in a 17 nucleotide oligomer corresponding to the T-arm of tRNA (Gu and Santi, 1991). Although many aspects of the mechanism are understood, stereochemical details are lacking. Such information is necessary to completely describe the chemical mechanism and to provide insight into RUMT-RNA-AdoMet interactions that contribute to catalysis. In this study, we employ ^{19}F NMR spectroscopy to elucidate the stereochemistry of addition of Cys 324 and the methyl moiety to a fluorinated T-arm analog, which functions to trap the methylated RUMT-RNA intermediate.

When fluorine is substituted for hydrogen at the 5-position of U54, RUMT forms an irreversible, covalent complex with the FURNA in the presence of AdoMet (Scheme II, Chapter 1)(Santi and Hardy, 1987). Because fluorine cannot be abstracted as F^+, the Michael adduct is trapped as the RUMT-FURNA-CH_3 complex. This trapped adduct mimics a steady state intermediate on the reaction pathway and is therefore a valuable tool for studying the mechanism of RUMT. Previously, this inhibitory complex was used to identify Cys 324 of RUMT as the nucleophilic catalyst (Chapter 2, Kealey and Santi, 1991).

---

[2]Abbreviations: RUMT, tRNA (m^5U54)-methyltransferase; m^5U54, 5-methyluridine at position 54 of tRNA; AdoMet, *S*-adenosyl-L-methionine; AdoHcy, *S*-adenosyl-L-homocysteine; FURNA, tRNA or T-arm of tRNA, containing 5-fluorouridine in place of uridine at position 54; FUtRNA, tRNA with the substitution of 5-fluorouridine for all uridines; dFUT-arm, T-arm analog in which U54 is replaced with 5-fluoro-2'-deoxyuridine (see Figure 1); RUMT-FURNA-CH_3, covalent complex containing RUMT, FURNA and the methyl derived from AdoMet; TS-FdUMP-CH_2H_4folate, covalent complex consisting of thymidylate synthase (TS), methylenetetrahydrofolate, and 5-fluoro-2'-deoxyuridine-5'-monophosphate; SDS, Sodium Dodecyl Sulfate; EDTA, Ethylenediaminetetraacetic acid; DTT, Dithiothreitol; PAGE, Polyacrylamide gel electrophoresis; DEAE, Diethylaminoethyl; CPG, controlled pore glass; TBAF, tetrabutylammonium fluoride; THF, tetrahydorfuran.

The RUMT-FURNA-CH_3 complex is also amenable to ^{19}F NMR spectroscopy. ^{19}F is a spin 1/2 nucleus with an NMR sensitivity of 83% of a proton. Moreover, since protein is devoid of fluorine, resonances from the protein will not contribute to signal overlap, as is often the case with proton NMR. Valuable structural and stereochemical information can be derived from the ^{19}F NMR spectrum of the covalent adduct. The magnitude of the three-bond H_6-F coupling contstant (J_{H6-F}) can be used to distinguish the isomer in which H_6 and F are *trans* from that in which H_6 and F are *cis*. When J_{H6-F} is a maximum value (30-40 Hz), then H_6 and F exist in a *trans* arrangement, whereas when J_{H6-F} is a minimum value (5 Hz), then H_6 and F are *cis*.

Using an RNA substrate containing a single FU at position 54, we prepared the RUMT-FURNA-CH_3 covalent complex. ^{19}F NMR analysis of the protease and nuclease digested complex yielded a signal consisting of a doublet of quartets, with a minimum J_{H6-F}. From the splitting pattern of the ^{19}F NMR spectrum, we confirmed the structure of the proposed intermediate **3** (Scheme II, Chapter 1), and deduced that addition of the catalytic nucleophile and the methyl electrophile to the pyrimidine occurs by the *cis* route. To date the steric course of nucleophilic addition has been determined for two mechanistically related enzymes, thymidylate synthase and *Hha*I methylase. In both cases, the reaction occurs by the *trans* route. The stereochemistry of the RUMT reaction represents the first example of *cis* addition to a pyrimidine, catalyzed by a C-5 methylase. Together with previous work, the data presented here allow us to describe a complete chemical mechanism of RUMT catalyzed methylation of U54 in tRNA.

MATERIALS AND METHODS

RUMT was prepared as described (Kealey and Santi, 1994). All RNA phosphoramidites and derivatized CPG column supports were purchased from Chemgenes Corporation, Waltham, MA. Phosphoramidites were dissolved in acetonitrile to a final concentration of 0.1 M. Reagents for solid phase RNA synthesis were obtained from Applied Biosystems Inc. (Foster City, CA.). Tetrabutylammonium fluoride was obtained from Aldrich. DEAE was DE-52 from Whatman. α-chymotrypsin was obtained from Worthington. *S*-adenosyl-L-[*methyl*-^{3}H]methionine (71 Ci/mmole) was purchased from Amersham.

Preparation of the RNA Substrate. The T-arm analog, 5' GUGUG(5-Fluoro-2'-deoxyU)UCGAUCCACAC 3' (Figure 5.1), was prepared by solid phase synthesis as follows: DMT ribocytidine-succinyl-aminopropyl CPG resin (0.43 gram, 6.5 μmole C) was loosely packed into a 0.7 x 5 cm column, and RNA synthesis was carried out on an Applied Biosystems 394 oligonucleotide synthesizer, using the 10 μmole RNA synthesis cycle provided by the manufacturer. Because the 0.7 x 5 cm column could only hold 6.5 μmole equivalent of CPG resin, a second round of RNA synthesis was performed as described above, using the remainder of the resin (ca. 0.3 grams). Following synthesis and cleavage from the solid support, base protecting groups were removed by incubating the RNA in 70% NH_4OH/ 30% ethanol (v/v) for 12 hours at 55°C. The ammonia was removed by evaporation with a steady stream of air, and the RNA was dried *in vacuo*. The RNA was dissolved in 1 M TBAF in THF (1 mL of TBAF per μmole RNA) and incubated at 25 °C in the dark for 5 hours. Complete silyl deprotection was verified by C-4 Reverse phase HPLC, as described (Webster et al., 1991). THF was removed by drying the 2' deprotected RNA to one-half its original volume. To the resulting viscous RNA solution were added 3 volumes of 0.3 M ammonium acetate, pH 7.0, and the RNA was

desalted in an Amicon Centriprep 3 concentrator by repeated dilution with ammonium acetate, followed by concentration, until the TBAF was 1.8 % of its original concentration (18 mM final). Tightly bound TBA ions were removed by adsorbing the RNA (3.8 mL) to a 10 mL DEAE column (2.5 x 10 cm), equilibrated with 20 mM Tris/HCl, 50 mM NaCl, pH 8. The column was washed with 45 mL of equilibration buffer, and the RNA was eluted in equilibration buffer, containing 0.5 M NaCl. The RNA (13 mL) was concentrated ca. 6-fold in an Amicon Centriprep 3 Concentrator, and then precipitated by addition of 2.5 volumes of cold 95% ethanol. Approximately 12 ODs of RNA were recovered per µmole of immobilized cytidine.

Formation and Protease and RNAse digestion of the RUMT-dFUT-arm-CH_3 Covalent Complex. A reaction mixture (11.9 mL) containing RUMT (16 mg), dFUTarm (110 ODs), [^{3}H]methyl-AdoMet (1.79 µmole, 0.055 Ci/mmole), 50 mM Tris-HCl, pH 7.6, 1 mM $MgCl_2$, and 1 mM DTT was incubated at room temperature, and the progress of the reaction was monitored by reverse phase HPLC of the free RNA. When all of the RNA had reacted (21 hours of incubation), the sample was clarified by centrifugation, diluted 3.5-fold with D_2O, and concentrated to about 0.5 mL in an Amicon Centriprep 30 concentrator. Formation of the covalent complex was verified by 12 % SDS-PAGE, with Coomassie and ethidium bromide staining, and by ^{19}F NMR (see below).

To the RUMT-dFUTarm-CH_3 covalent complex was added solid urea to a final concentration of 2 M, followed by 20 µl of α-chymotrypsin (200 µg). After 14 hours of incubation at 37 °C, a second aliquot (200 µg) of α-chymotrypsin was added, and the sample was incubated for an additional 8 hours at 37 °C. Upon digestion a large precipitate formed which was collected by centrifugation. The precipitate, which contained 25% of the total RUMT-dFUTarm-CH_3 complex,

was re-suspended in 400 μL of 8 M urea, diluted to 4 M urea with water, and another 200 μg of α-chymotrypsin was added. The sample was incubated at 37° C for 12 hours. The sample was clarified by centrifugation (the precipitate representing 5% of the total complex was discarded), and the supernatants from the chymotrypsin digests were combined, desalted and concentrated to 400 μL in an Amicon Centricon 3 microconcentrator. To the concentrated chymotrypsin digest (400 μl) was added 100 μg RNase A (10 mg/mL), and the sample was incubated overnight at 37°C. Protease and RNAse digestions of the covalent complex were monitored by reverse phase HPLC and ^{19}F NMR spectroscopy.

^{19}F NMR Spectroscopy ^{19}F NMR spectra were obtained at 282 MHz (25 °C) on a GE QE-300 pulsed FT NMR spectrometer, fitted with a 5 mm fluorine probe. For most samples, data were accumulated by using 16,000 data points, a 9 μsec pulse width, 1 sec relaxation delay, and a spectral width of 12,000 Hz. For the final spectrum of the nuclease and protease digested covalent complex, a spectral width of 5,681 Hz was employed. For each NMR experiment, about 16,000 scans were collected and averaged.

RESULTS

The RNA substrate used in this study was the dFU54T-arm analog shown in Figure 5.1. Because it could be synthesized chemically, the T-arm rather than full length tRNA was employed, thus allowing a unique 5FU to be placed at position 54. It was necessary to synthesize the T-arm with the 5-fluorodeoxy analog, because the corresponding 5-fluoro-ribo phosphoramidite was not commercially available. Although RUMT catalyzed methylation of the deoxy-U54 T-arm is 5-fold slower that of the wt T-arm, the reaction is essetial irreversible, and therefore could be driven to completion (J.T. Kealey,

unpublished observation). Solid phase RNA synthesis yielded 120 ODs (ca. 1 μmole) of RNA, following DEAE chromatography and desalting. The RNA was

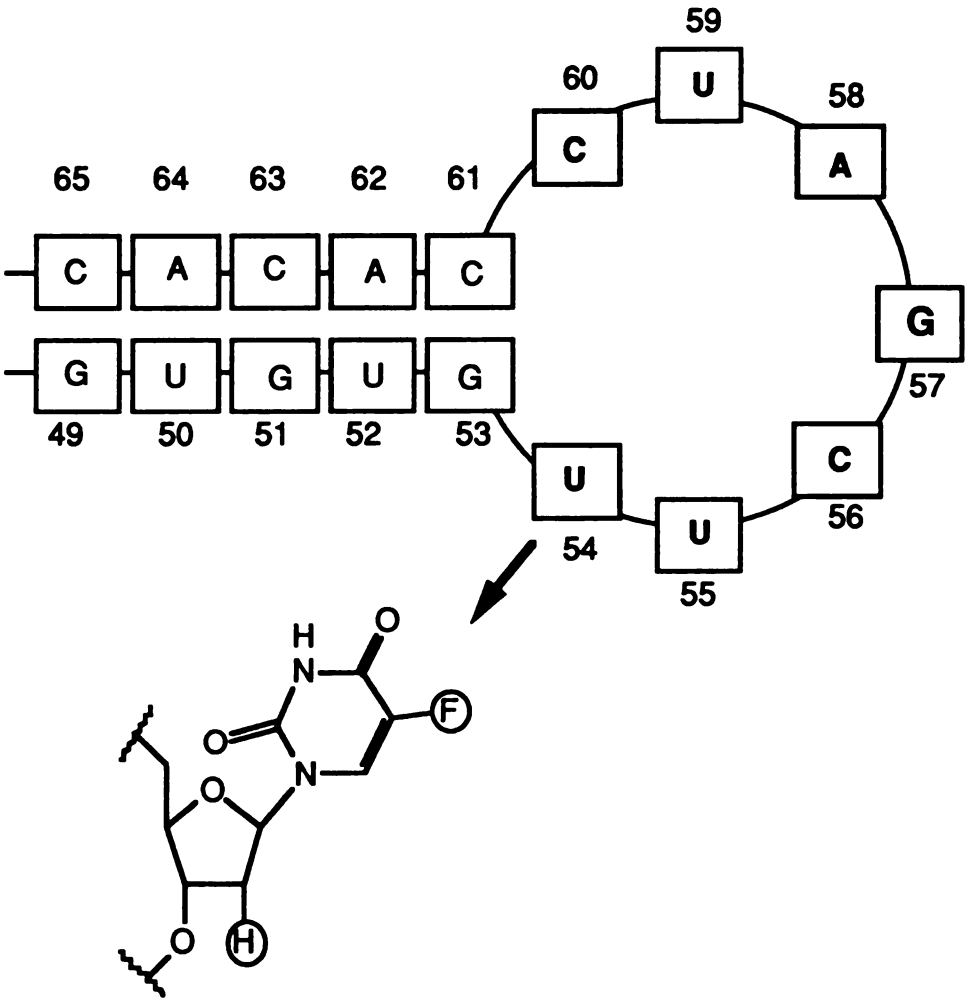

Figure 5.1. Structure of the T-arm analog of tRNA used to form the RUMT-FURNA-CH_3 covalent complex.

70-80% pure, as judged by denaturing PAGE . The formation of the RUMT-dFUTarm-CH_3 complex was followed by HPLC, which showed that >95% of the RNA reacted with RUMT and AdoMet to form the covalent complex. Formation of the covalent complex was also verified by SDS-PAGE and ^{19}F NMR spectroscopy. Upon formation of the RUMT-dFUTarm-CH_3 covalent

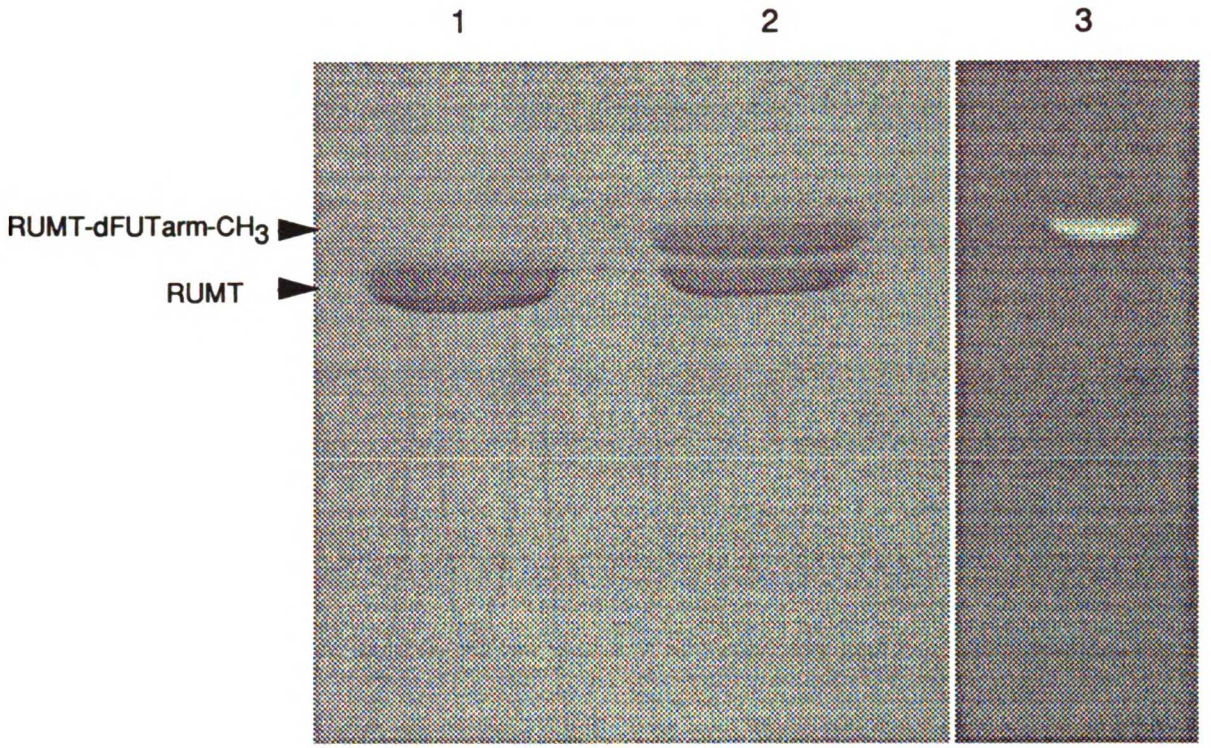

Figure 5.2. SDS-PAGE of the RUMT-dFUTarm-CH_3 covalent complex. Lane 1, RUMT stained with Coomassie R-250; lane 2, RUMT-dFUTarm-CH_3 stained with Coomassie R-250; lane 3, stained with ethidium bromide.

complex, the electrophoretic mobility of RUMT decreased slightly on SDS-PAGE (Figure 5.2). The complex stained with both Coomassie R-250 and ethidium bromide, indicating that it contained protein and nucleic acid. ^{19}F NMR of the complex revealed that all of the free RNA was consumed in the reaction, as evidenced by the disappearance of the ^{19}F resonance associated with free T-arm, and the appearance a new, extremely broad resonance characteristic of a large macromolecular complex.

Because of the severe line broadening associated with the fluorine signal in high molecular weight species, it was necessary to reduce the molecular mass of covalent complex by protease and nuclease digestion, prior

to further ^{19}F NMR experiments. Extensive chymotrypsin and RNAse A digestion of the RUMT-dFUTarm-CH_3 complex yielded a peptide-dFU(nucleotide)-CH_3 complex which was subjected to ^{19}F NMR. The peptide-

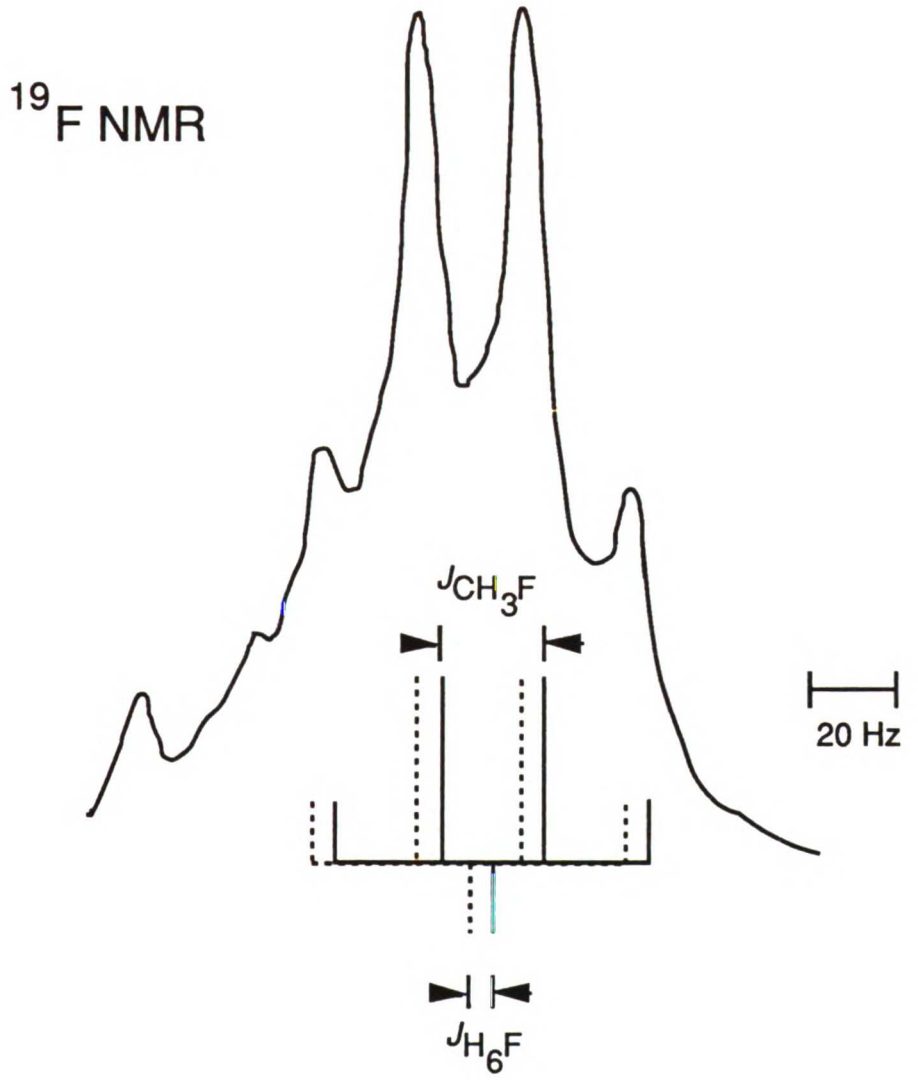

Figure 5.3. ^{19}F NMR spectrum of the peptide-dFU(nucleotide)-CH_3 complex, showing the proposed coupling constants. One of the quartets is represented in dashed lines to emphasize that the quartets overlap.

dFU(nucleotide)-CH_3 adduct yielded a multiplet as the major ^{19}F NMR signal (Figure 5.3), which was resolved into an apparent quartet, or overlapping

doublet of quartets. The theoretical ^{19}F NMR spectrum of the adduct should consist of a doublet of quartets, due to splitting of the ^{19}F signal by H_6 (J_{H6-F}) and by the C_5 methyl protons ($J_{F-C5\alpha H}$). The splitting pattern of the ^{19}F resonance is thus consistent with the proposed structure of the covalent adduct, **2.1** (Santi and Hardy, 1987; Kealey and Santi, 1991). The distance between the lines of the doublet (J_{H6-F}) depends on the dihedral angle between H_6 and F, and this dependence is described by the empirical Karplus equation (see, for example, Byrd et al., 1978). Maximum values of J_{H6F} (34-40 Hz) will be observed when the H_6-F dihedral angle is 180°, whereas a dihedral angle of 60-90° yields a minimum J_{H6F} (< 5 Hz) (Figure 5.4). Bovey et al. (1964) demonstrated that for fluorocyclohexanes the vicinal fluorine-proton coupling constants $J_{F_{eq}H_{eq}}$, $J_{F_{eq}H_{ax}}$, $J_{F_{ax},H_{eq}}$ were all less than 3-4 Hz, whereas $J_{F_{ax}H_{ax}}$ was 43.4 Hz. Moreover, the *trans* fluorine-proton vicinal coupling constant for $CHCl_2CHFCl$ is 38.0 Hz, while the *gauche* fluorine-proton coupling constant is 2.8 Hz (Gutowsky et al., 1962).The nuclease and protease digested *trans* adduct is expected to yield a maximum J_{H6F}, since H_6 and F are diaxial, with dihedral angle of 180° (Figure 5.4, path a). In the *cis* adduct, however, there is no conformation that places H_6 and F in a diaxial arrangement: either H_6 is axial and F is equatorial, or H_6 is equatorial and F is axial (Figure 5.4, path b). In either case, the H_6-F dihedral angle will be 60° and a minimum J_{H6F} will be observed. The magnitude of J_{H6F} can thus be used to distinguish *cis* from *trans* addition.

Shown in Figure 5.5a is the theoretical spectrum for a closely spaced doublet of quartets, which was calculated using a J_{H6-F} of 4 Hz, a $J_{F-C5\alpha H}$ of 22.4 Hz, and a 15 Hz linewidth. The actual ^{19}F spectrum closely resembles the theoretical spectrum, suggesting that J_{H_6-F} is about 4 Hz. The spacing between the lines of the quartet, $J_{F-C_5\alpha H}$, is 22.4 Hz which is close to the reported value

for the F-CH_2-THF coupling constant in the TS-FdUMP-CH_2-THF covalent complex (James et al., 1976; Byrd et al., 1978). The low J_{H6-F} found here is thus consistent with the structure of the covalent adduct shown in Figure 5.4 (path b), which could have only arisen by *cis* addition of the catalytic nucleophile and methyl electrophile.

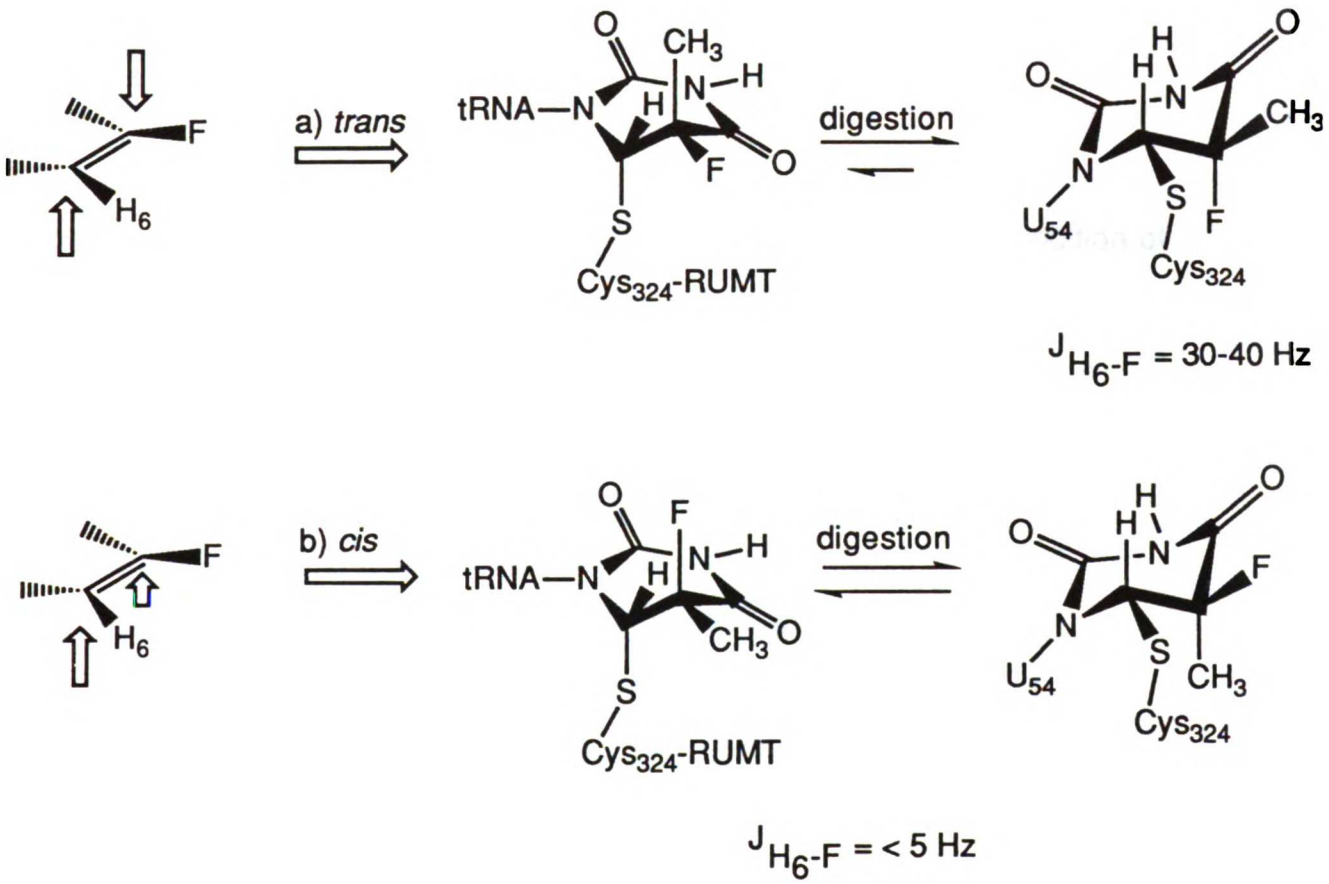

Figure 5.4. Stereochemistry of Addition. Upon denaturation, the stable form of the *trans* isomer (path **a**) is that in which the fluorine and H_6 are *trans* pseudoaxial; in *cis* addition (path **b**), there is no conformational isomer that directs the fluorine and H_6 *trans* pseudoaxial.

In the TS-FdUMP-CH_2H_4folate complex, which arises by *trans* addition of the catalytic nucleophile and the methylene, $J_{H6\text{-}F}$ is 34 Hz (James et al., 1976). Figure 5.5b shows the theoretical spectrum for a $J_{H6\text{-}F}$ of 34 Hz and a $J_{F\text{-}C_5\alpha H}$ of 22.4 Hz. In this case the theoretical spectrum does not match the experimentally obtained spectrum of the peptide-dFU(nucleotide)-CH_3 adduct, but the match between the experimental and theoretical spectra becomes progressively better as $J_{H6\text{-}F}$ approaches 4 Hz.

DISCUSSION

We have elucidated the stereochemical course of nucleophilic addition of Cys 324 of RUMT and the methyl electrophile from AdoMet to U54 of a T-arm analog of tRNA. The dFUT-arm substrate used in this study (Figure 5.1) was chosen because we desired a substrate that contained a single fluorine at the target nucleotide, U54. Employing such a substrate was crucial to success because previous experiments using FUtRNA to prepare the RUMT-FUtRNA-CH_3 covalent complex yielded uninterpretable NMR spectra (J. Kealey, unpublished observation). The spectral ambiguity was due to (i) uncertainty in peak assignment caused by multiple ^{19}F signals arising from multiple fluorouridines not removed by nuclease, and (ii) a poor signal to noise ratio of the FU54 signal, due to poor recovery of the nuclease and protease digested adduct after HPLC. The NMR sensitivity problem was further confounded by the fact that methylation of the RNA resulted in a ca. 4-fold loss in ^{19}F signal intensity due to the $J_{F\text{-}C_5\alpha H}$ coupling.

The spectral assignment and signal to noise issues were resolved by preparing an RNA substrate with a single fluorine, which significantly simplified spectral assignment and eliminated the need for extensive purification, following protease and nuclease digestion of the complex. Incorporation of a

single modified nucleoside (dFU) into RNA required chemical synthesis which, due to sequence length limitations inherent to this method, necessitated synthesis of a small RNA. We have previously shown that the 17 nucleotide T-arm of tRNA is an excellent substrate for RUMT, with kinetic parameters similar to intact tRNA (Gu and Santi, 1991). The small T-arm substrate thus proved ideal for this study. Since the 5-fluororibo phosphoramidite was not commercially available, we prepared the T-arm with the corresponding deoxyribo FU at position 54 (tRNA numbering, Figure 5.1). Since formation of the covalent complex is essentially irreversible, the reaction could be driven to completion, even though the dU54 T-arm is methylated by RUMT 5-fold slower than the wild type T-arm. The reaction conditions were chosen such that the RNA was the limiting reagent and virtually all of it was consumed in the reaction. Formation of the covalent complex was verified by SDS-PAGE, with Coomassie blue and ethidium bromide used to stain protein and nucleic acid, respectively (Figure 5.2), and by ^{19}F NMR spectroscopy.

Following formation of the covalent complex, the molecular mass of the adduct was reduced by both protease and nuclease digestion, prior to ^{19}F NMR. The reason for this was two-fold: first the severe line broadening of the fluorine signal in high molecular weight complexes required that the adduct be reduced to a small molecule in order to observe coupling constants less than ca. 30 Hz. Second, interpretation of the ^{19}F spectrum of the covalent adduct requires that the C_5-C_6 substituents adopt thermodynamically favorable conformations, as would be expected for a substituted cyclohexyl system. This requires denaturation or proteolysis of the protein component of the adduct, so that the conformation of the pyrimidine ring is not influenced by the enzyme. In the TS reaction, for example, the enzyme stabilizes a high energy conformation

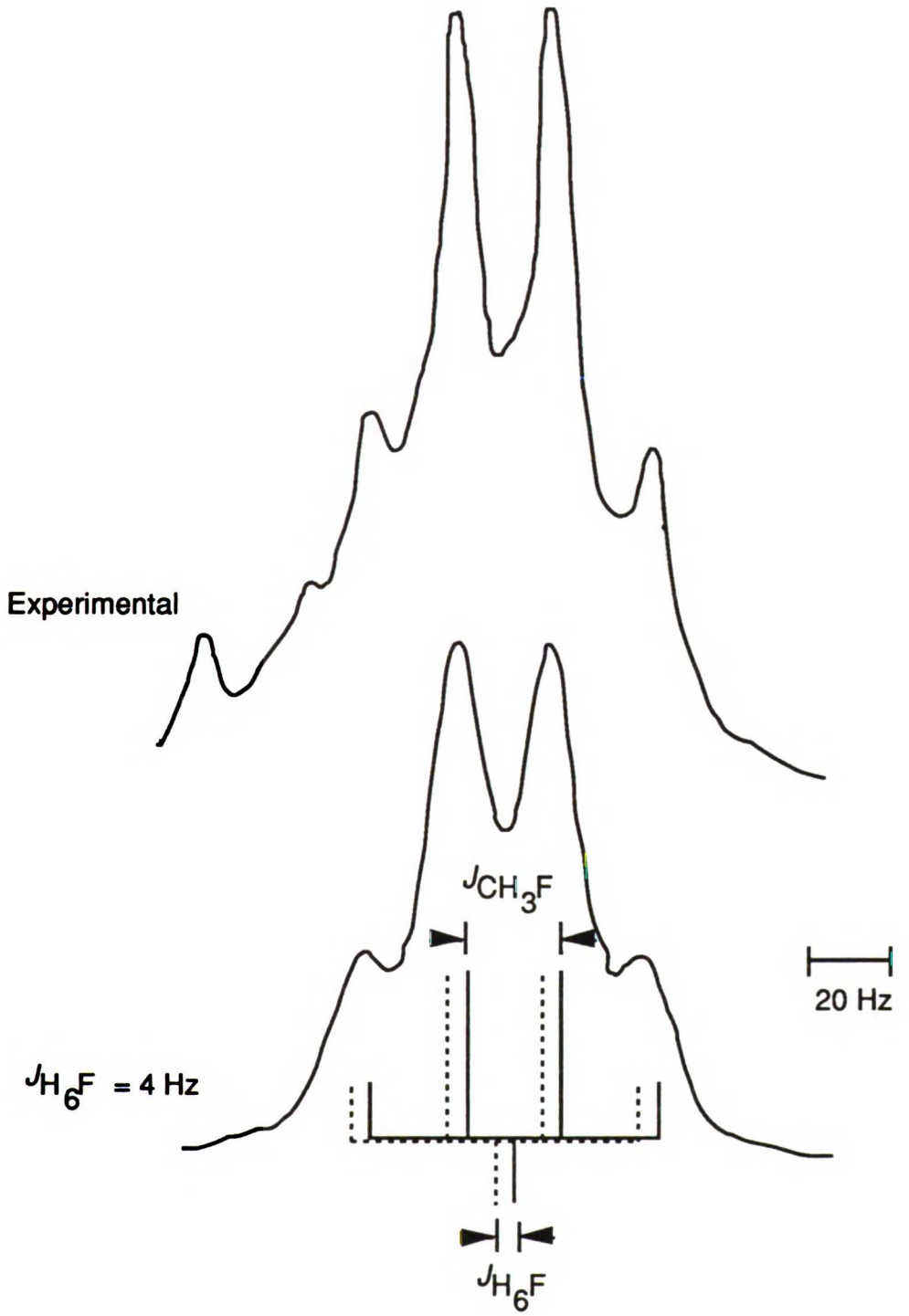

Figure 5.5 (a) 19F NMR spectrum of the peptide-dFU(nucleotide)-CH_3 complex, underlayed with the theoretical spectrum calculated by the program CHRSIM (QE-Charm software package), using experimentally determined coupling constants (J_{H6-F}, 4 Hz, JF-C5αH ,22.4 Hz), and a linewidth of 15 Hz.

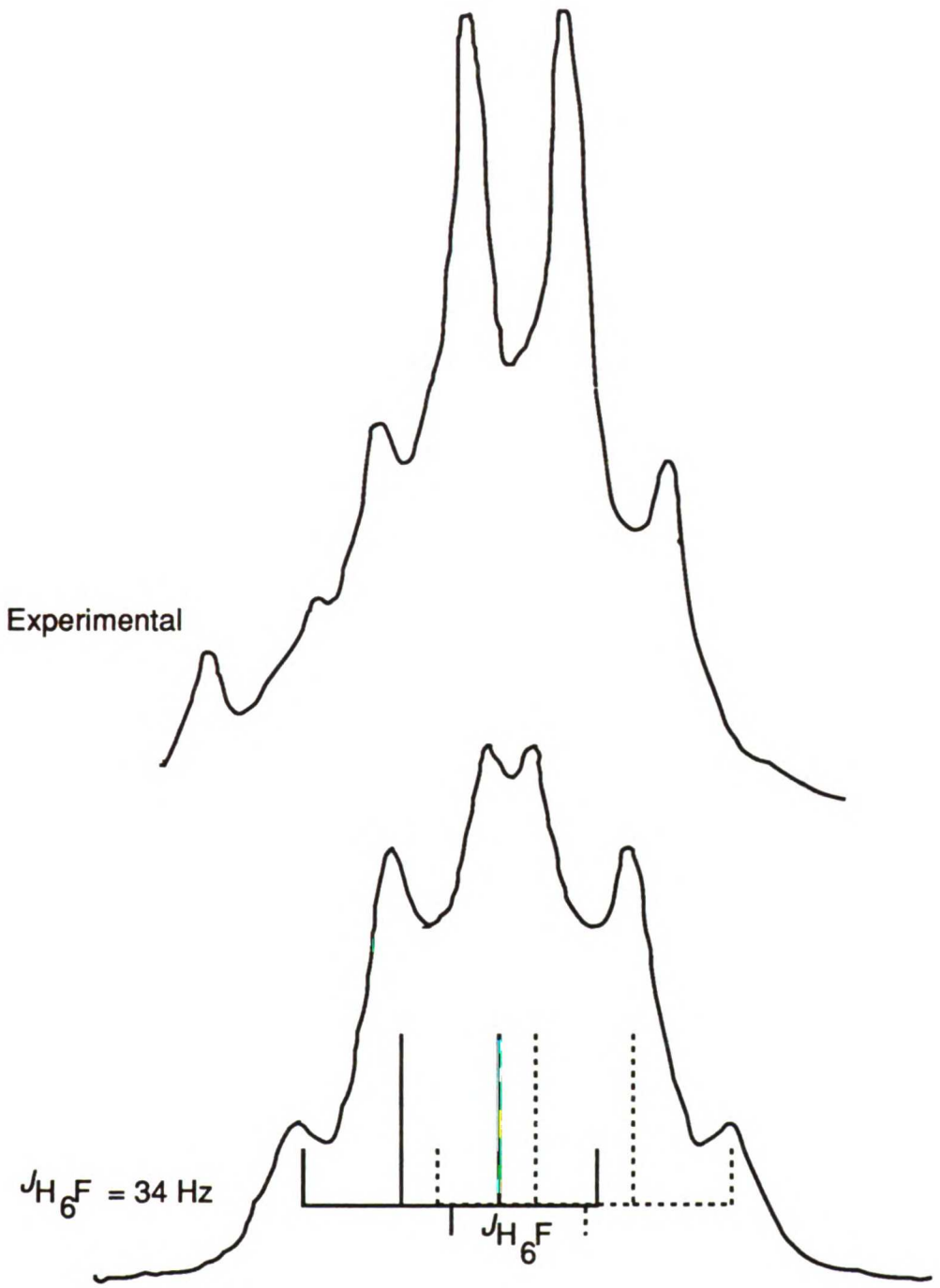

Figure 5.5 (b) Same as (a), except underlayed is the theoretical spectrum for a $J_{H6\text{-}F}$ of 34 Hz.

of the pyrimidine ring, in which the catalytic cysteine and TS-CH_2H_4folate are *trans* pseudodiaxial (James et al., 1976; Byrd et al., 1978; Matthews et al., 1990; Montfort et al., 1990). Upon denaturation or protease digestion of the TS-FdUMP-CH_2H_4folate complex, the catalytic Cys and methylene are directed *trans* pseudodiequatorial, which is the thermodynamically most favorable conformation of the C_5-C_6 saturated pyrimidine ring.

The ^{19}F NMR spectrum of the peptide-dFU(nucleotide)-CH_3 complex is shown in Figure 5.4. The spectrum consists of a doublet of quartets, with a minimum coupling constant, $J_{H6\text{-}F}$, between the lines of the doublet. Based on the empirical Karplus equation (see Byrd et al., 1978) and coupling constants of model compounds (Gutowsky et al., 1962; Bovey et al.,1964), the minimum $J_{H6\text{-}F}$ obtained here suggests that H_6 and F are *gauche*, as shown in Figure 5.4 (path b). This structure could only have arisen by *cis* addition of the catalytic nucleophile and methyl electrophile.

In small molecule chemical counterparts, both *cis* and *trans* additions are observed, with the preferred stereochemical course depending on the substrate and reaction conditions. For example, addition of *p*-toluenethiol to 1-*p*-tolylsulfonyl-cyclohexene under basic conditions in ethanol proceeds in a *trans* manner, yielding a cyclohexane in which the arylsulfonyl and the arylmercapto groups are *cis*. This is the thermodynamically less stable isomer, suggesting that the reaction is under kinetic control. When the same reaction is performed in a solvent of limited proton source, the thermodynamically favored *trans* isomer results, which was produced via *cis* addition (Truce and Levy, 1961). In an analogous reaction on a cyclopentene substrate, addition occurs by the *cis* route to yield the corresponding *trans* cyclopentane. In this case the stereochemical course is dictated by avoidance of unfavorable steric

interactions between the arylsulfonyl and arylmercapto groups in the transition state (Truce and Levy, 1963).

To date the stereochemistry of nucleophilic addition has been determined for two enzymes that are mechanistically similar to RUMT. Thymidylate synthase catalyzes the CH_2H_4folate dependent methylation of dUMP. Both NMR and crystallographic studies have shown that the catalytic nucleophile of TS and the methylene electrophile add *trans* across C_5-C_6 of the pyrimidine (James et al., 1976; Matthews et al., 1990; Montfort et al., 1990). Since dUMP is a mononucleotide, TS can access dUMP from both sides of the pyrimidine ring. *Hha*I methylase catalyzes the AdoMet-dependent methylation of a specific cytidine within a DNA double helix (Wu and Santi, 1987). In this case, the nucleotide substrate is buried within a double helix, and access to C_6 and C5 is restricted. It was recently shown by X-ray analysis that *Hha* I "flips" the target cytidine out of the double helix, and addition of the catalytic nucleophile and methyl electrophile occurs *trans* (Klimasauskas et al., 1994). By flipping cytidine out of the helix, *Hha* I can access C_5 and C_6 from above and below the plane of the pyrimidine, much like in the TS reaction.

The stereochemistry of nucleophilic addition reported here for RUMT represents the first case in which a Michael adduct is produced by addition of a catalytic nucleophile and a methyl electrophile to the same side of the pyrimidine ring. In the crystal structure of yeast $tRNA^{Phe}$, which serves as a model substrate for RUMT, U54 stacks between G53 and Ψ55. Solvent accessibility calculations have shown that C_5 of U54 is 95% buried and C_6 is solvent inaccessible. We have previously concluded that in order to form the covalent adduct between C_6 of U54 and Cys 324, RUMT must facilitate opening of the T-loop of tRNA (Kealey et al., 1991; Kealey and Santi, 1991). It is possible that structural constraints imposed on the reaction by the RNA substrate restrict

access to one side of the ring, so that the only accessible stereochemical pathway is *cis*. This proposal suggests that RUMT accesses the target atoms of U54 by a fundamentally different mechanism than that reported for *Hha*I (although it is hard to dismiss the simplicity and elegance of the "flip out" paradigm as a general mechanism that could be exploited by nucleic acid modification enzymes that must access buried atoms as part of their catalytic mechanism).

It is also conceivable that the *cis* addition observed here is purely a consequence of evolution. The only site of homology between RUMT and other AdoMet -dependent methylases is in the AdoMet binding consensus sequence (Gustafsson et al., 1991). The placement of this sequence relative to the catalytic nucleophile determines the stereochemistry of addition. If the AdoMet binding motif was modularly incorporated into RUMT, it could have been spatially located in a position that initially favored *cis* addition, which, by subsequent evolution would have locked it into that mode and ultimately dictated the stereochemistry of the reaction.

Together with previous studies, the elucidation of the stereochemistry of nucleophilic addition presented here enables a complete chemical mechanism of RUMT to be proposed. As shown in Figure 5.6, after accessing U54, Cys 324 of RUMT adds to either the top or the bottom of the pyrimidine ring (in Figure 5.6 Cys 324 is arbitrarily depicted as adding to the *si* face). This 1,4 addition reaction produces an anion equivalent at C_5, which is shown in Figure 5.6 as the protonated enol. Next, a ring flip occurs, which directs the Cys-peptide group pseudoequatorial, and out of the way of the incoming methyl group. By proceeding through a 1,4 enol intermediate (rather than a concerted 1,2 thiolate-methyl addition), RUMT is able to direct *cis* addition, while still maintaining maximum separation of negative charge in the transition state, and

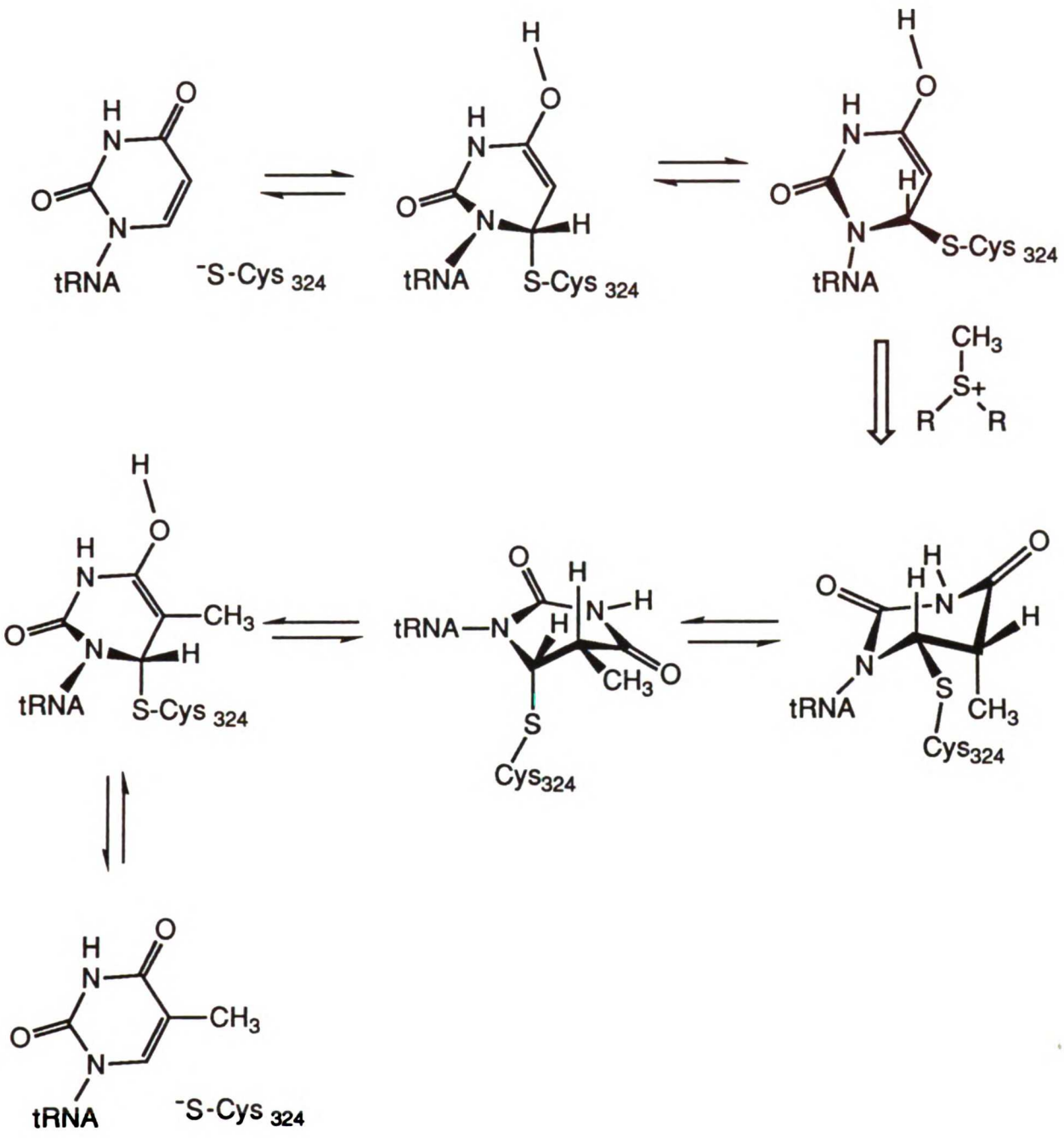

Figure 5.6. Proposed Catalytic Mechanism of tRNA (m^5U54)-methyltransferase showing the stereochemistry of addition. The absolute stereochemistry of the addition product, as shown, is arbitrary.

avoiding unfavorable steric clashes. Tautomerization results in attack of the C_5 anion on the activated methyl group from AdoMet, such that the methyl adds to same side of the ring as the catalytic nucleophile. Another ring flip occurs which places H_6 in optimal orientation for proton abstraction. The reaction can now proceed by one of two routes: 5-proton extraction and β-elimination of the enzyme, or formation of the methylated enol intermediate, with subsequent elimination of the enzyme. Gerlt and colleagues have argued that protonation of the carbonyl oxygen α to a carbon acid is necessary to reduce the pK_a of the acid sufficiently so that the proton can be abstracted by an enzymic base at a rate consistent with k_{cat} of the enzyme (for a review see Gerlt and Gassman, 1993). In light their proposals, we favor the elimination mechanism which proceeds via an enol intermediate, as shown. An attractive feature of the "enol intermediate" mechanism is that the final elimination step is the microscopic reverse of the initial 1,4 addition reaction. An understanding of the chemical mechanism at this level of detail places us in an excellent position for further study of RUMT-RNA-AdoMet interactions and how they contribute to catalysis. Particularly enlightening would be a structure of the FURNA-RUMT-CH_3 complex. Crystallographic studies of this complex are in progress.

REFERENCES

Bovey, F. A., E. W. Anderson, F. P. Hood and R. L. Kornegay (1964). NMR Study of Rotational Barriers and Conformational Preferences. I. Cyclohexyl Fluoride. *J. Chem. Phys.* **40**: 3099-3109.

Byrd, A. R., W. H. Dawson, P. D. Ellis and B. R. Dunlap (1978). Elucidation of the Detailed Structures of the Native and Denatured Ternary Complexes of Thymidylate Synthetase via ^{19}F NMR. *J. Am. Chem. Soc* **100**: 7478-7486.

Gerlt, J. A. and P. G. Gassman (1993). Understanding the Rates of Certain Enzyme-Catalyzed Reactions: Proton Abstraction from Carbon Acids, Acyl-Transfer Reactions, and Displacement Reactions of Phosphodiesters. *Biochemistry* **32**: 11943-11952.

Gu, X. and D. V. Santi (1991). The T-arm of tRNA is a Substrate for tRNA (m5U54)-Methyltransferase. *Biochemistry* **30**: 2999-3002.

Gustafsson, C., P. H. R. Lindsrom, T. G. Hagervall, B. K. Esberg and G. R. Bjork (1991). The trmA Promoter Has Regulatory Features and Sequence Elements in Common with the rRNA P1 Promoter Family of *Escherichia coli*. *J. Bacteriol.* **173**: 1757-1764.

Gutowsky, H. S., G. G. Belford and P. E. McMahon (1962). NMR Studies of Conformational Equilibria in Substituted Ethanes. *J. Chem. Phys.* **36**: 3353-3368.

James, T. L., A. L. Pogolotti, K. M. Ivanetich, Y. Wataya, S. M. Lam and D. V. Santi (1976). Thymidylate Synthetase: Fluorine-19 NMR Characterization of the Active Site Peptide Covalently Bound to 5-Fluoro-2'-Deoxyuridylate and 5,10- Methylenetetrahydrofolate. *Biochem. Biophys. Res. Comm.* **72**: 404-410.

Kealey, J. T., S. Lee, H. G. Floss and D. V. Santi (1991). Stereochemistry of Methyl Transfer Catalyzed by tRNA (m5U54)-methyltransferase-- Evidence for a Single Displacement Mechanism. *Nucleic Acids Res.* **19**: 6465-6468.

Kealey, J. T. and D. V. Santi (1991). Identification of the Catalytic Nucleophile of tRNA (m^5U54)Methyltransferase. *Biochemistry* **30**: 9724-9728.

Kealey, J. T. and D. V. Santi (1994). High Level Expression and Rapid Purification of tRNA m5U54 methyltransferase. *Prot. Exp. Purif.* in press

Klimasauskas, S., S. Kumar, R. R.J. and X. D. Cheng (1994). *Hha*1 Methyltransferase Flips its Target Base out of the DNA Helix. *Cell* **76**: 357-369.

Matthews, D. A., K. Appelt, S. J. Oatley and N. H. Xuong (1990). Crystal Structure of *Escherichia coli* thymidylate Synthase containing bound 5-fluoro-2'-deoxyuridylate and 10-propargyl-5,8-dideazafolate. *J. Mol. Biol.* **214**: 923-936.

Montfort, W. R., K. M. Perry, E. B. Fauman, J. S. Finer-Moore, G. F. Maley, L. Hardy, F. Maley and R. M. Stroud (1990). Structure, Multiple Site Binding, and Segmental Accommodation in Thymidylate Synthase on binding dUMP and an Antifolate. *Biochemistry* **29**: 6964-6976.

Santi, D. V. and L. W. Hardy (1987). Catalytic Mechanism and Inhibition of tRNA (Uracil-5-) methyltransferase: Evidence for Covalent Catalysis. *Biochemistry* **26**: 8599-8606.

Truce, W. E. and A. J. Levy (1961). The Stereochemistry of the Nucleophilic Addition of *p*-Toluenethiol to 1-*p*-Tolylsulfonyl-cyclohexene. *J. Am. Chem. Soc.* **83**: 4641-4643.

Truce, W. E. and A. J. Levy (1963). The Stereochemistry of Nucleophilic Addition of *p*-Toluenthiol to 1-*p*-Tolylsulfonylcyclopentene. *J. Org. Chem.* **28**: 679-682.

Webster, K. R., Y. Shamoo, W. Konigsberg and E. K. Spicer (1991). A Rapid Method for Purification of Synthetic Oligoribonucleotides. *Biotechniques* **11**: 658-661.

Wu, J. C. and D. V. Santi (1987). Kinetic and Catalytic Mechanism of *Hha*I Methyltransferase. *J. Biol. Chem.* **262**: 4778-4786.

Chapter 6

Purification of tRNA (m^5U54)-methyltransferase Containing Tightly Bound *S*-Adenosyl-L-methionine: Implications for the Mechanism of tRNA Methylation.

James T. Kealey and Daniel V. Santi*

Departments of Pharmaceutical Chemistry and Biochemistry and Biophysics

University of California, San Francisco, 94143-0446

* To whom correspondence should be addressed.

ABSTRACT

tRNA (m^5U54)-methyltransferase (RUMT, EC.2.1.1.35) catalyzes the methylation of uridine 54 in tRNA by *S*-Adenosyl-L-methionine (AdoMet). In purified preparations of RUMT, we found that the enzyme contained nearly equimolar amounts of bound AdoMet, which could methylate RNA. In vitro equilibrium dialysis experiments showed that the dissociation constant for the RUMT-AdoMet binary complex was about 1 μM in phosphate buffer; however, no RUMT-AdoMet binding was observed in Tris buffer. Kinetic models consistent with the data presented here and elsewhere are presented.

INTRODUCTION

tRNA (m^5U54)-methyltransferase (RUMT[3], EC.2.1.1.35) catalyzes the AdoMet-dependent methylation of uridine 54 (U54) in all *Escherchia coli* tRNAs (Steinberg et al., 1993), and in a 17-nucleotide oligomer correspoinding to the T-arm of tRNA (Gu and Santi, 1991). The mechanism of methylation involves (i) nucleophilic addition of Cys 324 of RUMT to the 6-position of U54 (Kealey and Santi, 1991), (ii) direct methyl transfer from AdoMet to the 5-position of the covalent adduct (Kealey et al., 1991), and (iii) 5-proton extraction and β-elimination to yield m^5U (Scheme I, chapter 1). In the absence of AdoMet, RUMT forms binary covalent complexes with tRNA, which are subsequently methylated by addition of AdoMet (Gu and Santi, 1992). Hence, the binding of the nucleic acid substrate to RUMT does not depend on prior AdoMet binding, as is the case with *EcoR*I methylase (Reich and Mashhoon, 1991).

In the course of studies on RUMT-RNA interactions employing enzyme overexpressed and purified to homogeneity (Kealey and Santi, 1994), we found that RUMT contained nearly equimolar bound AdoMet, which was capable of methylating RNA. In this paper we describe the identification and characterization of the purified RUMT-AdoMet complex. By employing equilibrium dialysis to recapitulate and quantitate the RUMT-AdoMet interaction in vitro, we found that the interaction depended on buffer components-- binding was observed in phosphate buffer, but not in Tris buffer.

---

[3]Abbreviations: RUMT, tRNA (m^5U54)-methyltransferase; m^5U, 5-methyluridine; AdoMet, S-Adenosyl-L-methionine; FUtRNA, unmodified yeast $tRNA^{Phe}$ with the substitution of 5-fluorouridine for all uridines; SDS, Sodium Dodecyl Sulfate; EDTA, Ethylenediaminetetraacetic acid; DTT, Dithiothreitol; PAGE, Polyacrylamide gel electrophoresis; DEAE, Diethylaminoethyl; MWCO, molecular weight cut-off; CH_2H_4folate, methylenetetrahydrofolate.

*Hha*I methyltransferase can also be purified with bound AdoMet (Kumar et al., 1992). Steady-state kinetic analyses showed that DNA and AdoMet bind to *Hha*I methyltransferase in an ordered-sequential fashion, with DNA binding first (Wu and Santi, 1987). The steady-state data are thus inconsistent with the observation that AdoMet is bound to *Hha*I methyltransferase in the absence of DNA. The conclusions presented here may, by analogy, shed light on the apparant DNA-AdoMet binding paradox observed for HhaI methyltransferase.

EXPERIMENTAL

General Material and Methods

RUMT was expressed from the plasmid, pJKtrmA, and purified as described (Kealey and Santi, 1994). The oligoribonucleotide, 5' GGCGGUUCGAUC CCGUC 3', corresponding to the T-arm of $tRNA^{Val}$ was synthesized on an Applied Biosystems (ABI) 394 oligonucleotide synthesizer, using ABI reagents, and the 1 μmole RNA synthesis cycle provided by ABI. RNA phosphoramidites and derivitized column supports were obtained from Glen Research Corporation (Sterling, VA). The RNA was cleaved from the solid support and 2'-deprotected as described (see Chapter 5), and the RNA was purified by C-4 HPLC, as described (Webster et al., 1991). $FUtRNA^{Phe}$ was prepared by *in vitro* transcription from the plasmid p67YFO (gift from O. Uhlenbeck, University of Colorado, Boulder), as described (Sampson and Uhlenbeck, 1988), using 4 mM NTPs and replacing UTP with FUTP. The transcript was purified on a Qiagen Tip 20 column, according to the instructions provided by Qiagen (Chatsworth, CA) . RNA was labeled at the 3' end with ^{32}pCp, as described (England et al., 1980), and purified on 15% polyacrylamide gels containing 7 M urea. Labeled RNA was extracted from the gel by soaking the gel piece in 0.5 M ammonium acetate, 1 mM EDTA, 0.1% SDS, pH 7, and the RNA was recovered

by ethanol precipitation. Buffer A consisted of 50 mM Tris/HCl, 2 mM $MgCl_2$, 1 mM DTT, pH 7.6. Buffer B consisted of 100 mM potassium phosphate, 10% (v/v) gycerol, 1 mM DTT and 0.1 mM EDTA, pH 7.2. TBE buffer consisted of 45 mM Tris-borate, 1 mM EDTA, pH 8.0. Dialysis membranes (10,000-12,000 MWCO) were obtained from Spectrum (Houston, TX), and prepared as described (Sambrook et al., 1989).

Indirect detection of bound AdoMet and stoichiometry of the RUMT-AdoMet complex

In initial experiments, 5 nM aliquots of ^{32}P-labeled T-arm were incubated in buffer A for 30 minutes at 15°C with the following concentrations of RUMT: 0, 0.02, 0.1, 0.27, and 1.34 μM). Binary complexes were trapped on nitrocelluose filters as described (Gu and Santi, 1992). Aliquots from each binding reaction were also analyzed on a 7 M Urea/15% polyacylamide gel (40 cm x 20 cm x 1 mm), run in TBE buffer at 1000 V. These experiments revealed that RUMT induced a change in the RNA substrate, which was manifested as both a decrease in the amount of binary complex formed with increasing RUMT concentration, and as a band shift of the RNA on the polyacylamide gel. It was hypothesized that the decrease in binding and accompanying band shift might be the result of methylation of the RNA. The band shift thus served as an assay to quantitate the methyl donating ability of RUMT.

RUMT (ca. 100 nM) was incubated with 26 nM, 47 nM , and 95 nM ^{32}P-labeled T-arm in buffer A, aliquots were removed at various times, and the reactions were terminated by freezing at -80°. Aliquots from the reaction mixtures were loaded onto polyacrylamide gels, and following electrophoresis, the radiolabeled bands were visualized and quantitated with a phosphorimager (Molecular Devices). In some experiments RUMT was further purified by Mono

S, or Mono Q, or tRNA affinity chromatography, and the purified enzyme was tested for the ability to methylate T-arm, as assessed by the band shift assay.

Direct detection and quantitation of bound AdoMet

The aforementioned experiments revealed that the AdoMet/RUMT ratio was suffieciently high (ca. 1:1) that the bound cofactor could be extracted from RUMT and analyzed directly on FPLC. To 2 nmole of RUMT was added an equal volume of 100 mM ammonium formate (pH 6) containing 8 M urea, and the sample was incubated for 30 minutes at 37°C. Protein was removed by spinning the sample through a centripor 25,000 MWCO dialysis filter (Ranin) at 12000 xg for 30 minutes, and the dialysate was loaded to the FPLC. FPLC was performed on a Hewlett Packard 1090 Liquid chromatograph, equipped with a Mono S HR 5/5 FPLC column (Pharmacia), and elution of AdoMet was accomplished isocratically, using 50 mM ammonium formate, pH 6 as the mobile phase at flow rate of 1 mL/min. The detection limit for AdoMet using this system was about 50 pmole. Using the HPLC assay to quantitate bound AdoMet, the half-life for removal of AdoMet from RUMT was determined. RUMT was added to a dialysis membrane (10,000-12,000 MWCO) and dialyzed against buffer B. Aliquots were removed at times ranging from 0 hours to 110 hours, and the amount of AdoMet bound to RUMT in each was determined by extraction/HPLC, as well as UV absorption.

To directly show that RUMT methylated the T-arm without exogeneously added AdoMet, RUMT was reacted with T-arm and the product m^5Urd was verified by HPLC. RUMT (2 nmole) and 1.2 nmole T-arm were incubated in buffer A at 15° in a 92 µl reaction mixture. After 3 hours, 10 µl of 300 mM sodium acetate, pH 5.3 and 10 µl (100 µg) of nuclease P1 were added, and the sample was incubated at 37°C for 30 minutes. The RNA hydrolysate was converted to

nucleosides with alkaline phosphatase, and nucleoside analysis was performed as described (Buck et al., 1983).

Chemical competence of bound AdoMet

An isotope trapping experiment was employed to determine if the bound AdoMet dissociated from RUMT prior to RNA binding and methylation, or if the bound AdoMet was chemically competent for methylation (i.e. did not dissociate prior to RNA binding and methylation). FUtRNA is a substrate analog of tRNA, and forms a methylated covalent complex with RUMT in the presence of AdoMet (Scheme II, Chapter 1). Hence, once the methyl is transferred, the enzyme is trapped, and the trapped adduct can be readily isolated on SDS-PAGE (Santi and Hardy, 1987). RUMT containing bound AdoMet was incubated in buffer A at 25°C with excess FUtRNA and [^3H]-*methyl* AdoMet. A control reaction contained FUtRNA, [^3H]-*methyl* AdoMet, and RUMT, which was dialyzed free of AdoMet. The final concentrations of reaction components were: RUMT (4.5 μM), FUtRNA (15 μM), and [^3H]-*methyl* AdoMet (40 μM, 2 Ci/mmole). Aliquots were removed at 2, 5 and 15 minutes and loaded to SDS-PAGE. ^{32}P-labeled bands were visualized by autoradiography and the bands associated with the RUMT-^{32}P-FUtRNA-CH_3 covalent complex were excised and the gel slices were incubated in 1 N NaOH at 55°C for 27 hours. Following neutralization, 5 mL of aquasol II was added to each solution of eluted complex, and the radioactivity of each sample was determined by liquid scintillation counting.

Equilibrium Dialysis

Equilibrium dialysis was employed to determine the RUMT-AdoMet dissociation constant (K_d) in the absence of RNA. Equilibrium dialysis was performed in an eight chamber apparatus (300 μl per chamber, 150 μl per side),

fitted with a dialysis membrane (10,000-12,000 MWCO). To the dialysis chambers on the "protein side" of the apparatus were added RUMT (dialyzed free of AdoMet, approximately 2 μM final), and to the chambers on the "ligand side" of the apparatus were added various concentrations of [^{3}H]-*methyl* AdoMet (0.1 μM to 7 μM final). The dialysis buffer consisted of either buffer A or buffer B, supplemented with 0.2 mg/mL BSA. Following dialysis at 4°C for 14 hours, aliquots from each chamber were removed and counted in 4 mL of Aquasol II until the standard error of counting was less than 1%. The concentrations of free and bound ligand were calculated as described (Klotz, 1989), and the data were fitted to equation 1 using the program, KaleidaGraph (Synergy Software, Reading, PA), run on a Macintosh computer.

$$[\text{bound ligand}] = [\text{total protein}] / 1 + \{(Kd / [\text{free ligand}])\} \qquad (1)$$

RESULTS

The impetus for this study derived from the observation that when ^{32}P-labeled T-arm was titrated with RUMT, after initial binding, the T-arm dissociated from the complex at high concentrations of RUMT (Figure 6.1A). Moreover, this "drop off" of the nitrocellulose binding isotherm correlated with a band shift of the RNA on 7 M urea-15% PAGE (Figure 6.1A). One possible explanation for these data was that RUMT alone (i.e. without exogeneously added AdoMet) methylated the RNA. The anomalous binding data thus reflected the difference in K_d between the non-methylated T-arm (low K_d) and the methylated T-arm (high K_d). Once methylated, the T-arm dissociated from the complex, due to the change in the RUMT-T-arm K_d. The band shift on 7 M urea-15% PAGE was apparently due to a difference in mobility between methylated and non-methylated T-arm on the gel system employed. Indeed, when excess

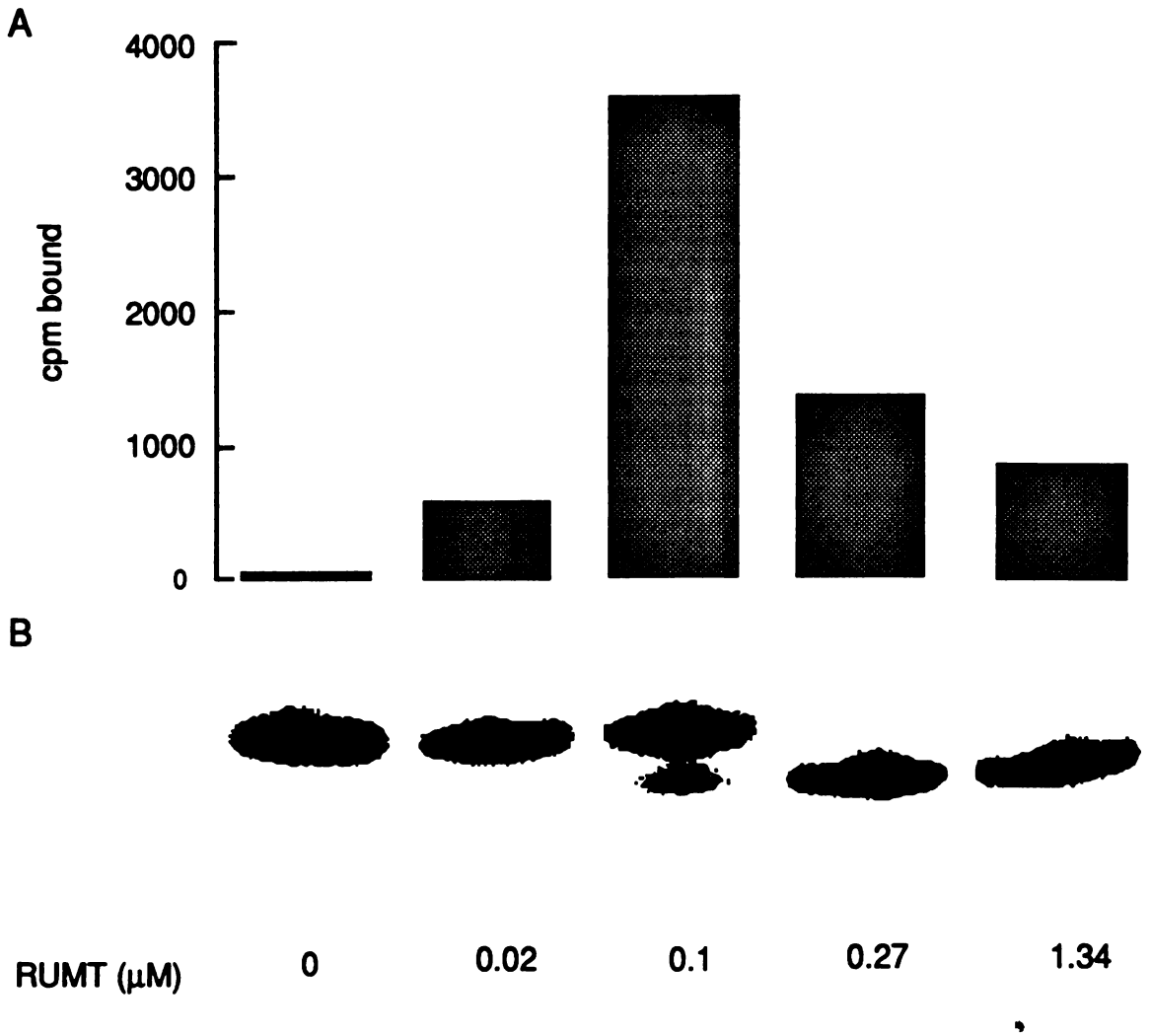

Figure 6.1 (A) Titration of ^{32}P-labeled T-arm with RUMT. The values on the y-axis represent the amount of RUMT-^{32}P-T-arm binary complex trapped on nitrocellulose filters, expressed in cpm of ^{32}P. (B) Semi-denaturing PAGE of aliquots from the binding assay.

exogenous AdoMet was added to reaction mixtures, all of the T-arm converted to the faster moving species (not shown).

Although the data strongly suggested that RUMT alone was able to methylate RNA, it was necessary to rule out the possibility that RUMT induced a 1 nucleotide truncation of the RNA, which was also consistent with the PAGE

results (Figure 6.1B). This interpretation, however, seemed unlikely for two reasons: First, since the K_d for the 11 mer T-arm is essentially the same as that of the 17mer T-arm (Xiangrong Gu and Daniel V. Santi, in preparation), a 1 nucleotide truncation of the 17mer T-arm should not dramatically affect RUMT binding. Second, the difference in mobility between RUMT-treated and untreated T-arm depended markedly on the gel conditions. Maximum separation of the two species was observed under semi-denaturing gel conditions (ca. 1000 V). However, when the gel was run under strictly denaturing conditions (2000 V), the difference in mobility between the two species was not apparent (Figure 6.2). This suggested that the two RNA species were of the same length, but differed in their stability of secondary structure.

To directly demonstrate that RUMT methylated the T-arm without exogeneously added AdoMet, the product of the reaction, ribothymidine, was identified by nucleoside analysis. After incubating the T-arm with RUMT, the RNA was digested with P-1 nuclease, and the hydrolysate was converted to nucleosides with alkaline phosphatase. HPLC of the resulting nucleosides clearly indicated the presence of ribothymidine (Figure 6.3).

Having established that RUMT methylated its substrate RNA without added cofactor, we determined the molar ratio of bound AdoMet to RUMT. Time courses of methylation were carried out at three RUMT:T-arm ratios, and the methylated ^{32}P-T-arm was isolated by PAGE and quantitated with a phosphorimager. As shown in Figure 6.4, up 80% of the RUMT was able to methylate the T-arm. The surprisingly high ratio of AdoMet:RUMT suggested that the AdoMet could be extracted from RUMT and detected by UV absorption on cation exchange FPLC. Treatment of RUMT with 2 M urea released a small molecule that co-migrated with authentic AdoMet under the chromatographic conditions employed. Based on a calibration curve, it was determined that 0.8

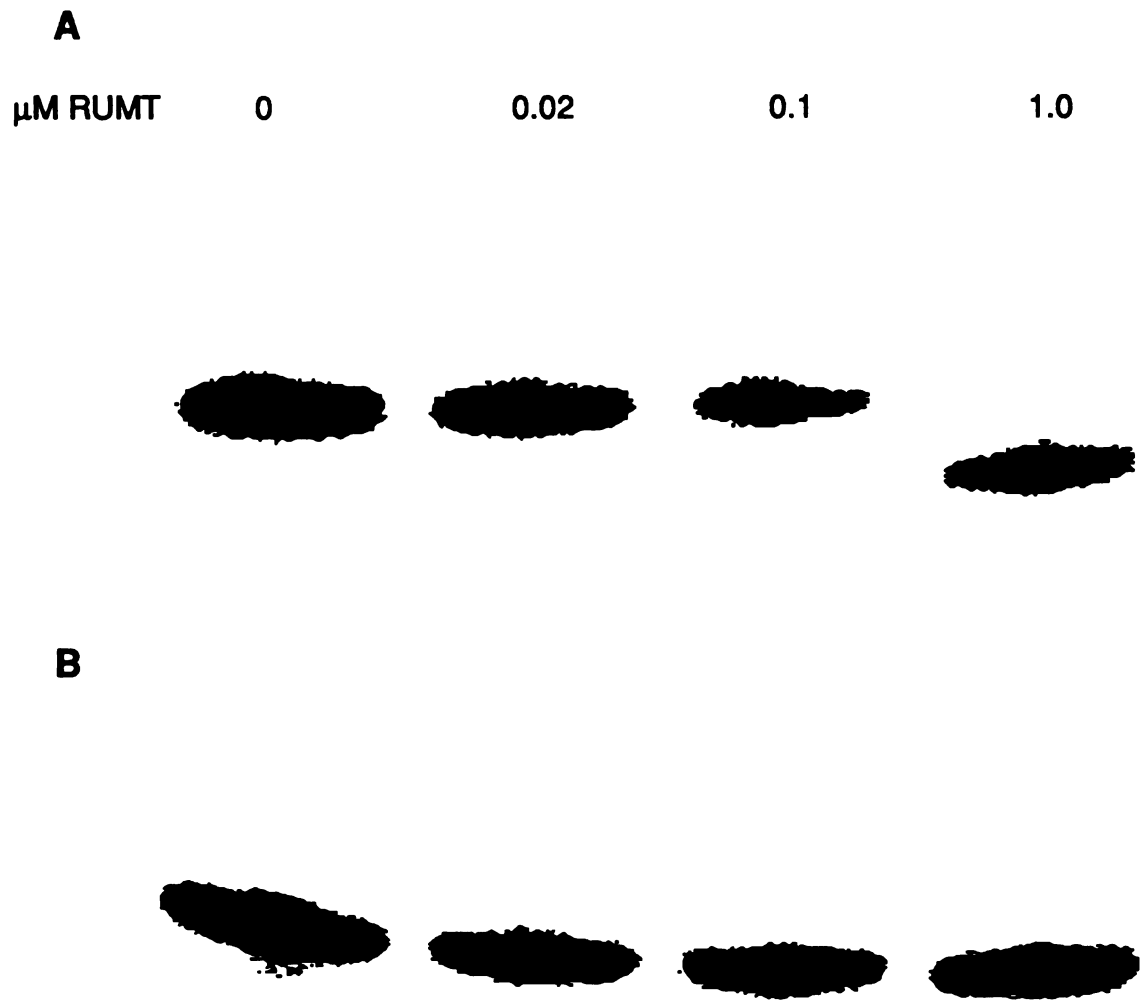

Figure 6.2. Electrophoresis of RNA derived from the binding assay. In (A) the gel was run at 900V and in (B) the gel was run at 2000 V. Identical aliquots were loaded to each gel.

mole AdoMet was present per mole of RUMT, which is consistent with the ratio obtained via the methylation assay.

In order to prepare RUMT without bound AdoMet, we determined the half-life for release of AdoMet from RUMT via dialysis. The amount of AdoMet bound to RUMT as a function of dialysis time was measured by the HPLC assay. As shown in Figure 6.5, the half-life for release of AdoMet from RUMT at 4° in buffer B was about 45 hours. In a parallel experiment, the A_{260}/A_{280} ratio of each aliquot from the time course was determined. An A_{260}/A_{280} ratio of ca. 0.62 reflected RUMT free of bound AdoMet, whereas an A_{260}/A_{280} ratio of 0.8 or more indicated that RUMT contained a significant amount (> 50% mol/mol) of bound AdoMet.

An isotope trapping experiment was used to determine whether the bound AdoMet directly methylated the RNA, or whether the AdoMet first dissociated from the enzyme upon RNA binding, and subsequently re-bound and methylated the RNA. RUMT, either containing or free of AdoMet, was incubated with ^{32}P-labeled FUtRNA, and saturating [^{3}H]-*methyl* AdoMet. The substrate analog, FUtRNA, was used to limit the enzyme to a single turnover, and the methylated product was isolated on SDS-PAGE. Since the bound AdoMet is not labeled with tritium, a low $^{3}H/^{32}P$ ratio in the product indicates that the methyl group is transferred directly to RNA without dissociation. On the other hand, if the unlabeled AdoMet dissociates prior to methylation, it will be "diluted" into the [^{3}H]-*methyl* AdoMet pool, a [^{3}H]-*methyl* AdoMet will re-bind, and the $^{3}H/^{32}P$ ratio will be high in the product. The change in specific activity of the [^{3}H]-*methyl* AdoMet due to release of the unlabeled AdoMet was negligible. As Figure 6.6 shows, the $^{3}H/^{32}P$ ratio in the product FUtRNA was significantly lower for RUMT containing AdoMet than for RUMT free of AdoMet. This strongly

suggested that the bound AdoMet does not dissociate from RUMT prior to methylation-- the bound AdoMet was thus chemically competent for methylation.

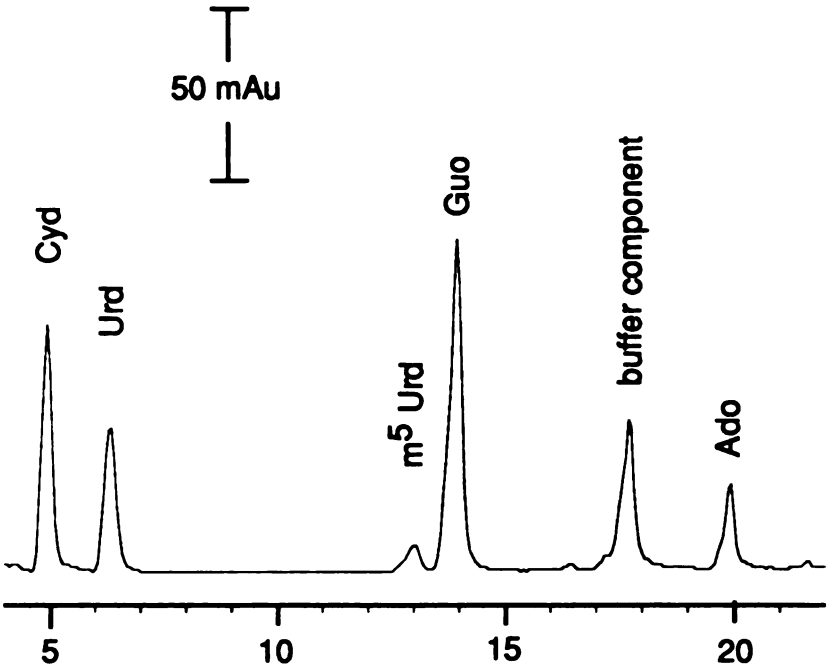

Figure 6.3. Nucleoside analysis following incubation of T-arm with RUMT. Time (min) is shown on the x-axis, and the absorbance at 260 nm is depicted on the y-axis.

Equilibrium dialysis was employed to study the RUMT-AdoMet interaction in vitro. In the absence of tRNA (but in the presence of 100 mM potassium phosphate), the RUMT-AdoMet dissociation constant was ca. 0.6 μM (Figure 6.7). In Tris buffer, no AdoMet-RUMT binding was observed, suggesting that in the absence of phosphate, the AdoMet-RUMT K_d is quite high (> 10 μM).

DISCUSSION

In this paper we showed that homogeneous RUMT methylates RNA, without exogeneously added AdoMet. The autogenous methylating activity of

RUMT persisted through phosphocellulose chromatography, followed by Mono S, Mono Q or tRNA affinity chromatography. Following autogenous

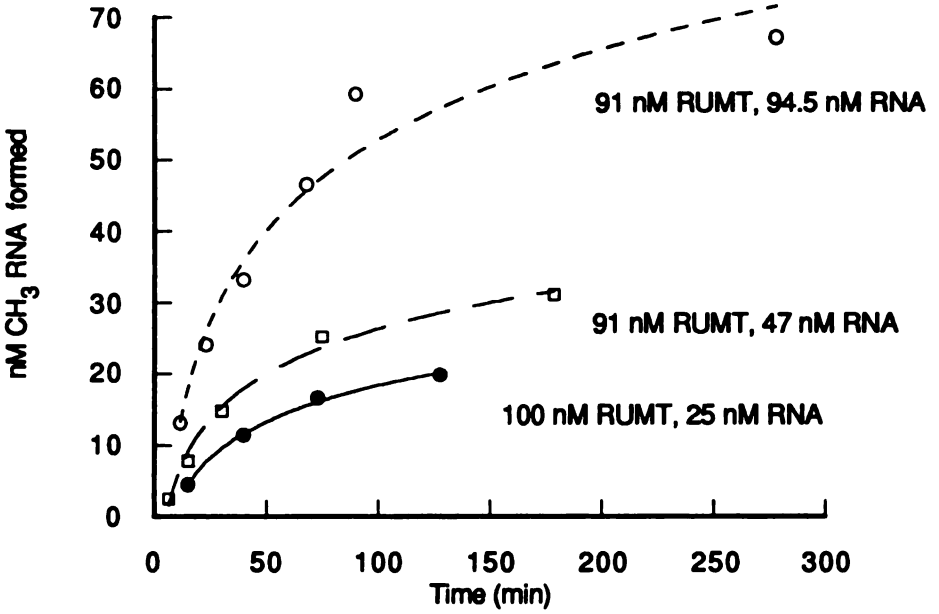

Figure 6.4. Time course for methylation of ^{32}P-labeled T-arm by RUMT

methylation of the RNA, the product of the reaction, m^5Urd, was verified by nucleoside analysis. By employing a band shift assay to separate methylated from non-methylated RNA, and by quantitating the methylated ^{32}P-labeled RNA, we determined that 80% of the RUMT was competent for methylation.

The in vitro methylation data is consistent with the methylated RNA arising by one of two conceivable routes: (1) methyl transfer from a methylated enzyme intermediate, or (2) methylation via tightly associated AdoMet. The first possibility is unlikely, since we have previously shown that the methyl transfer occurs by direct displacement of the sulfonium ion of AdoMet by C5 of the target

pyrimidine (Kealey et al., 1991). The direct displacement mechanism argues against the existence of a methylated enzyme intermediate. The possibility that

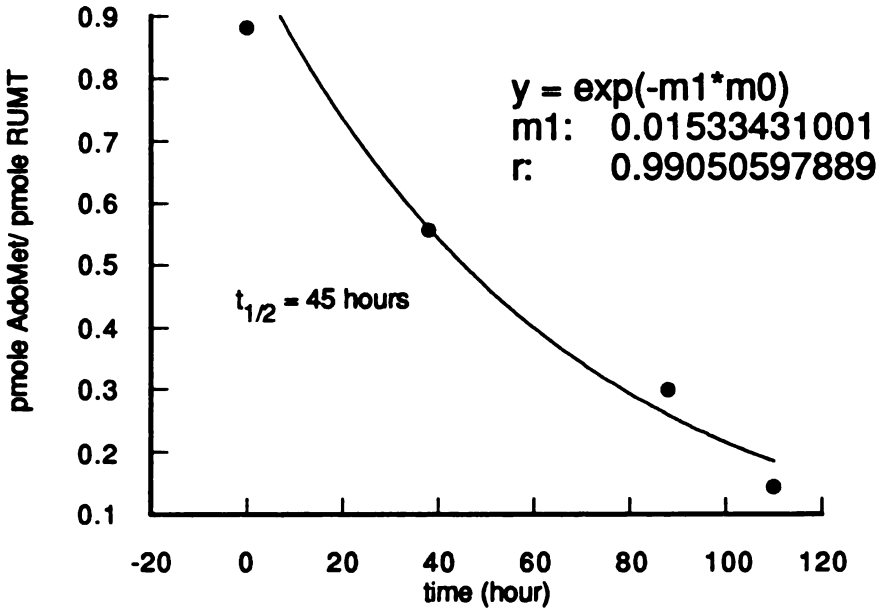

Figure 6.5. Release of AdoMet from RUMT via dialysis. At the indicated time, AdoMet was extracted from RUMT, isolated by HPLC, and quantitated by UV absorption.

RUMT contained bound AdoMet was directly addressed by extraction of the cofactor from the enzyme, with subsequent HPLC analysis of the filtrate. Treatment of RUMT with urea released a small molecule which exhibited chromatographic and UV absorption properties identical to those of authentic AdoMet. Based on a standard curve, approximately 0.8 mole of AdoMet was released per mole of RUMT. Hence, these data proved that homogeneous RUMT contained nearly equimolar bound AdoMet. The AdoMet could be slowly

removed from RUMT by dialysis-- the $t_{1/2}$ for release of the cofactor from RUMT at 4° in phosphate buffer was 45 hours.

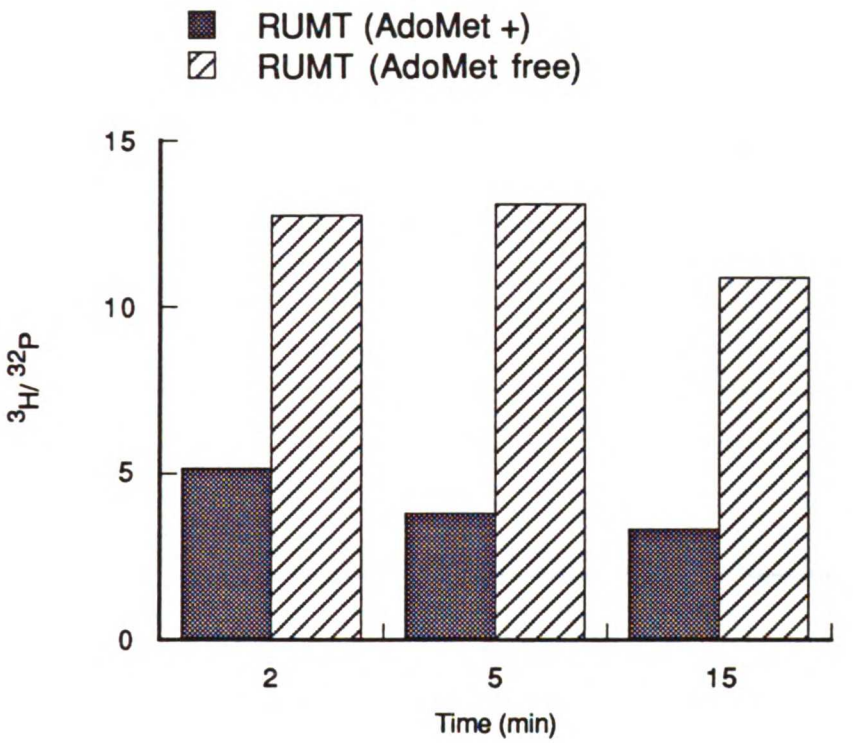

Figure 6.6. Isotope trapping. RUMT with AdoMet (AdoMet +) or RUMT without AdoMet (AdoMet free) was reacted with FUtRNA and [^3H]-*methyl* AdoMet. Shown is the $^3H/^{32}P$ ratio as a function of reaction time for the RUMT-FUtRNA-[^3H]-*methyl* covalent complex (see text for details).

In an attempt to relate the findings presented here to the mechanism of RUMT, we have constructed several plausible models for the RUMT-AdoMet-RNA interaction (Figure 6.8). In the discussion that follows, each model is evaluated with respect to experimental observations, and the model is ruled out if it is inconsistent with experimental data. Gu and Santi (Gu and Santi, 1992) have shown that RUMT binds RNA in the absence of AdoMet, and the data presented here suggest that RUMT binds AdoMet in the absence of RNA. This implies a random sequential binding mechanism, as outlined in Figure 6.8a.

The data are also consistent with the models presented in Figure 6.8b and 6.8c. In model 6.8b, the AdoMet site in the RUMT-AdoMet binary complex overlaps the AdoMet site in the RUMT-AdoMet-RNA ternary complex. Upon tRNA

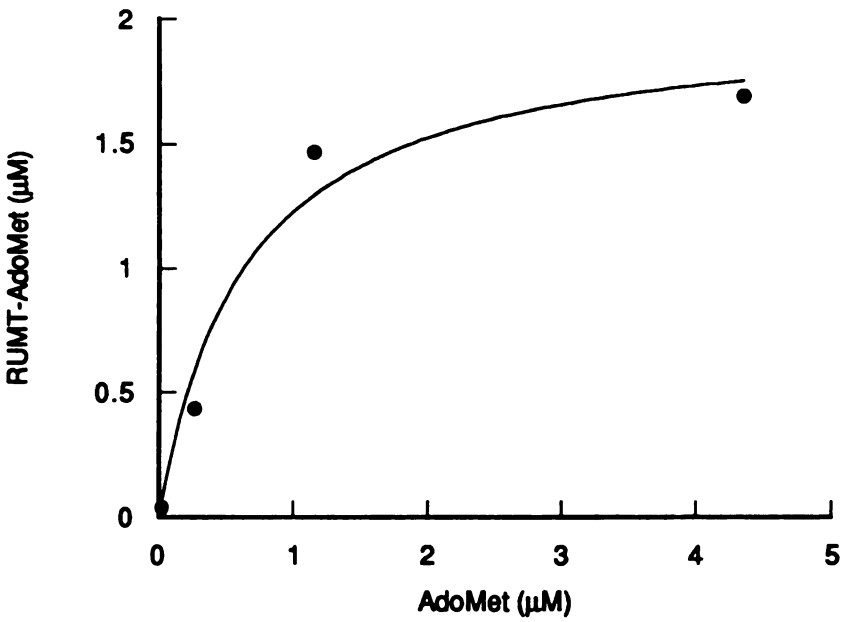

Figure 6.7. Determination of K_d of the RUMT-AdoMet interaction via equilibrium dialysis. The data, fitted to equation 1, yielded a K_d of about 600 nM.

binding, the AdoMet shifts to a methylation competent site, without dissociation from the enzyme. In model 6.8c, the bound AdoMet dissociates prior to, or concomitant with, tRNA binding, and then re-associates to a methylation competent site. This model predicts that there are two binding sites for AdoMet--an AdoMet storage site, and a methylation competent site, and the RNA serves to alter the AdoMet-RUMT affinity in favor of the methylation site. To experimentally distinguish models 6.8a,b from model 6.8c, we designed an isotope trapping experiment. RUMT was reacted with the mechanism-based

inhibitor, FUtRNA, in the presence of excess [^{3}H]-*methyl* AdoMet. A control reaction contained all of the above components, except that the RUMT was

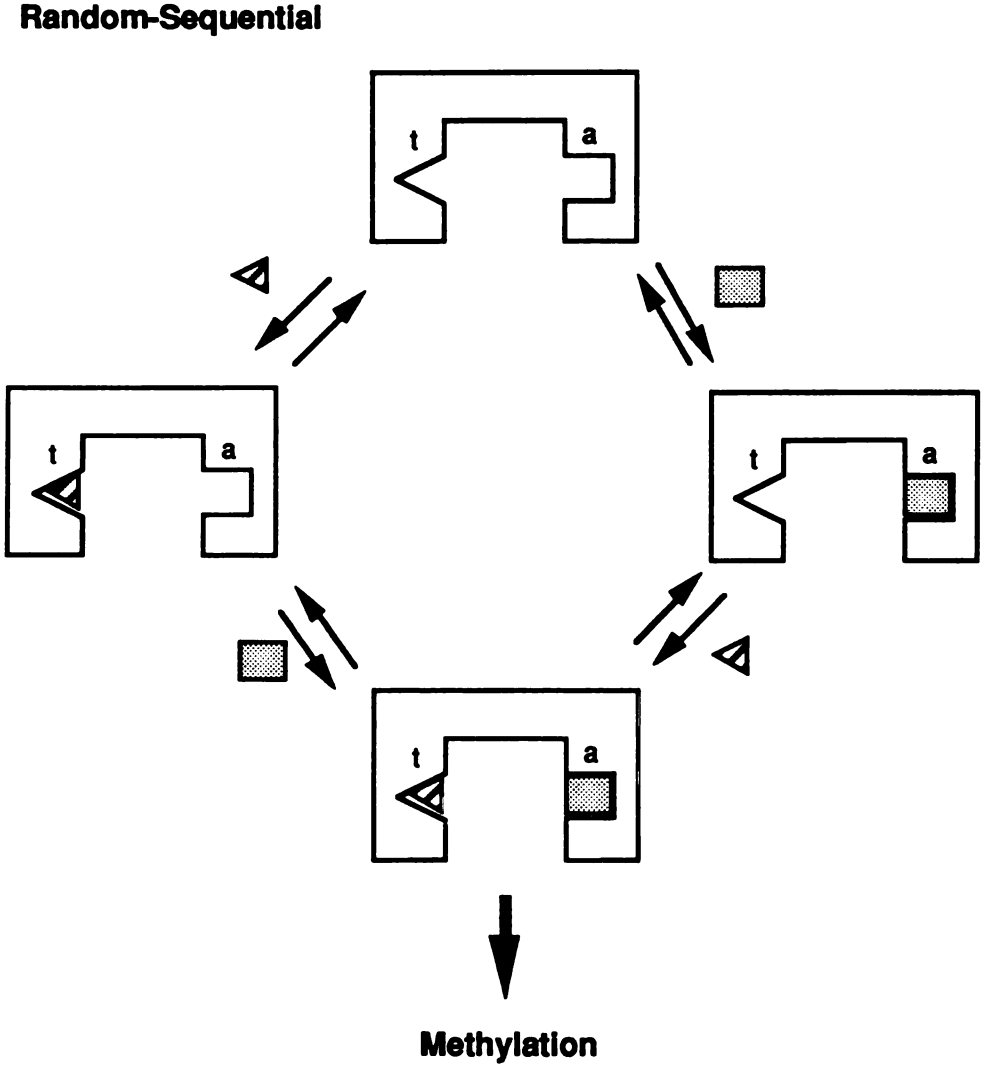

Figure 6.8a (Model 6.8a). Random-Sequential Mechanism. ◁, tRNA; , ▒ AdoMet. "t" indicates the tRNA binding site site, and "a" indicates the AdoMet site.

previously dialyzed free of AdoMet. Once the methyl is transferred, it is "trapped" in the RUMT-^{32}P-FUtRNA-CH_3 complex. If the ratio of $^{3}H/^{32}P$ in the RUMT-^{32}P-FUtRNA-CH_3 complex is low relative to the control, then the unlabeled bound

AdoMet must have transferred its methyl to the RNA prior to dissociating from the complex. As shown in Figure 6.6, this is indeed the case. These results thus rule out model 6.8c.

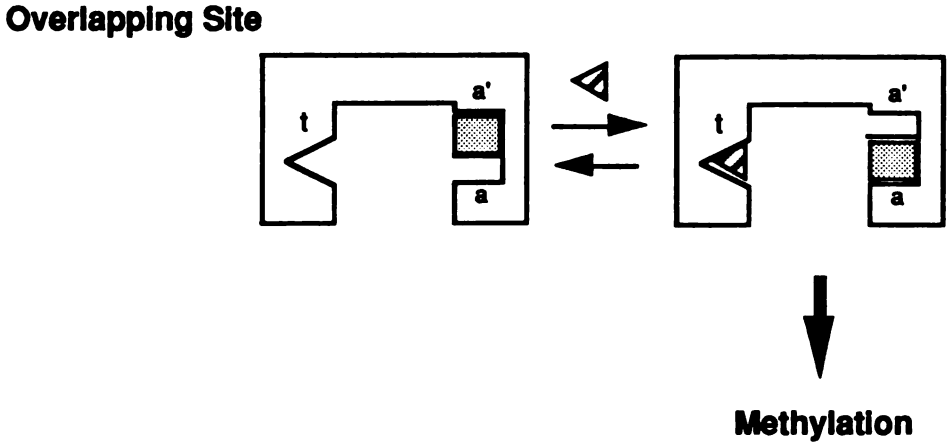

Figure 8.6b (Model 8.6b). Overlapping site model. " a' " indicates an alternative AdoMet binding site.

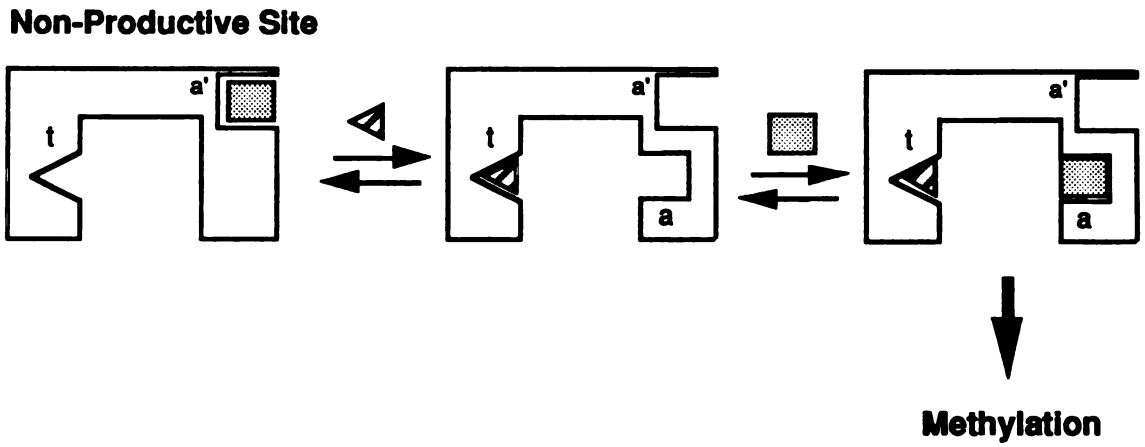

Figure 8.6c (Model 8.6c). Non-productive site model.

To further characterize the RUMT-AdoMet interaction, we sought to quantitate the protein-ligand binding in vitro. Equilibrium dialysis experiments revealed that the K_d of the RUMT-AdoMet complex was about 600 nM in phosphate buffer. Surprisingly, RUMT-AdoMet binding was highly dependent on buffer components-- binding was observed in phosphate, but not in Tris buffer. The observation that phosphate is required for AdoMet binding helps resolve two experimental anomalies. First, it explains why we have never observed RUMT-AdoMet complexes in previous preparations of RUMT. In the past, RUMT was purified by a multi-step, multi-column procedure, and many steps were performed in Tris buffer (Gu and Santi, 1991). Hence, by the time the enzyme was purified to homogeneity, most of the bound AdoMet would have dissociated and been removed by dialysis. In the stream-lined procedure employed in this study (Kealey and Santi, 1994), RUMT was purified in one day and the entire procedure was performed in phosphate buffer. Second, the phosphate requirement for AdoMet binding might also explain why we have never observed RUMT-AdoMet complexes on nitrocellulose filters, since those assays are not performed in phosphate buffer.

One interpretation for the phosphate dependence of AdoMet binding is that phosphate functions as an allosteric effector to induce an AdoMet binding site in RUMT. In this regard, phosphate could mimic RUMT's natural substrate, tRNA, and bind to RUMT in the tRNA binding site. In support of this hypothesis is the observation that the rate of RUMT catalyzed methylation of RNA substrates is markedly slowed in the presence of high a concentration of phosphate ($\geq$ 100 mM phosphate, J. Kealey, unpublished observation), suggesting that the RNA and phosphate compete for the same binding site. Moreover, it has been shown that the apoenzyme of thymidylate synthase, which catalyzes the CH_2H_4folate dependent methylation of deoxyuridine monophosphate, crystallizes with a

bound phosphate or sulfate in the dUMP binding site (Hardy et al., 1987, and references therein). This provides structural evidence that a buffer component, which shares common features with those of the natural substrate, occupies the substrate binding site in the absence of the natural substrate.

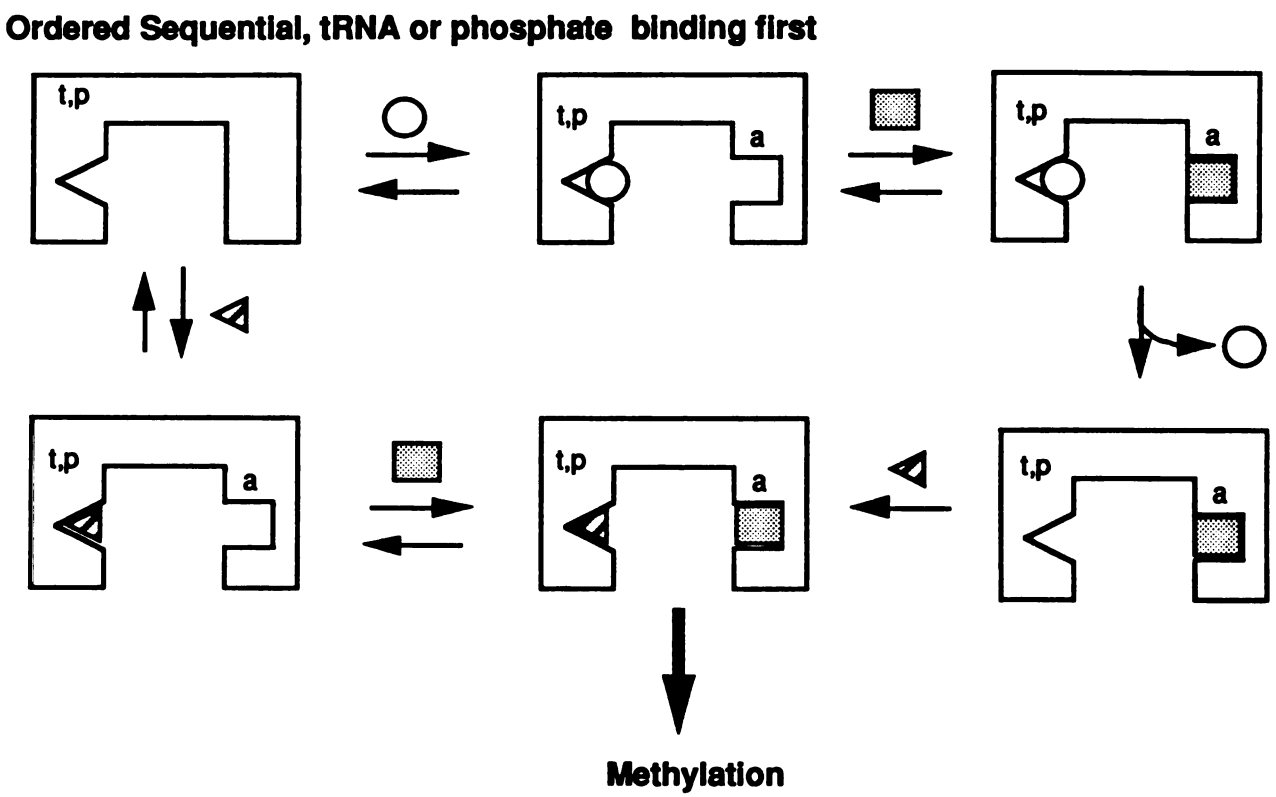

Figure 6.8d (Model 6.8d) Ordered-sequential mechanism. ○, phosphate.

Random -sequential binding, but AdoMet binding is only observed in the presence of phoshate or tRNA.

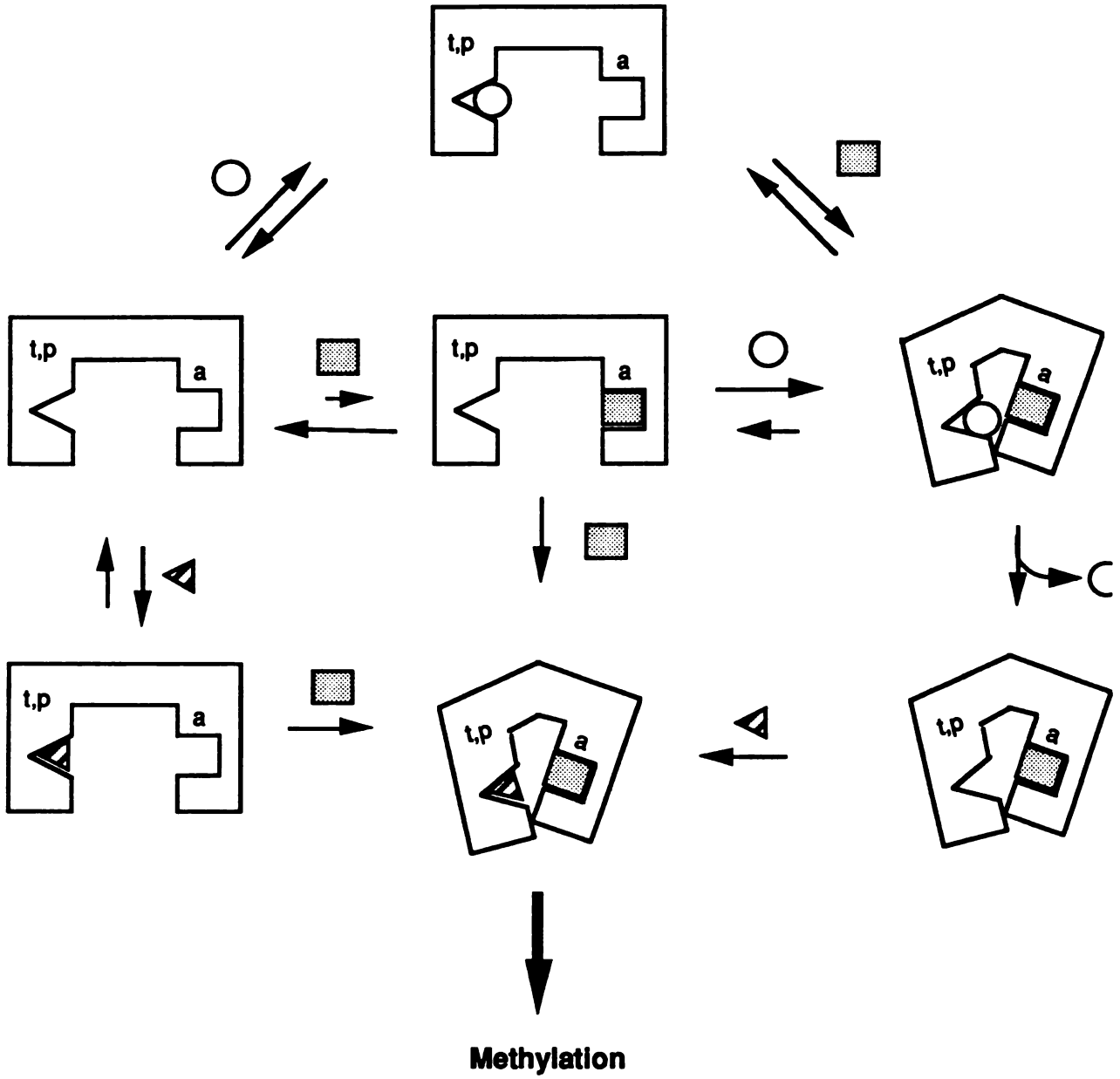

Figure 6.8e (Model 6.8e). Random sequential. The binding of phosphate or RNA is necessary to reduce the K_d (or decrease the off rate) of the RUMT-AdoMet complex so that it can be detected.

The ability of RUMT to bind AdoMet only in the presence of phosphate suggests that the substrate (phosphate or RNA) and the cofactor bind RUMT by an ordered sequential mechanism, as outlined in Figure 6.8d. This mechanism was originally discounted on the basis that AdoMet was found bound to RUMT in the absence of RNA, but in light of the observation that phosphate influences cofactor binding, the ordered-sequential mechanism must now be reconsidered. Note that in model 6.8d, the RNA can displace the phosphate without effecting the dissociation of the bound AdoMet. This feature was invoked to account for the results of the isotope trapping experiment, described above. A random-sequential model that is also consistent with the equilibrium dialysis data is shown in Figure 6.8e. In this model, AdoMet binds weakly to RUMT in the absence, but tightly to RUMT in the presence, of substrate (or buffer). In this way, the substrate or buffer acts as a "lid" to hold the AdoMet in place. The RNA or phosphate binds RUMT in the absence of AdoMet and the RNA can displace bound phosphate without causing the dissociation of bound AdoMet. Presently, models 6.8d and 6.8e are most consistent with the data in toto, but cannot themselves be distinguished based on the available data. It is predicted that RNA will affect AdoMet binding in a manner analogous to that of phosphate, and this hypothesis can be tested by investigating the binding of RNA and AdoMet to a mutant RUMT, which can bind substrates, but cannot turnover.

It is noteworthy that *Hha*I methylase, which catalyzes the AdoMet-dependent methylation of a specific cytidine in DNA (Wu and Santi, 1987), was also purified with bound AdoMet (Kumar et al., 1992). Moreover, the enzyme has been crystalized with bound AdoMet, but in the absence of DNA (Cheng et al., 1993). This finding was surprising considering that steady-state kinetic studies revealed that DNA and AdoMet bind to *Hha*I in an ordered-sequential

fashion, with DNA binding first (Wu and Santi, 1987). The steady-state kinetic data are thus in discord with the observation that AdoMet binds to *Hha*I in the absence of DNA. To reconcile this discrepancy, Cheng et al. (1993) have speculated that in the *Hha*I-Ado binary complex, the AdoMet could bind in a non-productive mode, which is kinetically incompetent for methylation (i.e. analogous to models 6.8b and 6.8c). Indeed, crystallographic data suggest that AdoMet occupies a different site in the *Hha*I-Ado complex than in the *Hha*I-AdoMet-DNA complex; however, this difference might be due to crystal packing forces (Klimasauskas et al., 1994). Alternatively, in light of the data presented here, it is tempting to speculate that a phosphate might occupy the DNA site in the *Hha*I-AdoMet complex. In support of this idea is the fact that *Hha*I is purified and crystallized in the presence of phosphate buffer (Kumar et al., 1992). Unfortunately, the crystallographic data of the *Hha*I-AdoMet complex are not of high enough resolution to unequivocally determine if phosphate (or some other ligand) is bound to *Hha*I along with AdoMet (X. Cheng, personal communication). The issue could be settled by employing an equilibrium dialysis experiment, analogous to the one reported here for RUMT, to determine if the *Hha*I-AdoMet interaction is phosphate (and by analogy DNA) dependent.

The fact that the RUMT-AdoMet complex remained intact through the RUMT purification procedure suggests that the off-rate of AdoMet from the binary complex is extremely slow. If the half-life of dissociation is estimated to be 6 hours (this is a minimum estimate, and is based on assuming that following a 6 hour purification, 50% of the bound AdoMet has dissociated), and considering a K_d of 600 nM, the bimolecular association constant (k_1) is calculated to be 32 $M^{-1}s^{-1}$. If in the crude cell lysate, the concentrations of RUMT and AdoMet were both about 100 μM (~ 4 mg/mL RUMT), then according to k_1, it would take about 5 minutes for the RUMT to be completely saturated

with AdoMet. Since it takes about one hour following cell lysis to prepare the enzyme for chomatrography, it is reasonable to assume that RUMT is saturated with AdoMet, prior to the first chromatographic step. It is noteworthy that the k_1 calculated above is about 300-fold lower than k_{cat}/K_m for RUMT catalyzed methylation of tRNA or T-arm. Since k_{cat}/K_m places a lower limit on the second order rate constant for association of enzyme and substrates, k_1 cannot reflect a kinetically competent interaction. The low value of k_1 relative to k_{cat}/K_m suggests AdoMet binding to the RUMT-phosphate complex proceeds by a different mechanism than AdoMet binding to the RUMT-RNA complex.

REFERENCES

Buck, M., M. Connick and B. N. Ames (1983). Complete analysis of tRNA-modified nucleosides by high-performance liquid chromatography: The 29 Modified Nucleosides of *Salmonella typhimurium* and *Escherichia coli* tRNA. *Anal. Biochem.* **129**: 1-13.

Cheng, X., S. Kumar, J. Posfai, J. W. Pflugrath and R. J. Roberts (1993). Crystal structure of the *Hha* DNA Methyltransferase complexed with *S*-Adenosyl-Methionine. *Cell* **74**: 299-307.

England, T. E., A. G. Bruce and O. C. Uhlenbeck (1980). Specific labeling of 3' termini with T-4 RNA ligase. *Methods in Enzymol.* **65**: 65-74.

Gu, X. and D. V. Santi (1991). Affinity chromatography of *Escherichia coli* (m^5U54)-Methyltransferase on tRNA-Agarose. *Protein Expression and Purification* **2**: 66-68.

Gu, X. and D. V. Santi (1991). The T-arm of tRNA is a substrate for tRNA (m^5U54)-Methyltransferase. *Biochemistry* **30**: 2999-3002.

Gu, X. and D. V. Santi (1992). Covalent adducts between tRNA (m^5U54)-Methyltransferase and RNA Substrates. *Biochemistry* **31**: 10295-10302.

Hardy, L. W., M. J. S. Finer, W. R. Montfort, M. O. Jones, D. V. Santi and R. M. Stroud (1987). Atomic structure of thymidylate synthase: target for rational drug design. . *Science* **235**: 448-55.

Kealey, J. T., S. Lee, H. G. Floss and D. V. Santi (1991). Stereochemistry of methyl transfer catalyzed by tRNA (m5U54)-methyltransferase-- evidence for a single displacement mechanism. *Nucleic. Acids. Res.* **19**: 6465-6468.

Kealey, J. T. and D. V. Santi (1991). Identification of the catalytic nucleophile of tRNA (m^5U54)Methyltransferase. *Biochemistry* **30**: 9724-9728.

Kealey, J. T. and D. V. Santi (1994). High level expression and rapid purification of tRNA (m^5U54) methyltransferase. *Prot. Exp. Purif.* **In press**:

Klimasauskas, S., S. Kumar, R. R.J. and X. D. Cheng (1994). *Hha*1 methyltransferase flips its target base out of the DNA helix. *Cell* **76**: 357-369.

Klotz, I. M. (1989). Ligand-protein binding affinites. Protein funtion: A practical approach. Oxford, IRL Press. pps. 24-54.

Kumar, S., X. Cheng, J. W. Pflugrath and R. Roberts (1992). Purification, crystallization, and preliminary X-Ray diffraction analysis of an M. *Hha*I-AdoMet Complex. *Biochemistry* **31**: 8648-8653.

Reich, N. O. and N. Mashhoon (1991). Kinetic mechanism of the *Eco*RI methyltransferase. *Biochemistry* **30**: 2933-2939.

Sambrook, J., E. F. Fritsch and T. Maniatis (1989). Molecular Cloning. A laboratory Manual. Cold Spring Harbor Laboratory Press.

Sampson, J. R. and O. C. Uhlenbeck (1988). Biochemical and physical characterization of an unmodified yeast phenylalanine transfer RNA transcribed *in vitro*. *Proc. Natl. Acad. Sci. USA* **85**: 1033-1037.

Santi, D. V. and L. W. Hardy (1987). Catalytic mechanism and inhibition of tRNA (Uracil-5-) methyltransferase: Evidence for Covalent Catalysis. *Biochemistry* **26**: 8599-8606.

Steinberg, S., A. Misch and M. Sprinzl (1993). Compilation of tRNA sequences and sequences of tRNA genes. *Nucleic Acids Res.* **21**: 3011-5.

Webster, K. R., Y. Shamoo, W. Konigsberg and E. K. Spicer (1991). A rapid method for purification of synthetic oligoribonucleotides. *Biotechniques* **11**: 658-661.

Afterward

... It is very easy to grow tired at collecting; the period of low tide is about all men can endure. At first the rocks are bright and every moving animal makes his mark on the attention. The picture is wide and colored and beautiful. But after an hour and a half the attention centers weary, the colors fade, and the field is likely to narrow to an individual animal. Here one may observe his own world narrow down until interest, and with it, observation, flicker and go out. And what if with age this weariness become permanent and observation dim out and not recover ? Can this be what happens to so many men of science? Enthusiasm, interest, sharpness, dulled with weariness until finally they retire into easy didacticism? With this weariness, this stultification of the attention centers, perhaps there comes the pained and sad memory of what the old excitement was like, and regret might turn to envy of the men who still have it. Then out of the shell of didacticism, such a used-up man might attack the unwearied, and he would have in his hands proper weapons of attack. It does seem certain that to a wearied man an error in a mass of correct data wipes out all the correctness and is a focus for attack; whereas the unwearied man, in his energy and receptivity, might consider a little dross of error a by-product of his effort. These two may balance and produce a purer thing than either in the end. These two may be the stresses which hold up the structure, but it is a sad thing to see the interest in interested men thin out and weaken and die. We have known so many professors who once carried their listeners high on their single enthusiasm, and have seen these same men finally settle back comfortably into lectures prepared years before and never vary them again. Perhaps this is the same narrowing we observe in relation to ourselves and the tide pool-- a man looking at reality brings his own limitations to the world. If he has strength and energy of mind the tide pool stretches both ways, digs back to the electrons and leaps space into the universe and fights out of the moment into non-conceptual time. Then ecology has a synonym which is ALL...

--- From *The Log From the Sea of Cortez*, John Steinbeck and Edward F. Ricketts